Diana Filipa Pereira Vaz

Graduated in Biochemistry

Dissertation presented to obtain the Master Degree in
Molecular Genetics and Biomedicine

Insights into *Campylobacter jejuni* Desulforubrerythrin catalytic mechanism

Supervisor: Prof. Miguel S. Teixeira, Professor, ITQB-UNL
Co-Supervisor: Dr. Célia V. Romão, Auxiliary Investigator, ITQB-UNL

Membros do júri:

Presidente: Doutora Paula Maria Theriaga Mendes Bernardo Gonçalves
Arguente: Doutor Carlos Aberto Gomes Salgueiro
Vogal: Doutora Célia Maria Valente Romão

FACULDADE DE CIÊNCIAS E TECNOLOGIA
UNIVERSIDADE NOVA DE LISBOA

November 2013

Diana Filipa Pereira Vaz

Graduated in Biochemistry

Dissertation presented to obtain the Master Degree in
Molecular Genetics and Biomedicine

Insights into *Campylobacter jejuni* Desulforubrerythrin catalytic mechanism

Supervisor: Prof. Miguel S. Teixeira, Professor, ITQB-UNL
Co-Supervisor: Dr. Célia V. Romão, Auxiliary Investigator, ITQB-UNL

Membros do júri:

Presidente: Doutora Paula Maria Theriaga Mendes Bernardo Gonçalves
Arguente: Doutor Carlos Aberto Gomes Salgueiro
Vogal: Doutora Célia Maria Valente Romão

FACULDADE DE CIÊNCIAS E TECNOLOGIA
UNIVERSIDADE NOVA DE LISBOA

November 2013

Direitos de cópia

Insights into Desulforubrerythrin catalytic mechanism

Diana Filipa Pereira Vaz

FCT/UNL, UNL

“The scientist does not study nature because
it is useful; he studies it because he delights
in it, and he delights in it because it is beautiful.”

Jules Henri Poincaré

Acknowledgments

Several people were indispensable for making of the work here described.

First, I would like to acknowledge the availability of my supervisors, Professor Miguel Teixeira and Doctor Célia Romão. To Prof. Miguel Teixeira, I would like to thank for giving me the opportunity to start my research work in his laboratory. I hope such an experience made me grow as a young scientist and also as a person. I am also grateful for all the advices, knowledge and work discussions. To Dr. Célia Romão, I acknowledge for all the advices and discussions, for always pushing me forward, and also for her interest and concern in subjects that go beyond the present work.

I also would like to acknowledge all the other members of the Metalloproteins and Bioenergetics Unit: Manuela Pereira, Afonso Duarte, Ana Paula Baptista, Patrícia Refojo, Vera Gonçalves, Sandra Santos, Bruno Marreiros, Elísio Silva, Filipa Calisto, Filipa Sena, Joana Simões, Paulo Castro, Cecília Miranda, Rodrigo David and Joana Carrilho. I would also like to thank to the former members of this unit Miguel Ribeiro and Liliana Pinto. To all of them I am grateful for the help and the advices, namely during my first stages in the laboratory, and also for all the good moments. The following people deserve a special word of gratitude: Liliana, who introduced the laboratorial work to me; Joana C., who was always available to help me; Rodrigo, who lots of times brought me to and from the lab.

I am grateful to my family, especially to my mother. Without her hard work and sacrifice I would have never made it so far.

A special acknowledgement to the following friends: Margarida who, especially since the beginning of the college was always there to listen to me; to André who, particularly during the write of this thesis, always had a word (to try) to keep me calm and focused.

Abstract

The following work aims to contribute to a better understanding of systems involved in resistance to oxidative stress species, namely hydrogen peroxide. The work is focused in one protein from the pathogen *Campylobacter jejuni*: desulforubrerythrin. Desulforubrerythrin is a non-heme iron protein in which the catalytic centre harbours a diiron cluster. Besides, the protein has a desulforedoxin domain at the N-terminal and a rubredoxin domain at the C-terminal. With the objective of understanding the protein catalytic mechanism three site-directed mutants, as well the wild type protein, were over expressed in *Escherichia coli*, purified and studied through biochemical and spectroscopic techniques. The amino acid residues selected for mutations are two tyrosines near the catalytic centre (residues 59 and 127). These residues are strictly conserved in rubrerythrins; moreover in diiron centres containing proteins tyrosines play a role in dissipating oxidizing species of iron (IV) by forming a tyrosil radical. The selected residues were replaced by a phenalanine residue which gave rise to three mutants: Y59F, Y127F and Y59F Y127F. These were characterized having as reference the wild type protein. All proteins have a molecular mass of 24 kDa and are tetramers in solution. The EPR and UV-visible techniques confirmed the presence of the three metallic domains in the wild type and Y59F mutant. The Y127F mutant was successfully used to test a protocol for diiron centre reconstitution in desulforubrerythrin.

Finally, crystals of the wild type and, for the first time, of the Y59F and double mutants were obtained. The X-ray data for the mutants were collected with a resolution of 1.9 Å and its structure will be determined.

Keywords: *Campylobacter jejuni*, desulforubrerythrin, hydrogen peroxide, crystallization, EPR.

Resumo

O trabalho aqui apresentado pretende contribuir para alargar o conhecimento sobre sistemas envolvidos na resistência ao *stress* oxidativo, nomeadamente na resistência ao peróxido de hidrogénio. O trabalho foi dirigido para o estudo de uma proteína do patogénio *Campylobacter jejuni*: desulforubreritrina. A desulforubreritrina é uma proteína com ferro não hémico cujo centro catalítico comporta dois átomos de ferro. Além disso, a proteína possui no N-terminal um dominio do tipo desulforedoxina e no C-terminal um domínio semelhante a uma rubredoxina

Com o objectivo de compreender o mecanismo catalítico da proteína três mutantes dirigidos, assim como a proteína selvagem, foram sobre expressos em *Escherichia coli*, purificados e caracterizados utilizando técnicas bioquímicas e espectroscópicas. Os resíduos de aminoácidos seleccionados para efectuar as mutações são duas tirosinas que se encontram junto do centro catalítico (resíduos 59 e127). Estes resíduos são estritamente conservados em rubreritrinas; além disso, em proteínas que contêm centros binucleares de ferro as tirosinas desempenham um papel importante na dissipação de espécies oxidantes de ferro (IV) à custa da formação de um radical tirosil. Os resíduos seleccionados foram substituídos por uma fenilalanina dando origem a três mutantes: Y59F, Y127F e Y59F Y127F. Os mutantes foram caracterizados tendo como referência a proteína selvagem. Todas as proteínas têm uma massa molecular de 24 kDa e são tetrâmeros em solução. As técnicas de Ressonância Paramagnética Electrónica (RPE) e de espectroscopia de UV-Vis confirmaram a presença dos três domínios metálicos na proteína selvagem e no mutante Y59F. A proteína com a mutação no resíduo 127 foi utilizada com sucesso para testar um protocolo de reconstituição de centros binucleares de ferro na desulforubreritrina.

Finalmente, cristais da proteína selvagem e, pela primeira vez, dos mutantes Y59F e Y59F Y127F foram obtidos. Os dados de difracção de raios-X para os mutantes foram recolhidos com uma resolução de 1.9 Å

Termos-chave: *Campylobacter jejuni*, desulforubreritrina, peróxido de hidrogénio, cristalização, RPE.

Table of contents

List of figures

List of tables

Abbreviations

Å	Angstrom (10^{-10} meters)
BCA	Bicinchoninc acid
BSA	Bovine Serum Albumine
Cia	*Campylobacter* invasion antigens
CDT	Cytolethal Distending Toxin
CD	Coestimulatory molecule
Da	Dalton
DC	Dendritic cell
DRbr	Desulforubrerythrin
DRbr Y59F	Desulforubrerythrin with residue 59 (tyrosine) replaced by a phenylalanine
DRbr Y127F	Desulforubrerythrin with residue 127 (tyrosine) replaced by a phenylalanine
DRbr Y59F Y127F	Desulforubrerythrin with residues 59 and 127 (tyrosines) replaced by phenylalanines
Dfx	Desulfoferrodoxin
DNA	Deoxyribonucleic acid
Dps	DNA binding protein from starved cells
Dx	Desulforedoxin
E'_0	Conditional reduction potential
e^-	Electron
ε	Molar absortivity
EPR	Electron paramagnetic resonance
FUR	Ferric uptake regulator
g	EPR-g factor
H^+	Proton
ICP	Induced Coupled Plasma
IL	Interleukine
IPTG	Isopropythiogalactoside
LB	Lysogeny broth
LOS	Lipooligossacharides
MES	2-(N-morpholino) ethanesulphonic acid
NADH	Reduced nicotinamide adenine dinucleotide
NF-κB	Nuclear factor κB
NADPH	Reduced nicotinamide adenine dinucleotide phosphate
O.D.	Optical density
PAGE	Polyacrylamide gel electrophoresis
PEG	Polyethylene glycol
PerR	Peroxide Regulator

PDB	Protein Data Bank
Rbr	Rubrerythrin
Rd	Rubredoxin
ROS	Reactive oxygen species
S	Spin quantum number
SDS	Sodium dodecyl sulphate
SOD	Superoxide Dismutase
TCEP	Tris-(2-Carboxyethyl)phosphine hydrochloride
TEMED	N, N, N', N'-tetramethylethylenediamine
TNF-α	Tumor Necrosis Factor α
TPTZ	2, 4, 6 – tripyridyl-triazine
Tris	Tris (hydroxymethyl)-aminomethane
UV	Ultraviolet
Vis	Visible
Wt	Wild type

Latin abbreviations

c.a.	*circa*, approximately
e.g.	*exempli gratia,* for example
et al.	*et alia*, and other people

1. INTRODUCTION

1.1. Reactive oxygen species (ROS) and oxidative stress

1.1.1. Oxygen

Molecular oxygen (O_2) is essential to all aerobic organisms but at the same time it can cause serious cellular damage. O_2 has a strong oxidizing potential, which makes this molecule very suitable for accepting electrons in reduction-oxidation reactions (Bartz and Piantadosi, 2010). The complete reduction of O_2 to water has a reduction potential of 0.815 V at pH 7.0 (Wood, 1988) (eq 1.1).

$$O_2 + 4\ H^+ + 4\ e^- \rightarrow 2\ H_2O_2 \quad \textbf{(eq 1.1)}$$

Oxygen has two unpaired electrons with the same spin, what limits its reactivity due to spin restriction rules (Fridovich, 2013).

1.1.2. Reactive oxygen species

Reactive oxygen species are molecules derived from oxygen reduction that can cause serious cell damaging. The most common ROS in living organisms are superoxide anion ($O_2^{\cdot-}$), hydrogen peroxide (H_2O_2), hydroxyl radical ($HO^{\cdot}$) and singlet oxygen ($^1O_2$) (Birben *et al*, 2012; Dröge, 2002).

These molecules can be free radicals on non-radicals with unstable bonds. In the first the high reactivity is due to the presence of unpaired electrons (Burton and Jauniaux, 2011).

Superoxide anion is formed by one electron reduction of oxygen (eq 1.2). It can react with another molecule of superoxide and form again oxygen and hydrogen peroxide in an autodismutation process (eq 1.3) (Jena, 2012).

$$O_2 + 1e^- \rightarrow O_2^{\cdot-} \quad \textbf{(eq 1.2)}$$

$$2O_2^{\cdot-} + 2H^+ \rightarrow O_2 + H_2O_2 \quad \textbf{(eq 1.3)}$$

Hydrogen peroxide can also be formed by the reduction of oxygen by two electrons (eq 1.4) or dimerization of two hydroxyl radicals (eq 1.5). In the case of hydrogen peroxide its reactivity is due to its low energy bonds when compared with O_2 and $O_2^{\cdot-}$ (Brieger *et al*, 2012).

$$O_2 + 2H^+ + 2e^- \rightarrow H_2O_2 \quad \textbf{(eq 1.4)}$$

$$2HO^{\cdot} \rightarrow H_2O_2 \quad \textbf{(eq 1.5)}$$

The hydroxyl radical, the most dangerous ROS for *in vivo* systems, can be formed by reacting superoxide and hydrogen peroxide, through the Haber-Weiss reaction (eq 1.6).

$$O_2^{\cdot-} + H_2O_2 \rightarrow HO^{\cdot} + OH^- + O_2 \quad \textbf{(eq 1.6)}$$

Singlet oxygen is very reactive and highly toxic in biological systems. This species corresponds to an excited form of molecular oxygen in which one of the electrons underwent a spin inversion, in an endothermic process (Fridovich, 2013). One of its sources is enzymatic reactions of photo-oxidation of biological compounds. Singlet oxygen reacts with DNA, particularly with guanine bases due to their lower redox potential (Agnez-Lima *et al.*, 2012).

1.1.3. Sources of ROS in living organisms

ROS are produced by all living organisms as a result of the normal aerobic metabolism and can be produced by external agents, such as ionizing radiation and transition metal ions (Birben *et al.*, 2012).

The production of ROS assumes particular importance in organisms in which O_2 is the final electron acceptor in the respiratory chain due to the leakage of electrons from respiratory enzymes. These electrons can lead to one electron reduction of O_2 and the subsequent formation of $O_2^{\cdot -}$, the most common radical in living organisms. The main source of hydrogen peroxide is the dismutation of $O_2^{\cdot -}$ by superoxide dismutase (SOD). This is readily converted to water by several enzymatic systems, such as catalase and glutathione reductase. When these systems fail, H_2O_2 becomes available to react with $O_2^{\cdot -}$ and yield the dangerous $HO^{\cdot}$. This radical has no known scavenger and reacts very rapidly with biological molecules. Besides, H_2O_2 can diffuse freely through biological membranes and cells have to cope with H_2O_2 produced in the outside of the cell (Brieger *et al.*, 2012).

Singlet oxygen can be formed by photo-oxidation of molecular compounds or by enzymatic reactions.

1.1.4. Iron and ROS

Iron is essential for all organisms. The couple Fe^{2+}/Fe^{3+} in biological systems has a redox potential that varies from -500 mV and +300 mV. This characteristic and its ability to exist in different redox states make iron a perfect co-factor for electron transfer reactions (van Vliet *et al.*, 2002). Iron can present oxidation numbers between -2 and +6, but in biological systems is only found Fe (II), Fe (III) and Fe (IV), respectively ferrous, ferric and ferryl forms (Cornelis and Andrews, 2010).

In biological systems iron is present in heme containing proteins and non-heme containing proteins, such as iron-sulfur proteins and non iron-sulfur proteins. These proteins have a wide diversity of functions, such as transcriptional regulation, electron transference, respiration or ROS detoxifying proteins (van Vliet *et al.*, 2002).

In spite of its importance, iron can cause serious injury when allowed to remain free in the cell, for its reaction with oxygen is one of the sources of ROS in the cell. This is mainly due to the Fenton reaction (eq 1.7) In the presence of iron (II) hydrogen peroxide is reduced and $HO^{\cdot}$ is formed. The cycle is completed by the regeneration of ferrous iron at the expense of one electron from superoxide radical (eq 1.8) (Birben *et al.*, 2012).

$$Fe^{2+} + H_2O_2 + H^+ \rightarrow Fe^{3+} + HO^{\cdot} + H_2O \quad \textbf{(eq 1.7)}$$

$$Fe^{3+} + O_2^{\cdot -} \rightarrow Fe^{2+} + O_2 \quad \textbf{(eq 1.8)}$$

To prevent these nefarious effects organisms have several proteins to capture free iron in a controlled way through sensor and regulatory systems. In more complex organisms this restriction is *per se* a defence against microbial colonization, given that all (pathogenic) organisms need iron (Holmes *et al.*, 2005), a process called nutritional immunity (Damo *et al.*, 2012). Also it is not surprising that iron and oxidative stress response genes are regulated by common mechanisms.

1.1.5. Toxicity of H_2O_2

The toxic effects of ROS, especially H_2O_2, for the bacterial cells can be used for human benefit. The immune system already takes advantage of ROS to kill invading pathogens and also to initiate the adaptive immune response. The great advantage of these substances is their non specific mode of action, thus they can be use against several bacteria (Linley *et al.*, 2012). But these compounds can also be use as disinfectant agents in industry or medical services. Its cellular targets are also very distinct. Hydrogen peroxide can react with co-factors from metallic proteins; can damage the DNA via Fenton reaction and lipids peroxidation which will lead to unstable cellular membranes (Finnegan *et al.*, 2010).

1.1.6. ROS detoxifying systems

Antioxidants keep ROS levels balanced by competing with other oxidizing substrates (Droge, 2002). Antioxidants can be enzymes, such as superoxide dismutase, catalase, or glutathione peroxidase, or small molecules as glutathione, vitamin C and vitamin E (Birben *et al.*, 2012).

When an organism reaches a state in which the amount of antioxidants and oxidative species is unbalanced favouring the later, we can say to have a situation of oxidative stress (Birben *et al.*, 2012).

Superoxide dismutases are enzymes responsible by dismutation of superoxide anion to hydrogen peroxide and oxygen. They can be separated in three families depending on the co-factor utilized. FeSOD/MnSOD can utilize iron or manganese as co-factor; the Cu, Zn SOD family in which the protein uses an atom of copper as co-factor and a zinc atom as structural element; and finally a family of SOD that uses nickel as co-factor (NiSOD) (Aguirre and Culotta, 2012).

Peroxidases are the mainly responsible enzymes for H_2O_2 reduction, being catalase a specific enzyme within this family. The first reduce hydrogen peroxide to water by oxidizing other substrates, while catalase catalyses the dismutation to water and oxygen (eq 1,9). This family includes gluthatione peroxidases and peroxiredoxins (Prx). Contrary to what is observed in many ROS destoxifying enzymes, Prx does not possess any metal co-factor. The reduction of hydrogen peroxide is performed by active cysteine residues and the resultant disulfide bond is reduced by thioredoxin (Rhee *et al.*, 2012).

$$2\ H_2O_2 \rightarrow 2\ H_2O + O_2 \quad \textbf{(eq 1.9)}$$

1.2. Rubrerythrins

Rubrerythrins (Rbr) are non-heme iron containing proteins. The first rubrerythrin was identified in *Desulfovibrio vulgaris* (Figure 1.1) (Legall *et al.*, 1988)**,** but other rubrerythrins were lately found in organisms from all life domains, mainly anaerobic and microaerophilic ones (*e.g.* Pütz *et al.*, 2005; Wakagi, 2003). They belong to the ferritin-like super family mainly by their four-helix bundle domain (Andrews, 1998; Cooley *et al*., 2011).

Most rubrerythrins are composed by two domains: a diiron oxo-bridged centre incorporated in a four-helix bundle and a rubredoxin domain at the N-terminal which contains an iron atom coordinated by four cysteines. Rubrerythrins are usually purified as homodimeric proteins with a "head to tail" arrangement (Coulter *et al.*, 2000; Lumpio *et al.*, 2001; Weinberg *et al.*, 2004).

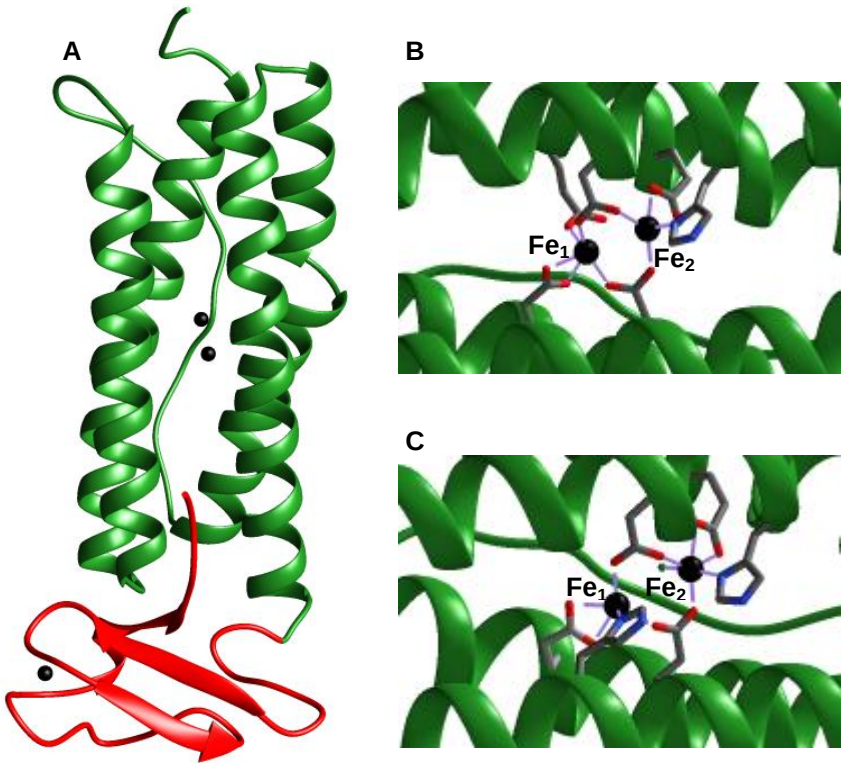

Figure 1.1: Structure of *Desulfovibrio vulgaris* rubrerythrin (PDB codes: A. 1RYT. B. 1LKM and C. 1LKO). The green area corresponds to the four-helix bundle domain and the red area is the rubredoxin domain. The iron atoms are represented in black. **(A)** Protein in a monomeric conformation. **(B)** Diiron centre all ferric. **(C)** Diiron centre all ferrous. Pictures created with Chimera.

1.2.1. Structural domains

The family of rubrerythrins is large and diverse due to the occurrence of several domains addition at the C and N-terminals (Figure 1.2).

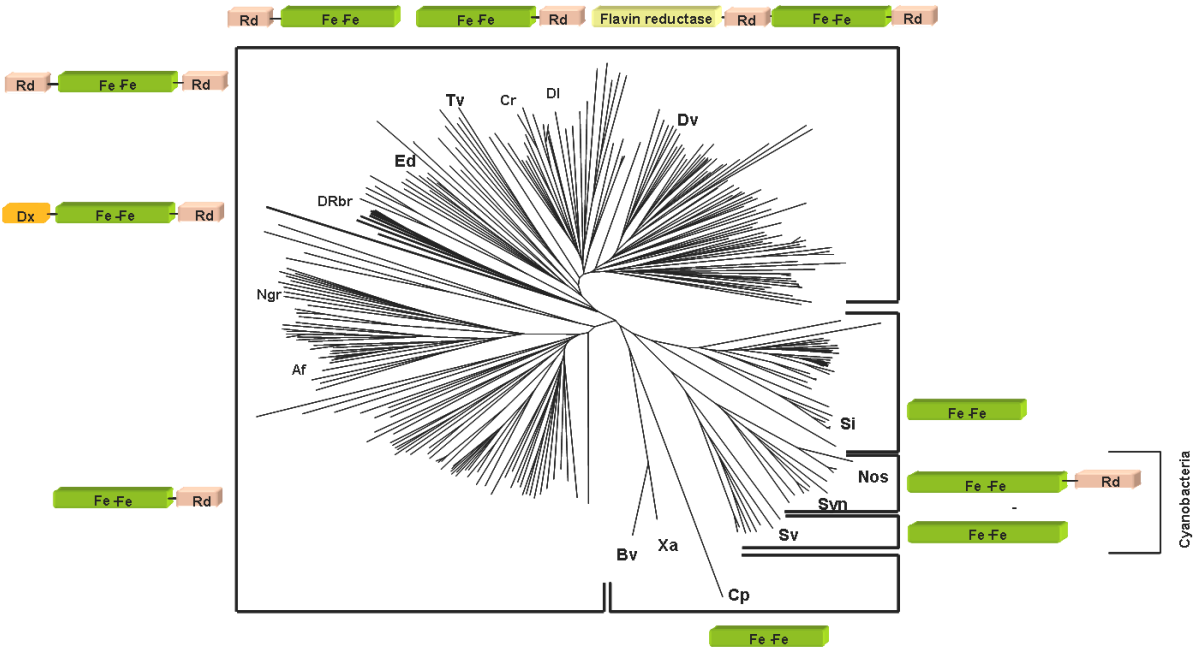

Figure 1.2: Dendogram of proteins from the rubrerythrin family (Pinto, 2012).

The simplest rubrerythrin contains only the four helix-bundle domain, like simerythrin from *Cyanophora paradoxa* or sulerythrin from the archeon *Sulfolobus tokodaii* (Cooley *et al.,* 2011; Wakagi, 2003). The four-helix bundle carries a diiron centre responsible for the catalytic activity of the protein. The iron ligands are two histidines, four carboxylates and one glutamate, depending upon its oxidation state. When oxidized the Fe_1 is coordinated by four glutamate residues and Fe_2 is coordinated by three glutamates and one histidine. The two iron atoms are connected by two of the glutamate residues ligands and one molecule of solvent. In the reduced form the molecule of solvent disappears and each iron is coordinated by one histidine, three glutamates and one molecule of water (Figure 1.1) (Pinto, 2012).

Given the high similarity of helix A/B and helix C/D it is proposed that rubrerythrins ancestors were homodimeric proteins containing only replicas of helix A and B (Figure 1.3) and the appearance of the actual rubrerythrins was probably due to a gene duplication event (Andrews, 2010).

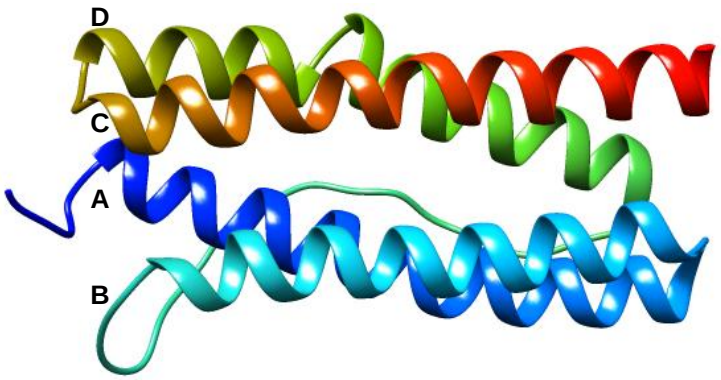

Figure 1.3: Four-helix bundle of *D. vulgaris* rubrerythrin. Image coloured from blue (N-terminal) to red (C-terminal). PDB code: 1ryt. The helixes are designated by the letters (A-D). Picture created with Chimera.

The C-terminal of rubrerythrins usually has a rubredoxin domain. Rubredoxins are iron-sulfur proteins harbouring an iron atom coordinated by four cysteine residues (Bentrop *et al.*, 2001).

Two types of rubredoxin proteins are so far described in literature. The difference between type I and type II rubredoxins is based on the distance between the cysteine ligands to the iron. Type I rubredoxins have a binding motif of the type $CX_2CX_nCX_2C$ and are the most common rubredoxins. Type II rubredoxins have two extra residues between the first pair of cysteines. In rubrerythrins the rubredoxin like domain resembles a type I rubredoxin. Desulforedoxin is a rubrerythrin-like protein in which the amino acids between the first pair of cysteines are absent, that causes a distortion in the protein structure (Figure 1.4) (Archer *et al.*, 1995).

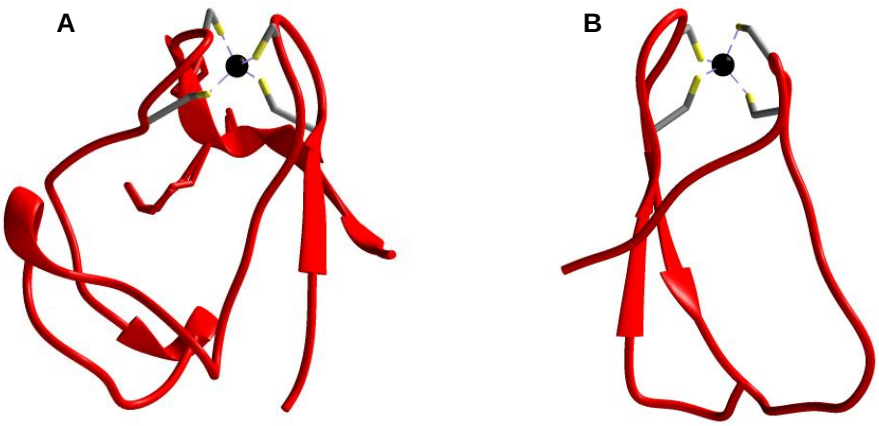

Figure 1.4: Comparison between rubredoxin and desulforedoxin. **(A)** Three-dimensional structure of *Desulfovibrio vulgaris* rubredoxin. Structure 1RB9 from PDB. **(B)** Three-dimensional structure of *D. vulgaris* desulforedoxin. Structure 1DXG from PDB. Iron atoms are coloured in black. Figures created with Chimera.

1.2.2. Physiological activity

Considering the structural domains present in rubrerythrins it was initially thought that they can be involved in iron storage or in protection against oxidative stress. The diiron centre of rubrerythrins has a three-dimensional structure similar with that of ferritins and is able to oxidize ferrous iron (eq 1.10

and 1.11) (Coulter *et al.*, 2000), however rubrerythrins do not form a hollow sphere that could store iron.

$$Fe^{2+} + Rbr_{ox} \rightarrow Fe^{3+} + Rbr_{red} \quad \textbf{(eq 1.10)}$$

$$Rbr_{red} + O_2 \rightarrow Rbr_{ox+} [O_2]_{red} \quad \textbf{(eq 1.11)}$$

To study the possible role of rubrerythrin, Lumppio and collaborators transformed an *Escherichia coli* strain (QC774) deficient in *sodA* and *sodB* that requires supplementation of the minimal medium in order to grow in aerobic conditions. This observed phenotype is probably due to the accumulation of superoxide anion and free iron. They transformed this strain with a plasmid coding for rubrerythrin and compared the growth rates of the non-transformed strain *versus* the transformed strain and found no significant differences, excluding the hypothesis of this protein acting as a superoxide dismutase. On the other hand they also transformed an *E. coli* strain (NC202) deficient in *katG* and *katE* (genes that encode catalase) and observed that the strain expressing the rubrerythrin had a higher survival rate when aerobically exposed to 2.5 mM H_2O_2 than that of the wild type strain. Similar results were obtain for nigerythrin, a Rbr-like protein also identified in *D. vulgaris*, thus indicating a role in hydrogen peroxide detoxification for these proteins (eq 1.12 and eq 1.13) (Lumpio *et al*., 2001).

$$NADH + Rbr_{ox} \rightarrow Rbr_{red} + NAD^+ + H^+ \quad \textbf{(eq 1.12)}$$

$$2\ H^+ + Rbr_{red} + H_2O_2 \rightarrow Rbr_{ox} + 2\ H_2O \quad \textbf{(eq 1.13)}$$

In another work the authors studied the ability of wild type and mutant rubrerythrins from *D. vulgaris* to perform the referred functions attributed to rubrerythrins (peroxidase and ferroxidase). The work was performed with wild type and rubrerythrin mutants. The results obtained for Rbr Y27F and hydrogen peroxide are of particular importance, given the subject under study in this work. Observing the results obtained for the wild type protein the NADH peroxidase activity (251 ± 3.2 $\mu M\ min^{-1}$) seems to be more likely to occur *in vivo* than the ferroxidase activity (2 ± 0.3 $\mu M\ min^{-1}$). Furthermore, the Y27F mutant showed only 30% of the wild type peroxidase activity, thus indicating the residue in position 27 as being important to this activity. (Coulter *et al.*, 2000).

In *Pseudomonas gingivalis* W83 was detected the presence of a Rbr. Initial studies done by M. Sztukowsaka and collaborators showed the impact of Rbr gene disruption. They showed an increase in Rbr gene transcription upon exposure to oxygen or hydrogen peroxide and also the *P. gingivalis rbr*$^-$ mutant is more sensitive to oxygen and hydrogen peroxide (Sztukowsaka *et al.*, 2002). Later, Mydel and collaborators studied the importance of Rbr for *P. gingivalis* infection using a murine model. Although they showed the importance of Rbr in *P. gingivalis* proliferation *in vivo* through protection against reactive nitrogen species (RNS) (Mydel *et al.*, 2006). Having in mind the previous results this is a little intriguing and the physiological role of rubrerythrins as well their physiological electron donors needs further investigation.

1.2.3. Desulforubrerythrin

Desulforubrerythrin (Figure 1.5) was identified in *Campylobacter jejuni* NCTC11168. After exposing cells to H_2O_2, it was observed that a protein of approximately 27 kDa started to degrade. After N-terminal sequencing it was identified as the product of the gene *cj0012c* (Yamasaki *et al.*, 2004).

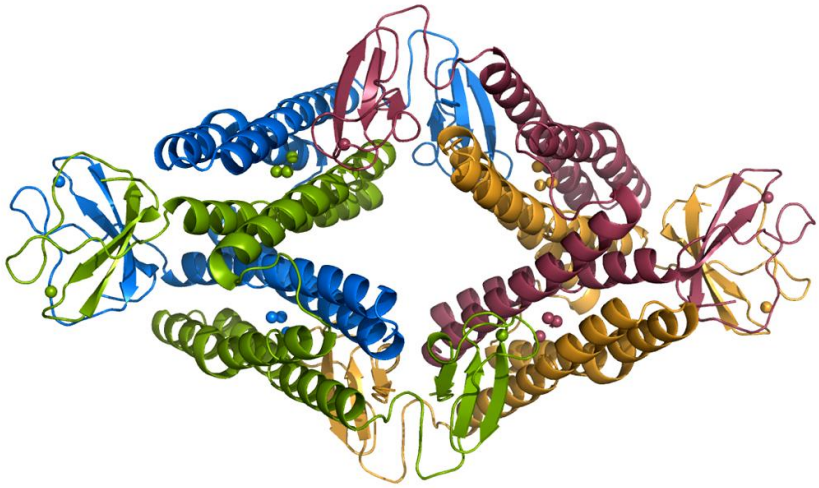

Figure 1.5: Desulforubrerythrin in a tetrameric conformation. Each monomer is represented with a different colour. (Unpublished data under refinement).

The sequence analysis of the protein revealed the presence of a desulforedoxin like domain at the N-terminal, wrongly labelled by the authors as rubredoxin oxidoreductase (Rbo) and a rubrerythrin like domain at the C-terminal, leading to the first designation of the protein: Rrc (Rbo/Rbr like protein from *C. jejuni*). Lately the domain at the N-terminal was identified as a desulforedoxin domain, leading to the actual denomination of the protein: desulforubrerythrin - DRbr (Pinto *et al.,* 2011). This similarity with rubrerythrins leaded the authors to speculate about the protein function as being related with oxidative stress protection. Although the levels of protein decrease upon cells exposure to hydrogen peroxide, no significant alterations were detected in the mRNA levels (Yamasaki *et al.*, 2004).

In case the protein is involved in hydrogen peroxide reduction its degradation at higher levels of its substrate may be an auto-regulation mechanism. It is clear that the protein needs to be reduced by some enzymatic system which in last instance should lead to NAD(P)H consumption. Thus, in elevated concentrations of hydrogen peroxide exists the serious possibility of depletion the cell of its reducing equivalents.

Lately, A.F. Pinto and collaborators showed that the protein has NADH-linked hydrogen peroxidase activity. They showed that the protein is able to reduce hydrogen peroxide to water in the presence of NADH, flavorubredoxin oxidoreductase and rubredoxin domain of flavorubredoxin, both from *Escherichia coli* (Pinto *et al.*, 2011). The same work also showed that the protein is isolated as a tetramer and has an isoelectric point of 5.37.

To better understand the catalytic mechanisms of the reaction with hydrogen peroxide, three mutant proteins were here studied. Two single mutant proteins and one double mutant comprising both mutations. The residues chosen were tyrosine 59 and 127. These residues are strictly conserved

in rubrerythrins and are hydrogen bounded to iron ligands (Figure 1.6). Besides, tyrosines surrounding diiron centres are known for being important in dissipation of oxidizing species such as Fe (IV) by formation of a tyrosil radical (Pinto, 2012). The residues were replaced by a phenylalanine, a structuraly similar amino acid but lacking the hydroxyl group. This difference should be enough to induce changes in protein activity (in case the residues are important for its activity) but should not be enough to change the three-dimensional structure around the catalytic centre.

The work here presented was based in expression, purification and characterization of the mutant proteins having as reference the wild type protein.

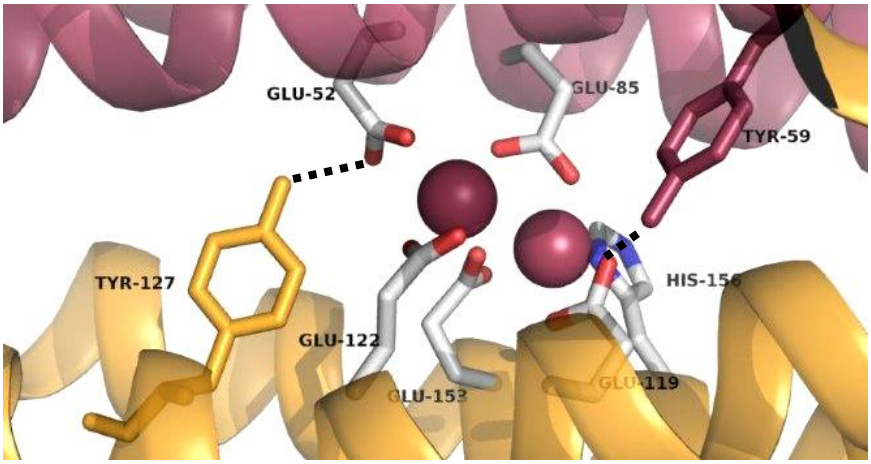

Figure 1.6: Depiction of the diiron centre evidencing its surrounding tyrosines. Iron atoms are represented in red; tyrosine 59 is represented in red; tyrosine 127 is represented in yellow. The dashed black lines represent hydrogen bonds between the tyrosines and glutamates. (Unpublished data under refinement).

1.3. *Campylobacter jejuni*: an overview

Campylobacter jejuni is a microaerophilic Gram-negative bacterium. It belongs to the delta-epsilon class of proteobacteria (Figure 1.7) and is a flagellate spiral bacterium (Figure 1.8). This species is the main cause of foodborne gastroenteritis in the world. The infection is acquired by consumption of contaminated meat, especially poultry. In developing countries contaminated water can also be a source of infection. The symptoms include fever, abdominal pain and diarrhoea (Dasti *et al.*, 2010; Young *at al.*, 2007). The disease can cause different symptoms apparently depending on the socio-economic level of the country. In developed countries the infection causes bloody diarrhoea with mucus while in developing countries the infection is more common in children and causes watery diarrhoea (Young *et al.*, 2007). This could be due to the fact that in developing countries people are exposed to the pathogen at early stages of life and this could confer a certain immunity against subsequent infections. In any case the infection in self-limiting, but in more severe cases antibiotic therapy may be required, generally erythromycin but also quinolones. Initially erythromycin was the chosen antibiotic to treat campylobacteriosis, being replaced nowadays by fluroquinolones. Although initially these drugs were efficient in treating the infection, soon cases o antibiotic resistance started to emerge due to the indiscriminate use of antibiotics in animals (Engberg *et al.*, 2001), making urgent the identification of alternative targets to other drugs.

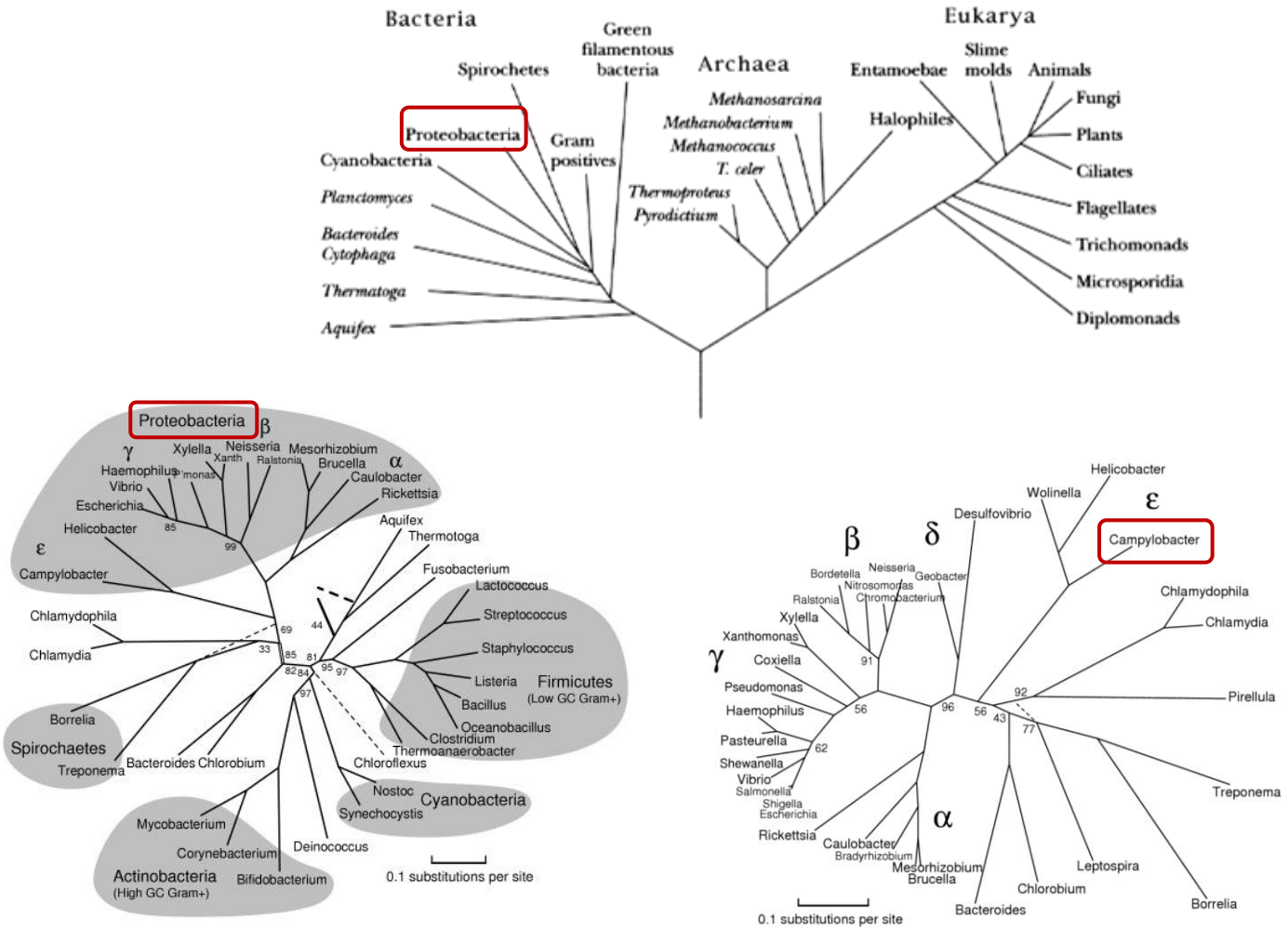

Figure 1.7: Localization of *Campylobacter* genus in the tree of life. **(A)** Tree of life based on ssRNA Adapted from Todar 2012. **(B)** Phylogenetic tr ee of Bacteria based in proteins. **(C)** Phylogenetic tree of Proteobacteria based on proteins. The numbers represent bootstrap support. Adapted from (Gupta, 2006).

The infection can cause serious sequelae, such as reactive arthritis and Guillian-Barre syndrome (GBS), a muscular neuropathy (Altekruse *et al.*, 1999; Kassem *et al.*, 2012; Young et al, 2007). The GBS seems to be an auto-immune response to the infection to the lipooligosacharides (LOS) of *C. jejuni* that are similar to human gangliosides. This results in temporary paralysis of the peripheral nerves and more rarely it can lead to death (Bingham-Ramos and Hendrixson, 2008; Kaakoush *et al.*, 2007).

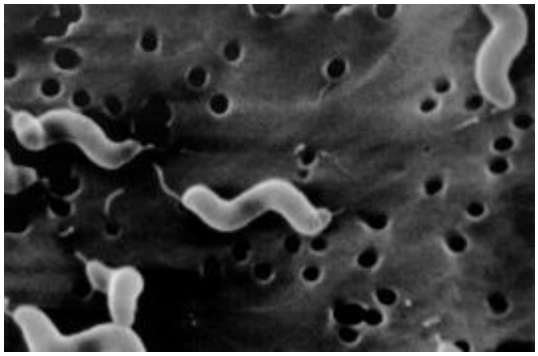

Figure 1.8: *Campylobacter jejuni* scanning microscopy image (Altekruse *et al.*,1999)

The genome of *C. jejuni* NCTC11168 has 164 148 base pairs, from which 94.3% encodes proteins making it one of the densest genomes sequenced. The analysis of the genome revealed homopolymeric tracts with great variability, probably coding for LOS, flagellar systems or other extracellular components (Parkhill *et al,* 2000). This diversity in extracellular surface structures may be one way to escape the immune system.

C. jejuni requires low O_2 concentrations (5-10%) and 5-10% of carbon dioxide to grow, which makes this microorganism microaerophilic and capnophilic, respectively. Its optimum growth temperature is 42ºC, just the same temperature of the chicken gut: its commensal host. *In vitro* growth of this microorganism requires media supplemented with blood or fetal bovine serum (Atack and Kelly, 2009). This makes one wonder how *C. jejuni* survives in the environment while travelling between hosts (see section 3.1).

Campylobacter members have a full tricarboxylic acid cycle (TCA) but are unable to utilize carbohydrates as energy source; they rely on intermediates of the TCA cycle (Brenner *et al.*, 2005).

C. jejuni possesses a highly branched respiratory chain allowing the organism the use of a wide range of substrates, including formate, malate, succinate and lactate, amongst others (Hoffman and Goodman, 1982; Kassem et al., 2012).

1.3.1. *C. jejuni*, oxidative stress and iron

Although *C. jejuni* requires specific conditions for optimal growth it has the ability to colonize different hosts and to survive in different environments, where may face different type of stresses: nutrients depletion (namely iron), atmospheric concentrations of O_2, ROS produced by the host, amongst others. To be able to survive these stressful conditions *C. jejuni* needs oxygen consuming enzymes and reactive oxygen species scavengers.

The respiratory chain of *C. jejuni* possesses a cbb_3 type oxygen reductase and a *bd*-type quinol: O_2 oxidoreductase, which are important for O_2 consumption (Smith *et al.*, 2000).

C. jejuni is a catalase-positive organism. Its genome analysis shows the presence of only one catalase coding gene named *katA*. W. A. Day and collaborators showed that a *C. jejuni* catalase deficient strain loses its viability after 15 minutes exposure to H_2O_2, while the wild type bacteria maintains a viability of approximately 60% after 1 hour in the same conditions. They also showed that the wild type strain could survive upon uptake by murine and porcine macrophages, while the mutant bacteria were not able to recover. Moreover, in macrophages treated with an oxidative burst inhibitor no differences were detected between the wild type and catalase deficient strains. Altogether these results show the importance of catalase in H_2O_2 resistance for *C. jejuni* (Day *et al.*, 2000).

The superoxide dismutation is performed by an iron superoxide dismutase (Fe-SOD). A mutant strain lacking the *sodB* gene was less able to survive inside human embryonic intestinal cells when compared with the wild type strain (Pesci *et al.*, 1994).

Proteins belonging to the family of peroxiredoxins were also identified in *C. jejuni*. These are alkyl hydroperoxide reductase (AhpC), thiol peroxidase (Tpx) and bacteoferritin comigratory protein (Bcp). The AhpC protein was showed to increase the aerotolerance under normal atmospheric conditions of *C. jejuni* but showed no detected effects in H_2O_2 resistance (Baillon *et al.*, 1999). Studies with Tpx and Bcp suggest that these two proteins may have a redundant role by comparing the phenotype of a wild type *C. jejuni* strain with *tpx* and *bcp* single mutants and with a double mutant. When growing the strains microaerobically the single mutants showed growth profiles very similar with the wild type strain. The double mutant reached the same cellular density than the wild type strain, but took more than twice as long. This was also verified when the cells were exposed to 1 or 2 mM of H_2O_2. The same study shows that Tpx and Bcp have substrate specificity. Both enzymes can reduce H_2O_2 in the presence of thioredoxin, thioredoxin reductase and NADH but only Bcp was able to reduce cumene hydroperoxide and tert-butyl-hydroperoxide, common artificial substrates to measure peroxidase activity (Atack *et al.*, 2008).

C. jejuni also contains a DNA binding protein from starved cells (Dps). Dps are DNA binding proteins, that also bind iron, thus preventing the production of $HO^{\cdot}$ (Miyamoto, *et al.*, 2011). It was observed that the Dps confers H_2O_2 resistance by binding iron in the cell, because bacteria lacking the Dps showed the same H_2O_2 resistance than the wild type bacteria when an iron chelator was added to the growth medium (Ishikawa *et al.*, 2003). Just recently was shown that the *C. jejuni* Dps has DNA binding ability in the presence of H_2O_2 and Fe^{2+}, thus protecting DNA from the nefarious effects of H_2O_2 (Huergo *et al.* 2013).

A truncated globin (Ctb) was identified in *C. jejuni* as important to bacteria survival even under microaerophilic conditions, the *ctb* mutant showed a slower growth when compared with the wild type protein (Wainwrigh *et al.*, 2005).

Although *C. jeujuni* seems to be lacking siderophores (iron chelators exported by microorganisms (Pi *et al.*, 2012)) it is able to use siderophores from other bacteria present in the bowel and iron is then transported to the cell by a ferric-enterobactin (CfrA). Furthermore, *C.jejuni* is able to use the heme group from exogenous proteins through the heme uptake system ChuABCD (Butcher *et al.*, 2010).

All these ROS detoxifying systems need to be tightly regulated. Contrarily to other bacteria *C. jejuni* lacks the regulators OxyR and SoxR, respectively involved in hydrogen peroxide and superoxide sensing. Instead, this bacterium possesses the PerR protein, usually found in Gram-positive bacteria, which is an hydrogen peroxide regulator (Butcher *et al.*, 2010) The iron uptake also needs to be carefully controlled since it is involved in the generation of the dangerous hydroxyl radical. This is regulated by the ferric uptake regulator (Fur), a member of the PerR family. Fur is a repressor that in the presence of ferrous iron Fur binds itself to the promoter of iron uptake genes and inhibits their transcription (Palyada *et al.*, 2004). Fur also represses genes involved in ROS detoxifications (*katA*, *ahp*C) (Table 1.1) (Butcher *et al.*, 2010). This last result seems contradictory given that iron is tightly connected to the formation and elimination of ROS via the Fenton reaction and by its role in detoxifying enzymes, respectively. So under iron rich conditions an over expression in iron-containing proteins would be expected to avoid the dangers of free iron in the cell.

PerR works by inhibiting the transcription of genes involved in oxidative stress response. Its own expression is iron-dependent but not H_2O_2 dependent and is auto regulated by binding to the *perR* promoter (Kim, *et al.*, 2011). In the absence of iron Apo-PerR is unable to bind to the promoter region in the DNA resulting in induction of oxidative stress resistance genes, even in the absence of ROS (Butcher *et al.*, 2010)

The implication of PerR in H_2O_2 resistance is corroborated by studies where a strain lacking *perR* is more resistant to H_2O_2, due to continuous transcription of *katA* and *ahpC* (Palyada *et al.*, 2009).

Due to the close relation between iron and oxidative stress several genes are co-repressed by PerR and Fur (Figure 1.9).

In a *fur* mutant c*j0012c* transcription is activated under iron rich conditions and is repressed in the absence of iron. In the wild type strain its transcription is also decreased when iron is not available (Butcher *et al.*, 2012; Holmes *et al.*, 2005). Furthermore *cj0012c* is also repressed by PerR (Palyada *et al.*, 2009), which is in agreement with the results shown by Yamazaki *et al.* that observed unchanged levels of *cj0012c* transcripts in the presence of hydrogen peroxide.

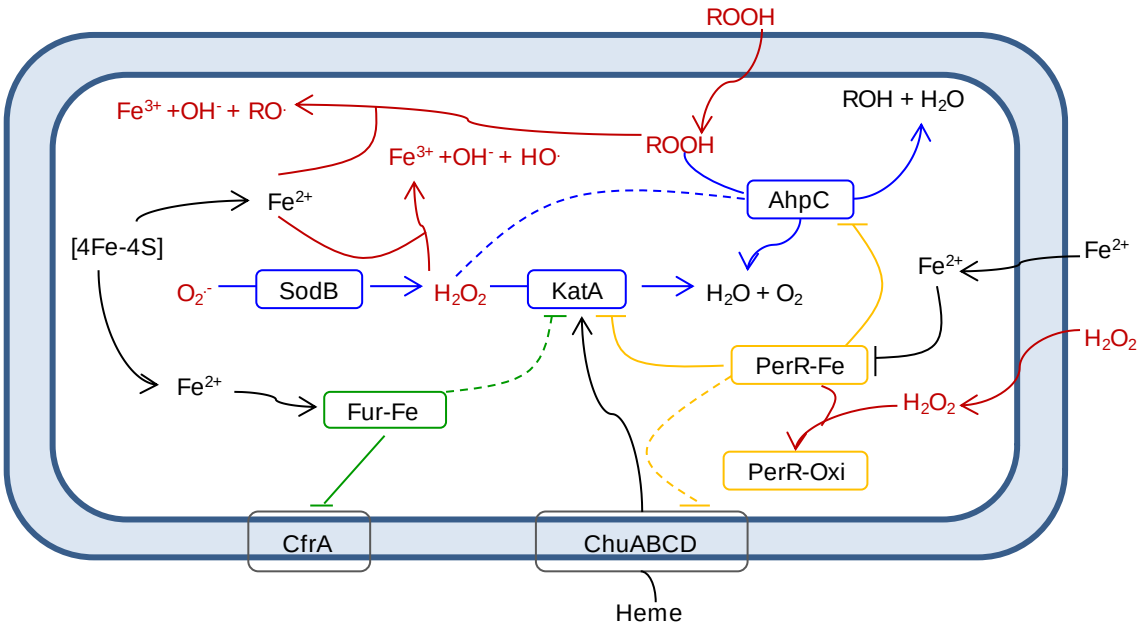

Figure 1.9: Simplified representation of oxidative stress regulation in *Campylobacter jejuni*. Anti-oxidant systems are in blue coloured boxes; oxidants species are coloured in red; Fur is coloured in the green box; Per-R is in the yellow coloured box. Full trace lines represent primary repression and dashed lines represent secondary repression. Adapted from Palyada *et al.*, 2009.

Table 1.1: Example of genes up and down regulated by Fur, PerR and iron. The signals "-" and "+" stand for repression or activation, respectively. Adapted from Butcher *et al.*, 2010.

Gene name and category	Fur-Fe	Fur+Fe	Fe	PerR-Fe	PerR+Fe
Iron transport					
cfrA		-	-		
chuABCD		-	-	-	
Oxidative stress defense					
ahpC		-	-	-	
cft			-		
katA		-	-	-	-
rrc	-	+	+		-

1.3.2. Pathogenesis mechanisms

Approximately 90% of the campylobacteriosis cases are due to *Campylobacter jejuni* and the other cases are almost entirely attributed to *Campylobacter coli*.

Based on the symptoms two disease mechanisms are hypothesised: adherence of the bacteria to the intestine and production of toxins or invasion and replication inside the host cells which will initiate an inflammatory disease. In the first case the symptoms include watery diarrhea, while in the second bloody diarrhea (Janssen *et al.*, 2008).

Colonization of the host occurs in the small bowel and in the colon (Altekruse *et al.*,1999). The first barrier that the bacteria should overcome is the acidic environment of the stomach, followed by the barrier of the gastrointestinal tract, namely the mucus layer. The bacteria overpass the mucus layer thanks to their corkscrew shape, motility and chemotaxis (Altekruse *et al.*, 1999; Young *et al*., 2007; Kassem *et al.*, 2012). To fulfil the colonization process the bacteria must adhere to the epithelial cells through membrane proteins. Several proteins are involved in cell adherence: CadF, CapA, PEB1 and JlpA (Dasti *et al.*, 2010). CadF is also required for cell invasion in a fibronectin dependent way. Mutants in CadF and JlpA have shown impaired ability to invade several cell lines *in vitro* and are also less prone to colonize chicken gut (Dasti *et al*., 2010; Young *et al.*, 2007).

More than being involved in motility the flagella also seem to be important for cell invasion and toxicity. The flagellar filament is composed by two proteins: FlaA and FlaB. Deletion studies in a human clinical strain showed that deletion of *flaA* results in impaired motility and invasion, but the adherence ability of the bacteria was enhanced. The double mutant in *flaA* and *flab* showed even a greater adherence improvement but the invasion was poorer than in the *flaA* mutant. (Konkel *et al.*, 2004).

The secretion mechanisms are not yet clear, but no type III secretion system was identified. It is believed that secretion is dependent on the flagellar machinery due to homology of secreted proteins with flagellins. These secreted proteins are named *Campylobacter* invasion antigens (Cia) and their functions are still unknown. The secretion pathway via flagellum is corroborated by mutagenesis studies. In the mutant *flaAflaB* no secretion of this CiaB was detected although the protein was expressed (Konkel *et al.*, 2004). This highlights the importance of the flagellar apparatus in secretion and consequently on the disease.

The only toxin identified so far in *C. jejuni* is the cytolethal distending toxin (CDT) which is also found in other species in the same genus and in *Escherichia coli*. CDT is a holotoxin composed of smaller proteins: CdtA, CdtB and CdtC. This toxin arrests the cellular cycle at G2 phase and causes cell distension. CdtB is responsible for the protein activity, while CdtA and CdtC probably play a role in the uptake by the host cells but there is no evidence if these subunits enter the cell or not. The sequence of the CdtB subunit showed similarity with DNase-I like proteins, and CdtB was showed to have DNase activity in plasmidic DNA (Ohara *et al.*, 2004).

The mechanism by which CDT is exported from the bacterial cell is unknown but one study suggests that outer membrane vesicles (OMV) may be a vehicle for toxin export (Lindmark *et al.*, 2009). CdtB is probably translocated to the nucleus of the host cell via via retrogade transport (Young *et al.*, 2007).

1.4. *Campylobacter jejuni*, ROS and the immune system response

The role of ROS in the immune system concerns both the innate and acquired immunity.

After ingestion of microorganisms by phagocytic cells a “respiratory burst” takes place inside the phagolysosome. This process starts with the production of $O_2^{\cdot-}$ by the NADPH oxidase enzyme present in the phagossome membrane (NOX2) that transfers electrons from NADPH to two O_2. As seen in section 1.1, $O_2^{\cdot-}$ production will lead to production of several oxidant molecules, namely H_2O_2 and $HO^{\cdot}$. The hydrogen peroxide can also be converted in hypoclorous acid, a strong oxidant, by mieloperoxidase or eosinophil peroxidase (Winterbourn, 2008) (Figure 1.10). These molecules will hopefully cause serious damage in the pathogenic bacteria. The importance of NOX is corroborated by a reduced resistance to infections in mice lacking NOX subunits (Alfadda and Sallam, 2012;, Droge, 2002). Besides, NOX1 is present at the cellular membrane and transfers electrons to O_2 present at the outside of the cell (Winterbourn, 2008), allowing to fight bacteria that resist phagocitosis.

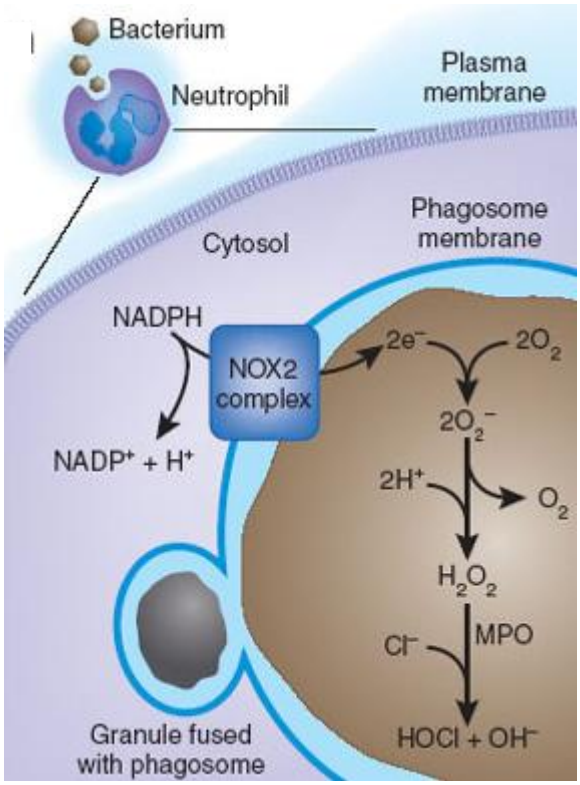

Figure 1.10: NOX role in generation of ROS in phagosomes. NOX generates $O_2^{\cdot-}$ that dismutes into H_2O_2. Myeloperoxidase converts hydrogen peroxide in hypochlorous acid. Image from Winterbourn, 2008.

The role of ROS goes beyond this non-selective response. The production of ROS at the infection local decreases the threshold activation of T -lymphocytes due to amplification in signalling cascades (Figure 1.11) (Kaakoush *et al.*, 2007).

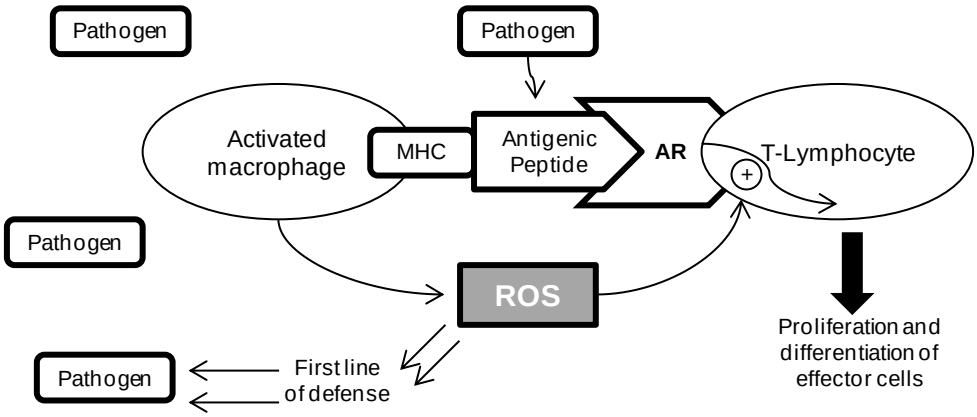

Figure 1.11: Importance of ROS in the immune system. ROS production by activated macrophages is a non-specific defence against invading pathogens. ROS also play an important role in activation of T-lymphocytes along with pathogen determinants presented by Major Complex of Histocompatibility (MHC) molecules. (Adapted from Droge, 2002)

After interaction of *C. jejuni* with epithelial cells cytokine production is induced, namely IL-8. IL-8 secretion leads to recruitment of dendritic cells (DCs), macrophages and neutrophils (Zheng *et al.*, 2008).

Dendritic cells (DC) seem to play a fundamental role in the immune response to *C. jejuni* activation. Based on *in vitro* results *C. jejuni* is rapidly internalized by DC promoting the DCs maturation verified by expression of coestimulatory molecules (CD40, CD80 and CD86) (Hu *et al.*, 2006). In the same study production of cytokines by infected DC was also observed, especially IL-8 and TNF-α (Tumor Necrosis Factor α) as well NF-κB (Nuclear Factor-κB) activation. The activation of DCs is extremely important to stimulate naive T cells through antigen presenting. The same study also points LOS as one important feature in cytokine production (Young *et al.*, 2007).

The production of IL-8 by epithelial cells seems to be dependent of the flagellum and the CDT given that mutants in one of these features are less efficient in promoting IL-8 secretion. Furthermore this secretion also seems to be dependent of NF-κB activation (Figure 1.12) (Zheng *et al.*, 2008).

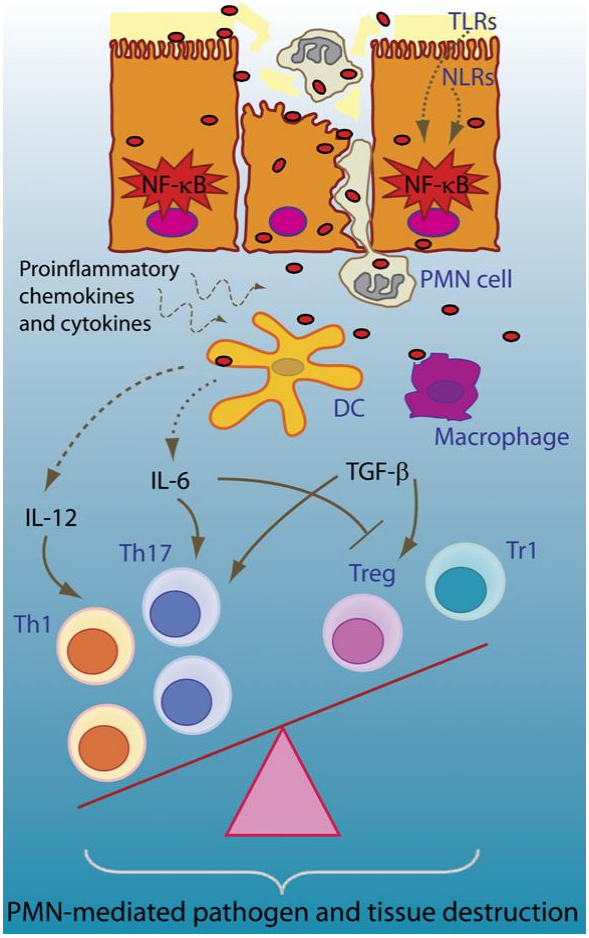

Figure 1.12: Representative scheme of pathological inflammation. This response of the immune system is triggered by "pathogen-associated molecular motifs (PAMP)". Bacterial cells interact with the epithelium inducing realising of pro-inflamatory cytokines (CXCL20, IL-8). This leads to the recruitment of dendritic cells (DCs), macrophages and neutrophils. The internalization of the bacteria by DCs will initiated the activation of the NF-κB via. Image from Sansonetti and Santo, 2007.

2. MATERIALS AND METHODS

Unless stated otherwise all procedures were performed with wild type and DRbr mutants.

2.1 Strains and resistances

Competent *Escherichia coli* strain BL21DE3GOLD cells were used to over express the proteins under study. In the expression assays BL21DE3 and STAR strains from *E. coli* were also used.

2.2 Gene cloning

The pMAL system from New England Biolabs was used for cloning the gene *cj0012c* from *C. jejuni* NTTC11168 with and without the desired mutations. The clone for the wild type protein was provided by Yamazaki M.[1,2], Amano F.[2] and Ignimi S[3].

The clones for the mutant proteins were done by Pinto, A. using the Quick Change Multi-Site Directed Mutagenesis Kit from Agilent Technologies. The residues chosen for mutation were tyrosines 59 and 127. In two mutants one of the residues was replaced by a phenylalanine and in a third both tyrosines were replaced, also by two phenylalanines.

2.3 Cells transformation

Competent *E. coli* BL21DE3 GOLD cells were transformed with plasmids containing the gene for the wild type or mutant proteins. To 100 μL of competent cells were added 2 μL of plasmid at *c.a.* 83 ng/μL. The mixture was incubated in ice for 30 minutes. Afterwards cells were heated at 42ºC during 20 seconds and then immediately put in ice for 2 more minutes. To the cells were added 900 μL of lysogeny broth (LB) medium (Table 2.1) and the mixture was incubated for 1 hour at 37ºC with shaking. Cells were harvested by centrifugation and resuspended in 100 μL of supernant before plating in LB agar (LA) medium (Table 2.1) supplemented with 100 μg/mL ampicilin. The plates were incubated at 37ºC overnight.

Table 2.1: Instructions for LB and LA media preparation.

Components	LB medium (Adjust pH to 7.0)	LA medium
Tryptone	10 % (w/v)	10 % (w/v)
Yeast extract	10 % (w/v)	5 % (w/v)
NaCl	10 % (w/v)	10 % (w/v)
Agar	-	5% (w/v)

[1] Faculty of Agriculture, Tokyo University of Agriculture and Technology, Japan
[2] Department of Hygienic Chemistry, Osaka University of Pharmaceutical Sciences, Japan
[3] Division of Biomedical Food Research, National Institute of Health Sciences, Japan

2.4 Protein expression tests for DRbr mutants

A few colonies from the LA plates were used to inoculate 25 mL of LB medium with 100 μg/mL ampicilin. Cells were grown at 37ºC until the optical density (OD) at 600 nm reached 0.6. Then 250 μM of isopropyl-1-thio-β-D-galactopyranoside (IPTG) was added. After 4 hours cells were harvested by centrifugation at 5000 g during 10 minutes at 4ºC. Two samples were analyzed, corresponding to the cells before and after induction. Both samples were disrupted by freezing/thawing cycles with liquid nitrogen. The levels of protein in the soluble fraction were evaluated by sodium dodecyl sulfate polyacrylamide gel electrophoresis (SDS-PAGE).

2.5 Expression of the recombinant DRbr and DRbr mutants

A pre-inoculum of 100 mL with 100 μg/mL of ampicilin was prepared overnight at 37ºC, from fresh colonies (prepared plate).

Over-expression of DRbr and mutants was achieved by growing the cells aerobically at 37ºC in M9 minimal medium supplemented with 20 mM glucose, 400 μM $FeSO_4$ and 100 μg/mL ampicilin. The medium was inoculated with 1% from the pre-inoculum. At OD_{600} of 0.3 it was added 250 μM IPTG. Cells were grown overnight and then the cells were harvested by centrifugation at 7000 g during 10 minutes and 4ºC and then stored at -20ºC.

Minimal medium M9 was prepared accordingly the following instructions: for 1 litre of medium 5 times concentrated the following quantities were dissolved in deionized water: 64 g of $Na_2HPO_4.7H_2O$, 15 g of KH_2PO_4, 2.5 g of NaCl and 5 g of NH_4Cl.

2.6 Recombinant proteins purification

The purification process was performed in anaerobic conditions in a Coy glove box under an atmosphere of approximately 95% argon and 5% hydrogen at room temperature. All buffers were previously degassed and the atmosphere was replaced with nitrogen, prior to their introduction in the glove box

The cells were unfrozen and washed in a buffer containing 10 mM Tris-HCl H 7.2 for three times, then were harvested by centrifugation and resuspended in a buffer containing 50 mM Tris HCl pH 8, 100 mM NaCl, 1 mM $MgCl_2$, 0.1 mg/mL lysozyme and 20 μg/mL DNase I. The cellular extract (supernatant) was obtained by passing the cells three times through a French Press at 35 000 psi. Soluble fraction was collected after ultracentrifugation the cellular extract at 125 000 g for 1 hour at 4ºC. The atmosphere of the soluble extract was replaced with nitrogen and applied in a Q-Sepharose Fast Flow column XK 26 (XK26/20, GE Healthcare) equilibrated with 20 mM Tris-HCl pH 7.2. The protein was eluted with a linear gradient from 0 to 1 M NaCl at 2 mL/min. The DRbr and its mutants eluted between 0.2 M and 0.3 M NaCl and were then dialyzed overnight against 10 mM KPi pH 7.2. This fraction was subsequently applied in a Bio-gel hydroxyapatite (HTP) type II (XK 16/20 GE Healthcare) column previously equilibrated with 10 mM KPi pH 7.2. The protein was eluted with a

linear gradient from 10 mM to 1M of KPi pH 7.2. Fractions containing the protein were collected at approximately 0.3 M of KPi pH 7.2 and concentrated to a maximum volume of 2 mL in a Diaflo (Amicon) using a YM30 membrane. Finally the protein was applied to a Superdex-200 (XK 16/170, GE Healthcare) column equilibrated with 20 mM Tris-HCl pH 7.2 and 150 mM NaCl and eluted with the same buffer. The final fraction was concentrated using a Diaflo (Amicon) and stored at -20ºC in anaerobic conditions.

The purity of the final fractions was accessed by 15% SDS-PAGE.

2.7 Electrophoretic analysis

All SDS-PAGE analysis were performed in a 15 % gel with 1 mm thickness. The solution components and volumes are listed in Table 2.2

Table 2.2: Instructions for preparation of SDS-PAGE gels. Components and volumes for preparing one resolving 15% SDS-PAGE gel and one stacking 5% SDS-PAGE gel.

Solution components	Stacking gel (mL)	Resolving gel (mL)
30% Acrylamide mix	0.67	5
1.5 M Tris-HCl pH 8.8	-	2.5
1 M Tris-HCl pH 6.8	500	-
Deionised Water	2.7	2.3
10% SDS	0.04	0.1
10% Ammonium persulfate (APS)	0.04	0.1
N, N, N', N'-tetramethylethylenediamine (TEMED)	0.004	0.004

The electrophoresis were performed with a BioRad MiniProtean system and a power supply from Amershan Biosciences at 180 V during approximately one hour. The running buffer contained 0.6 % (w/v) Tris-(hydroxymethyl) aminomethane (Tris), 4 % (w/v) glycine and 0.2 % (w/v) SDS. The pH was adjusted to 8.3 with HCl.

The molecular weight of the samples was inferred from the low molecular mass markers from GE Healthcare.

Sample visualization was achieved by staining the gel in a solution containing 0.1% Coomassie G, 50% methanol and 10 % acetic acid for approximately 30 minutes. Next the gel was submersed in a destaining solution with 40 % acetic acid and 10 % methanol for 30 minutes. The gels were left in water overnight.

Depending upon the origin of the sample to analyze, its pre-treatment was different.

Induced *versus* non-induced cells: 1 mL of culture media before and after induction was centrifuged to collect the cells. Next, 30 µL of Loading Buffer with urea (Table 2.3Table 2.4) was added to resuspend the pellet and the mixture was heated at 100 ºC during 5 minutes. Finally the mixture was centrifuged for 2 minutes at 14 000 g and 15 µL of the supernatant were applied in the gel.

Soluble *versus* non-soluble fraction: 2 mL of culture media was collected after finishing the protein expression tests or the growths and centrifuged to collect the cells. Cells were lysed by adding 500 µL of lysis buffer (Table 2.4) and by doing freezing/ thawing cycles with liquid nitrogen. The mixture was centrifuged and the supernatant was collect and once more centrifuged. The supernatant and the pellet were both collected corresponding to the soluble and non-soluble fractions respectively; to both were added 30 µL of Loading Buffer with urea and applied in the gel after heating at 100 ºC for 5 minutes and centrifuged at 14 000 g.

Table 2.3: Solution components for preparing loading buffer with and without urea.

Solution components	Loading buffer with urea (2x)	Loading buffer (2x)
500 mM Tris-HCl pH 8.0	4 mL	-
500 mM Tris-HCl pH 6.8	-	1.5 mL
SDS	0.8 g	0.8 g
Glycerol (88%)	4.6 mL	2.5 mL
β-mercaptoethanol	400 µL	500 µL
Bromophenol blue	0.04 g	0.04 g
Urea	4.8 g	-
Water	-	4.25 mL

Table 2.4: Components and respective concentrations of the lysis buffer.

Lysis buffer
50 mM Tris-HCl pH 8.0
20 % (w/v) sucrose
100 mM NaCl
1mM $MgCl_2$
0.1 mg/mL lysozyme
20 µg/ mL DNase I

Protein samples: To 15 μL of sample 15 μL of Loading Buffer were added (Table 2.3). The mixture was heated at 100º C during 5 minutes, centrifuged at 14 000 g and applied in the gel.

2.8 Determination of protein and iron concentration

Protein concentration was determined using the bicinchoninic acid (BCA) (Pierce) method and the iron content was assayed using 2, 4, 6-tripyridyl - 1, 2, 3-triazine (TPTZ) method and by Inductevily Coupled Plasma Atomic Emission spectroscopy (ICP). The zinc content was also determined by ICP. The ICP was performed at REQUIMTE Analysis Laboratory at Faculdade de Ciências e Tecnologia da Universidade Nova de Lisboa.

For the BCA method were prepared 8 tubes with BSA (Bovine Serum Albumin) concentrations between 0 and 1 mg/mL, plus the samples tubes. To each tube was added 1 mL of BCA solution previously prepared by mixing 50 parts of reagent A (Bicinchonic acid and tartrate in an alkaline carbonate buffer) with one part of reagent B (4% copper sulfate pentahydrate). This method is based in the chelation of Cu^{1+} with protein in an alkaline buffer, the biuret reaction, which forms a light blue complex. The second step is the reaction of the BCA reagent with the Cu^{1+} to yield a purple product, which increases the sensitivity of the method 100 times when compared with the traditional biuredtmethod. After 30 minutes incubation on the dark the absorbance at 562 nm was registered. The calibration and the samples were prepared in triplicates.

For the TPTZ method a calibration was performed by preparing tubes with iron concentrations between 0 and 25 μM. The tubes with the samples were also prepared by diluting a small amount (≈5 μL) with water. To all tubes was added 100 μL of 8 M HCl followed by mixing in the vortex to remove the iron from the protein. Next, 100 μL of a solution of TCA (Trichloroacetic acid) 80% was added to precipitate the protein and the mixture was again homogenised in the vortex. The standards and the samples were centrifuged during 10 minutes at 14 000 g and 800 μL of supernatant were transferred to a new vial. To each tube was added 200 μL of 75% of ammonium acetate to set the pH around 4.5 and 80 μL of 10% ammonium hydroxide which reduces the iron to ferrous. The solutions were mixed and finally 80 μL of 4 mM of TPTZ was added. After incubation for 10 minutes in the dark, the absorbance was measured at 593 nm (Fischer and Price, 1964).

2.9 Molecular mass determination

The molecular mass in solution was determined by size exclusion chromatography with an analytical Superdex 200 column (10/300 GE Healthcare). The column was equilibrated with 50 mM KPi pH 7.2 with 150 mM NaCl. A calibration was performed in which the following commercial proteins were used: aprotinin (Mm = 6500 Da), myoglobin (Mm = 17600 Da), chymotrypsinogen (Mm = 25 000 Da), albumin (Mm = 66 000 Da), canalbumin (Mm = 76 600), aldolase (Mm = 158 000 Da), catalase (Mm = 240000 Da) and ferritin (Mm = 440 000 Da). Dextran blue (Mm = 2 000 000 Da) was used in all standards and samples as internal control.

2.10 N-terminal sequencing

All solutions used in the protocol for N-terminal sequencing were prepared with ultra pure MiliQ water except TEMED.

To perform the N-terminal sequencing a sample of protein was applied in 15% SDS - acrylamide gel. The running buffer was prepared with 1.5 % (w/v) Tris, 7.2 % (w/v) glycine, 25 mL 0.5 % (w/v) SDS and the pH was set to 8.3. All solutions were prepared following the instructions in section 2.7.

A pre-run with 40 μM glutathione added in the cathode was performed at 100 V during 2 hours. Subsequently the buffer inside the cathode was removed and new buffer was added, alongside 6 μL of thioglycolic acid. The sample was applied and the run was performed at 150 V during approximately one and a half hour. The run was tracked by the addition of molecular mass marker pre-coloured from Bio-Rad.

The transference to a PVDF membrane with 0.2 μm pore was performed using a Trans-Blot SD semi-dry transfer cell at 15 Volts for 20 minutes at room temperature. The transference buffer was 1 x CAPS (Cyclohexylamino propanesulphonic acid) (w/v) and 10 % methanol (v/v). Before the transference the membrane was activated in 100 % methanol for 15 seconds followed by washing with water for 5 minutes and finally was submersed in transference buffer. The gel and the filter paper were also submersed in transference buffer immediately before the assembly of the system.

To visualize the bands corresponding to the samples the membrane was submersed in a solution of Coomassie R followed by alternate washing with water and a solution of 50 % methanol.

The sequencing was performed at the Analytical Laboratory, Analytical Services Unit, Instituto de Tecnologia Química e Biológica, Universidade Nova de Lisboa.

2.11 Spectroscopies

UV-Vis spectra, as well all spectrophotometric data, were collected with a Shimadzu UV-1603 or Shimadzu UV-1700 spectrophotometers.

EPR spectra were acquired with a Bruker EMX spectrometer, equipped with an ESR 900 continuous-flow helium cryostat from Oxford Instruments.

2.12 Redox titrations

Redox titrations were analysed by EPR spectroscopy and performed under argon at room temperature. At appropriate potentials a sample was collected into an EPR tube and immediately frozen in liquid nitrogen. The assays were performed in 50 mM Tris-HCl pH 7.2 by stepwise addition of sodium dithionite as a reducing agent. The protein final concentration was 80 μM as well the following redox mediators: potassium ferricyanide (E'0 = +430 mV), N,N dimethyl-pphenylenediamine (E'0 = +340 mV), tetramethyl-p-phenylenediamine (E'0 = +260 mV), 1,2-naphtoquinone-4-sulphonic acid (E'0 = +215 mV), 1,2-naphtoquinone (E'0 = +180 mV), trimethylhydroquinone (E'0 = +115mV), 1,4-naphtoquinone (E'0 = +60 mV), menadione (E'0 = 0 mV), plumbagin (E'0 = -40 mV), indigo trisulphonate (E'0 = -70 mV), phenazine (E'0 = -125 mV), 2-hydroxy-1,4-naphtoquinone (E'0 = -152

mV) and anthraquinone-2-sulphonate (E'0 = -225 mV). The electrodes were previously calibrated with a saturated quinhydrone solution at pH 7.0. All data were analyzed using the Nernst equation and the reduction potential values are reported in relation to the standard hydrogen electrode.

2.13 Reconstitution of the binuclear centre

The procedures were performed in an anaerobic chamber under an atmosphere of argon.
To 100 µM of DRbr Y127F sample in 20 mM Tis-HCl with 150 mM NaCl were added 2 M of dithiothreitol (DTT) and 300 µM of Fe^{2+} (Ammonium iron (II) sulfate hexahydrate). The mixture was incubated during 30 minutes and then 50 µL of sample were applied in a desalting column (Micro Spin 6 from Bio-Rad) and eluted in the sample buffer by centrifugation at 1000 g during 4 minutes. The binuclear centre reconstitution was assessed by EPR.

2.14 Protein crystallization

Proteins were dialyzed against 100 mM MES pH 6.2 with 500 mM NaCl and then concentrated to *c.a.* 25 mg/mL using a Vivaspin of 10 kDa from Startorius.

The first trials were done using a Cartesian Crystallization Robot Dispensing System (Genomics Solutions) and round-bottom Greiner 96-well CrystalQuick^{TM} plates. This allowed the use of protein quantities at the nanolitre scale. Structure Screen 1 & 2 HT-96 from Molecular Dimensions was used and the plate remained at 20ºC as well all the plates that would follow.
Crystals appeared when the crystallization solutions included 0.1 M Hepes pH 7.5, 0.1 M, Bicine pH 9 or 0.1 M Tris-HCl pH 8.5. To improve the crystals quality the hanging-drop vapor diffusion technique was used. In these trials crystals appeared only when the buffer was Hepes, so the optimization proceeded only with this buffer. The optimization followed varying the type and concentration of precipitant agents (several PEGs - Polyethylene glycol, isopropanol and glycerol) and also with the additive TCEP (Tris-(2-Carboxyethyl)phosphine hydrochloride), but the later did not improve the results.

The selected crystals were frozen in liquid nitrogen in the reservoir solution plus 20% glycerol as cryo-protectant. Some crystals were also incubated with 10 mM H_2O_2 or 50 mM sodium dithionite as reductant or oxidant, respectively. The crystals were tested at the ALBA synchrotron in Barcelona, Spain.

3 RESULTS

3.1 Protein expression tests for the Desulforubrerythrin mutants

The expression tests were performed in LB medium at 37ºC. The cells were induced with IPTG and harvested after 4 hours. The samples corresponding to non-induced and induced cells were analyzed by a 15% SDS-PAGE gel. The location of the protein in the induced samples was also analyzed (soluble fraction and pellet that includes membranes and inclusion bodies) (Figure 3.1.)

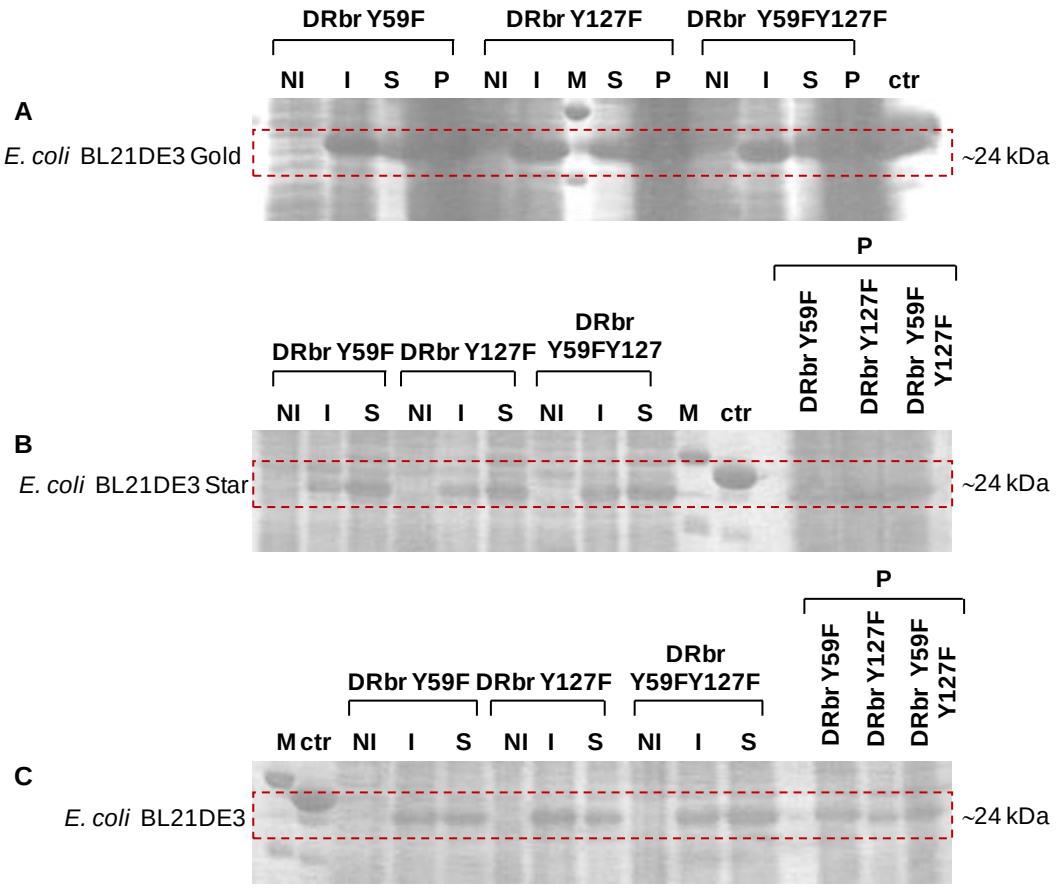

Figure 3.1: SDS-PAGE of non-induced and induced cell samples of the protein expression tests for DRbr mutants. **(A)** Mutant proteins expressed in *E. coli* BL21DE3 Gold. **(B)** Mutant proteins expressed in *E. coli* BL21DE3 Star **(C)** Mutant proteins expressed in *E. coli* BL21DE3. NI: Non-induced cells; I: Induced cells; S: Soluble fraction; P: Pellet (non-soluble fraction); ctr: DRbr WT previously purified.

As can been seen in Figure 3.1 all proteins were successfully over expressed in all cellular strains tested. Given that the wild type protein had already been over expressed in *E. coli* BL21DE3 Gold cells this was the strain chosen to express the mutant proteins.

3.2 Proteins expression

The cells were grown in minimal medium supplemented with iron and induced with IPTG when the O.D. at 600 nm reached 0.3. Each growth was performed in erlenmeyers of 2 litres capacity filled with 1 Litre of medium and 1% of pre-inoculum. Cells were grown overnight and were harvested by centrifugation. Samples of the non induced and induced cells were analyzed by 15% SDS-PAGE (Figure 3.2). For each protein were performed two independent growths. Given that all procedures were the same and the results were very similar, here will be presented only one example of one growth for each protein.

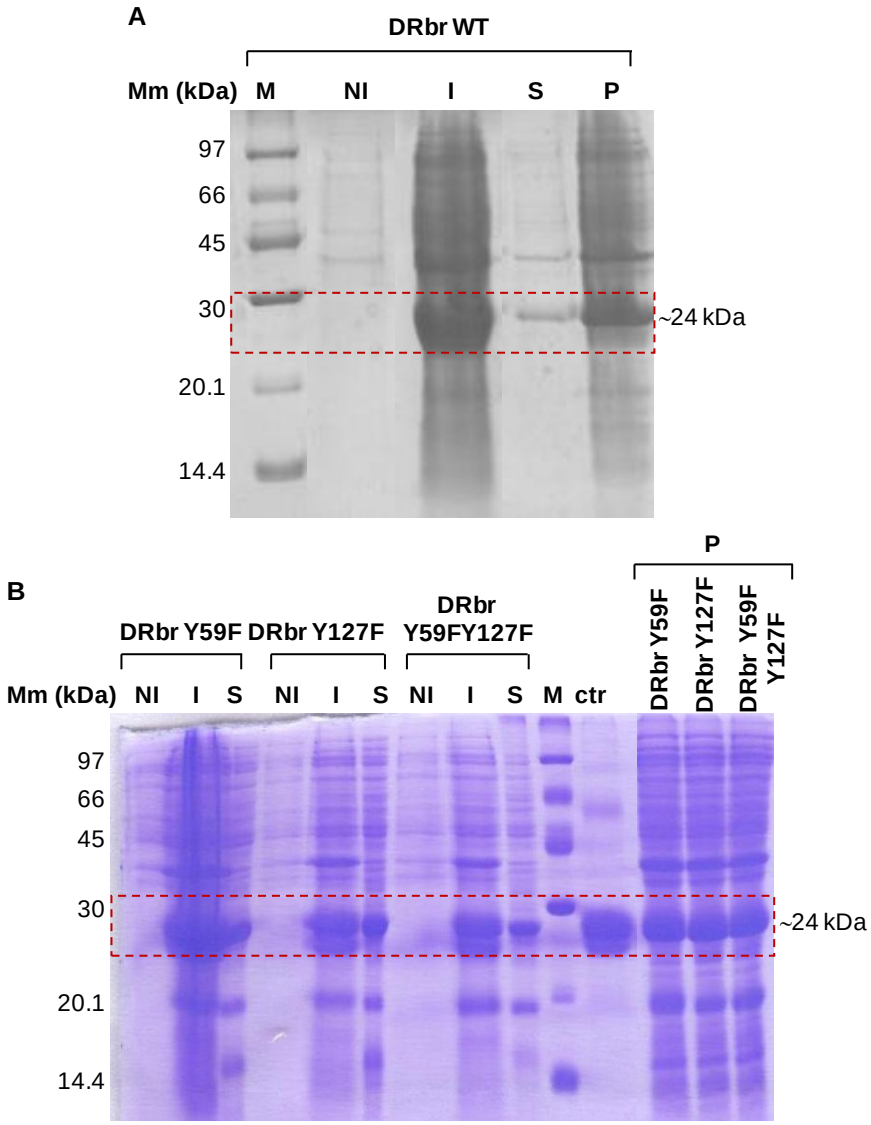

Figure 3.2: SDS-PAGE of samples from protein expression. **(A)** DRbr WT and **(B)** DRbr mutants in non-induced (NI) and induced (I) cells: soluble fraction (S) and pellet (P). ctr: Wild type protein previously purified.

As can be seen in Figure 3.2, all proteins were over expressed and are present in both soluble and non soluble fraction.

3.3 Biochemical characterization

3.3.1 Protein purification

After harvesting the cells and collecting the soluble fraction all proteins were purified in an O_2 free atmosphere. Since the protocol was always the same and the results were also very similar next will be presented one example for each protein.

Wild type desulforubrerythrin

After ultracentrifugation the soluble fraction was applied to a Q-Sepharose FF column and eluted with 20 mM Tris-HCl pH 7.2 plus a linear gradient from 0 to 1 M NaCl. The selection of fraction was based on the chromatogram and on the colour of the protein eluted. The oxidized protein is pink or red depending on its concentration, but when reduced it is colourless. After eluting the Q-Sepharose column the protein is in the reduced state. To ascertain its localization 2 μL of sample corresponding to the chromatograms peaks were removed from the glove chamber. After exposure to O_2 the protein reoxidizes and its identification was made by analyzing the colour of the sample. The protein eluted between 0.2 and 0.3 M NaCl. This fraction was dialyzed overnight at 4ºC against 10 mM KPi pH 7.2 and was applied in a HTP column. After this step the protein was oxidized making possible its prompt identification by the colour of the fractions. The protein was eluted with a linear gradient from 10 mM to 1 M KPi pH 7.2 and the fraction containing the protein eluted at approximately 0.3 M KPi. This fraction was concentrated to a maximum volume of 2 mL using a Diaflo and was applied in a size exclusion column and eluted with 20 mM Tris-HCl pH 7.2 with 150 mM NaCl; the retention time of the protein was around 150 minutes. After this step the protein was considered pure and was stored at -20 ºC in aliquots of 500 μL.

During the purification, samples from the eluted fractions containing protein were stored and afterwards were applied in a 15% SDS-PAGE gel to evaluate the efficiency of the process. The chromatograms and the gel can be seen in Figure 3.3

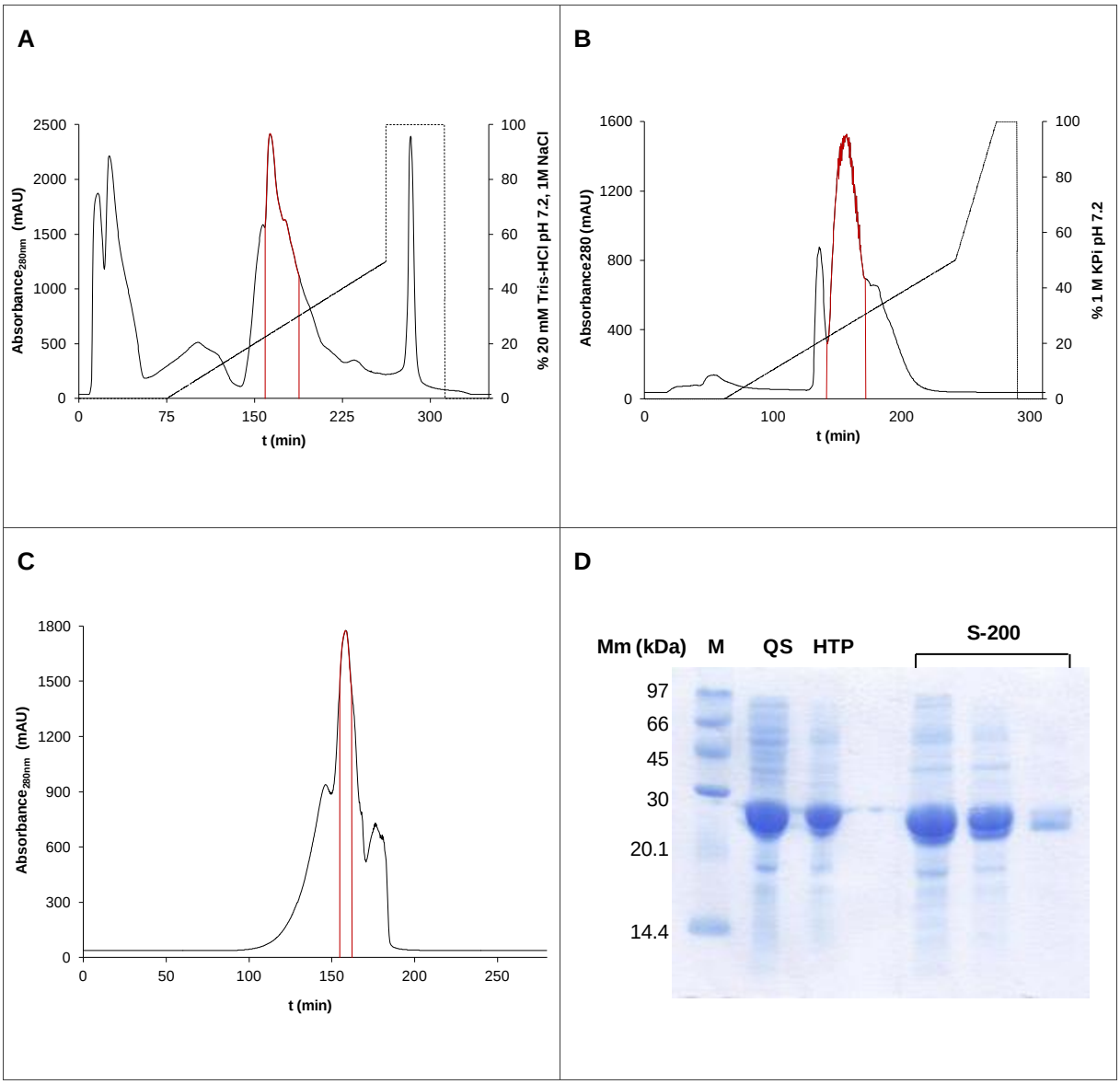

Figure 3.3: Resume of WT DRbr purification. **(A)** Chromatogram of the elution of the soluble fraction from the Q-Sepharose FF column. The solid black line corresponds to the absorbance at 280 nm and the dashed line is the percentage of 20 mM Tris-HCl pH 7.2 with 1 M NaCl. **(B)** Elution of the sample from the Q-Sepharose FF column in the HTP column. The solid black line corresponds to the absorbance at 280 nm and the dashed line is the percentage of 1 M KPi pH 7.2. **(C)** Chromatogram showing the DRbr WT elution profile in the size exclusion column. The solid black line corresponds to the absorbance at 280 nm. The red line corresponds to the elution of DRbr WT. **(D)** SDS-PAGE with samples of each eluted fraction containing DRbr WT. In the last step of the purification were obtained three fractions containing the protein. The peak line coloured in red in panel C corresponds to the elution of the sample shown in the last lane of the gel presented in panel D.

Desulforubrerythrin mutants

The procedure to purify the DRbr mutants was equal to that of the DRbr WT procedure. The elution profiles were also very similar. The chromatograms and the gels are shown in Figures 3.4, 3.5 and 3.6, respectively for DRbr Y59F, DRbr Y127F and the double mutant.

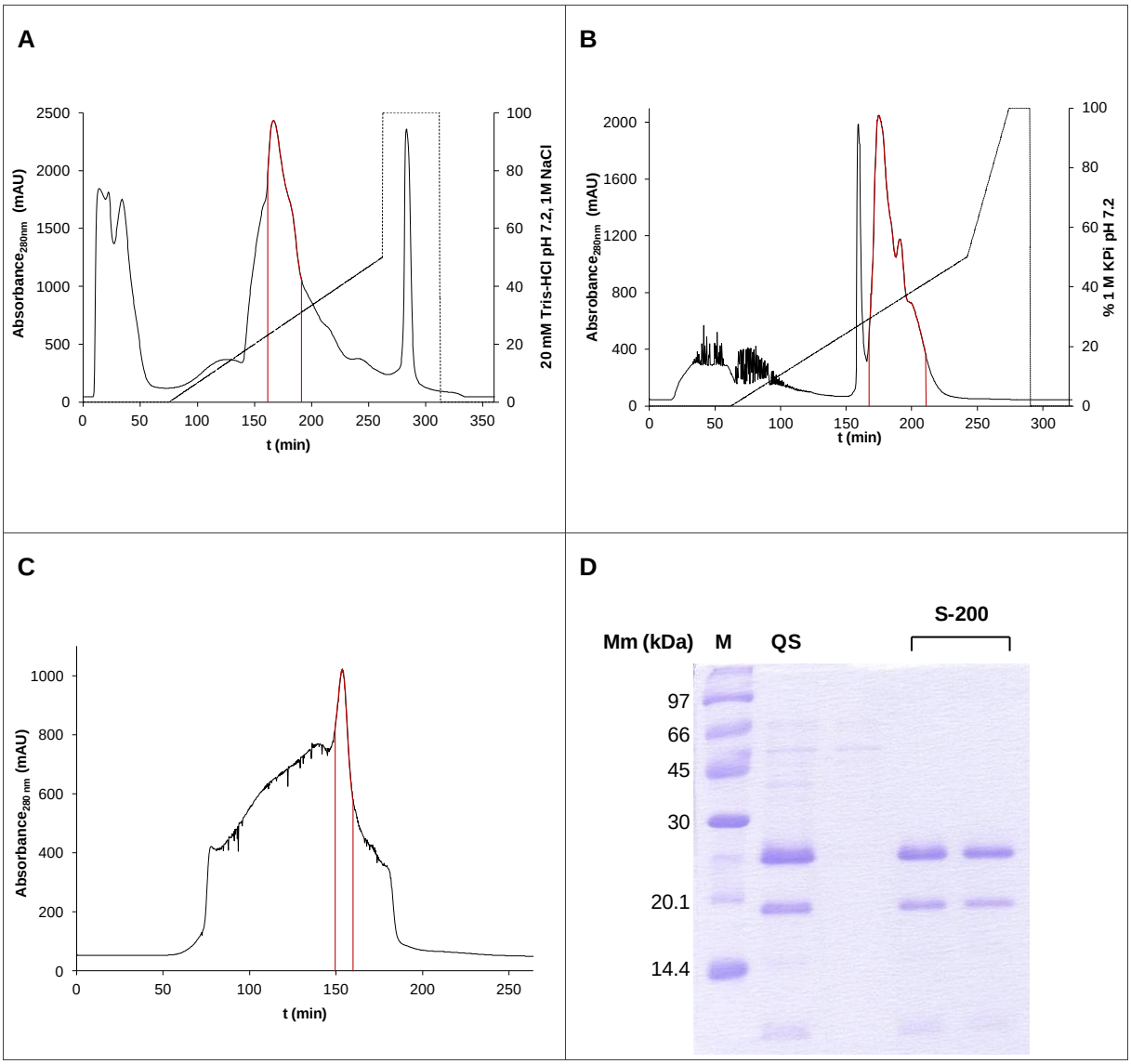

Figure 3.4: Resume of the DRbr Y59F purification. **(A)** Chromatogram of the elution of the soluble fraction from the Q-Sepharose FF column. The solid black line corresponds to the absorbance at 280 nm and the dashed line is the percentage of 20 mM Tris-HCl pH 7.2 with 1 M NaCl. **(B)** Elution of the sample from the Q-Sepharose FF column in the HTP column. The solid black line corresponds to the absorbance at 280 nm and the dashed line is the percentage of 1 M KPi pH 7.2. **(C)** Chromatogram representing the DRbr Y59F elution profile in the size exclusion column. The solid black line corresponds to the absorbance at 280 nm. The red line corresponds to the elution of DRbr Y59F. **(D)** SDS-PAGE with samples of each eluted fraction containing DRbr Y59F. In the last step of the purification were obtained two fractions containing the protein. The peak line coloured in red in panel C corresponds to the elution of the sample shown in the last lane of the gel presented in panel D.

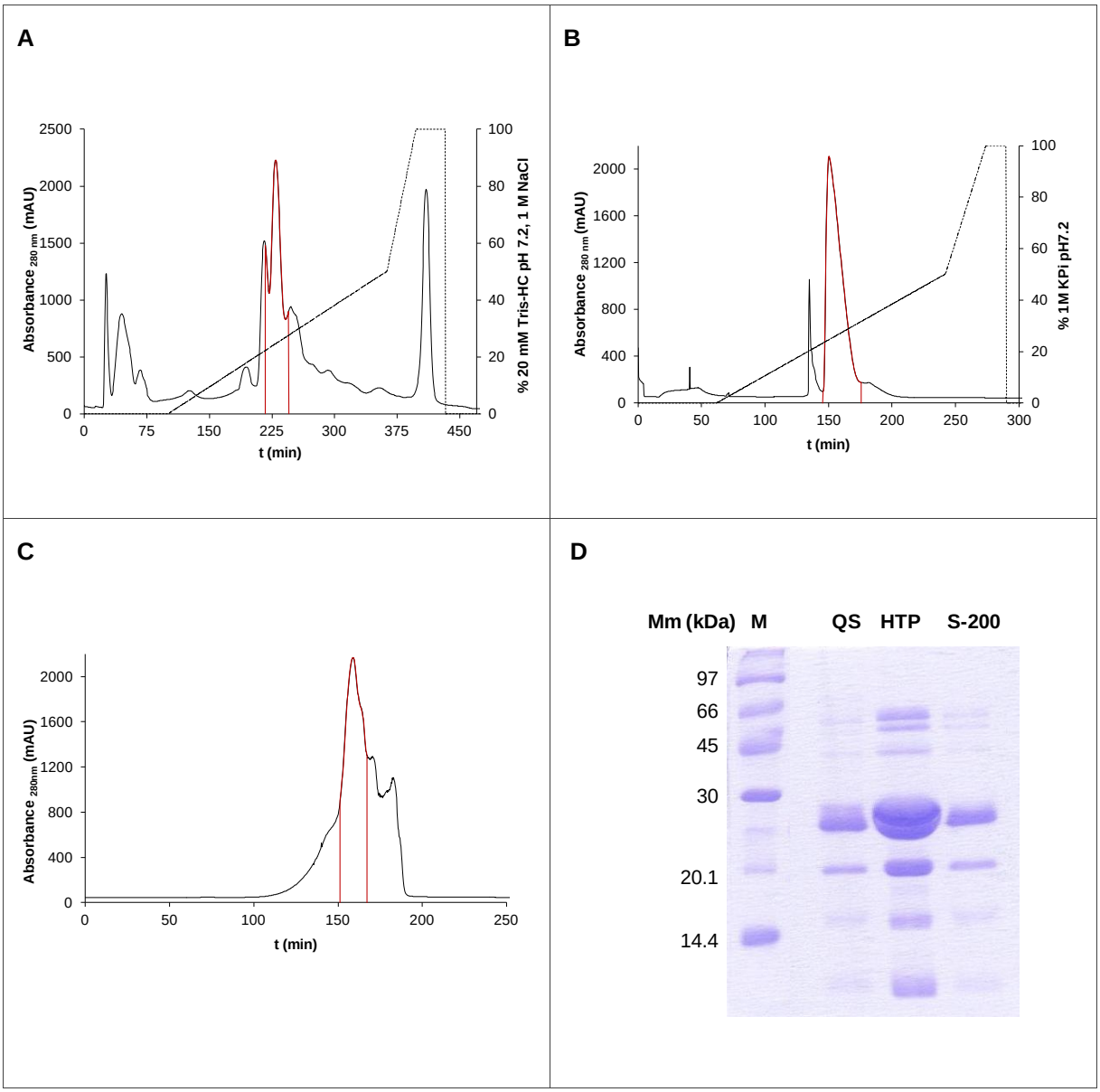

Figure 3.5: Resume of the DRbr Y12F purification. **(A)** Chromatogram of the elution of the soluble fraction from the Q-Sepharose FF column. The solid black line corresponds to the absorbance at 280 nm and the dashed line is the percentage of 20 mM Tris-HCl pH 7.2 with 1 M NaCl. **(B)** Elution of the sample from the Q-Sepharose FF column in the HTP column. The solid black line corresponds to the absorbance at 280 nm and the dashed line is the percentage of 1 M KPi pH 7.2. **(C)** Chromatogram representing the DRbr Y127F elution profile in the size exclusion column. The solid black line corresponds to the absorbance at 280 nm. The red line corresponds to the elution of DRbr Y127F. **(D)** SDS-PAGE with samples of each eluted fraction containing DRbr Y127F.

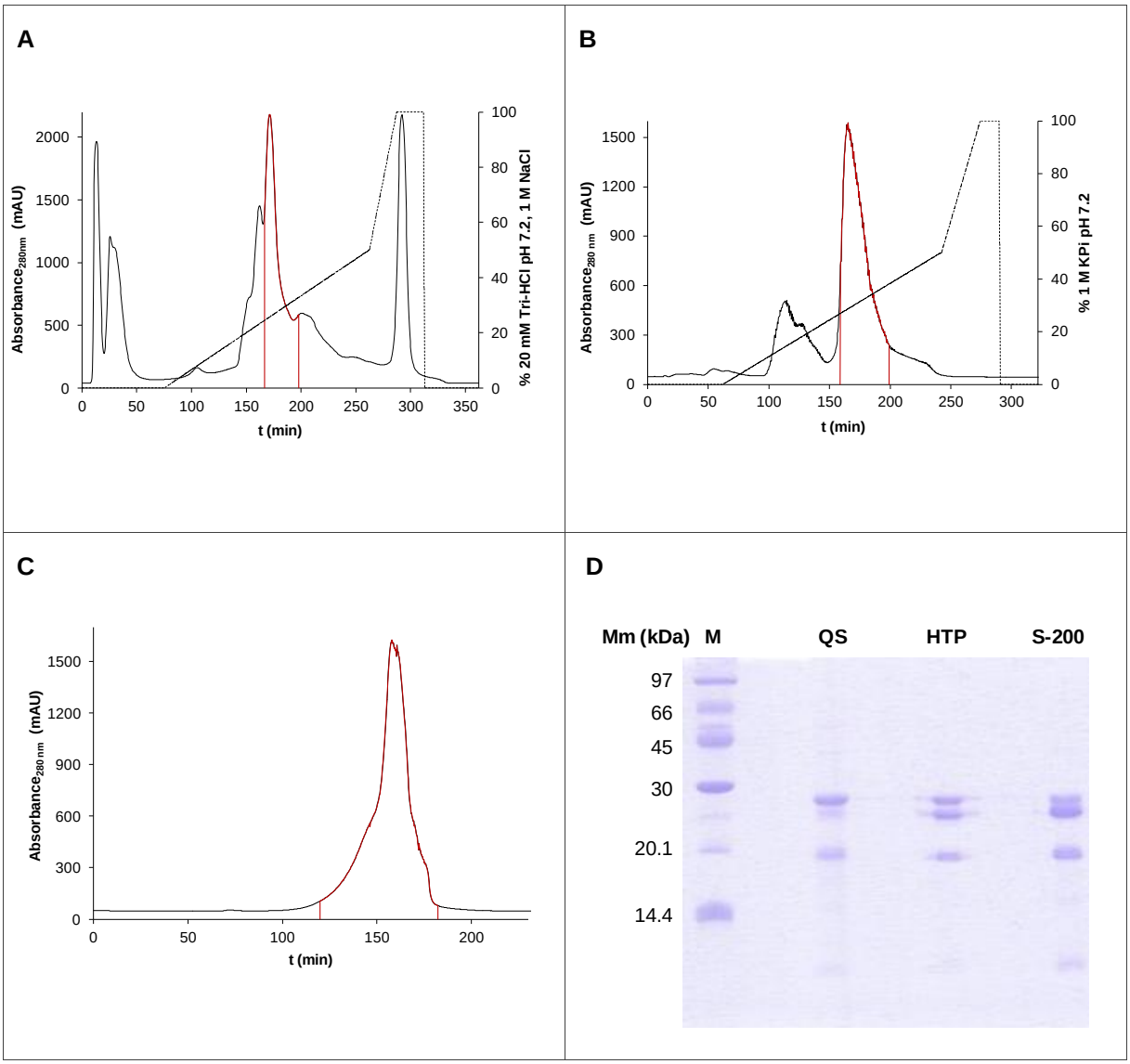

Figure 3.6: Resume of the DRbr Y59F Y127F purification. **(A)** Chromatogram of the elution of the soluble fraction from the Q-Sepharose FF column. The solid black line corresponds to the absorbance at 280 nm and the dashed line is the percentage of 20 mM Tris-HCl pH 7.2 with 1 M NaCl. **(B)** Elution of the sample from the Q-Sepharose FF column in the HTP column. The solid black line corresponds to the absorbance at 280 nm and the dashed line is the percentage of 1 M KPi pH 7.2. **(C)** Chromatogram representing the DRbr Y59F Y127F elution profile in the size exclusion column. The solid black line corresponds to the absorbance at 280 nm. The red line corresponds to the elution of DRbr Y59F T127F. **(D)** SDS-PAGE with samples of each eluted fraction containing DRbr Y59F Y127F.

3.3.2 Quantifications

The concentrations of the final fractions were determined through the BCA method. The iron was quantified by the TPTZ method and also by ICP. The content of zinc was also determined by ICP.

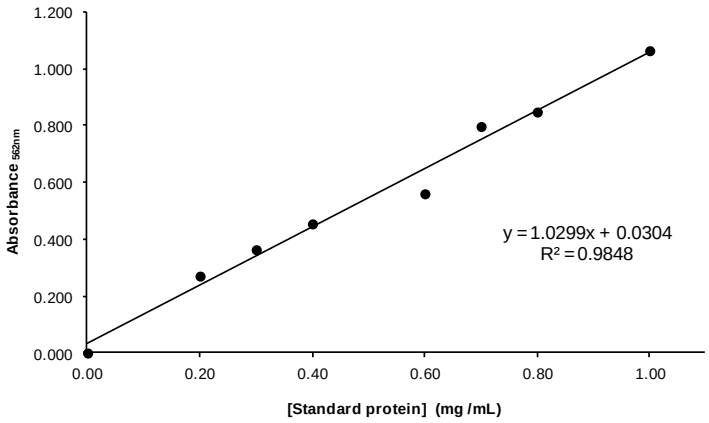

Figure 3.7: Calibration curve to determine the protein concentration through the BCA method. The results are the median calculated from three replicas. The curve was adjusted by the mean root square method.

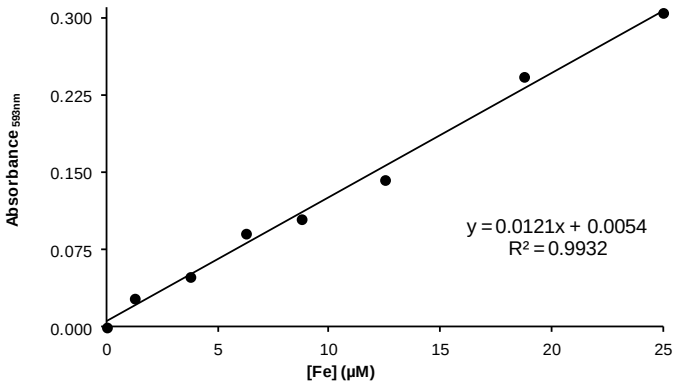

Figure 3.8: Calibration curve to determine the iron concentration through the TPTZ method. The experimental results are the median calculated from three replicas. The curve was adjusted to the results by the mean root square method.

The expected result of 4 atoms of iron per monomer of protein was observed for some fractions of WT, DRbr Y59F and DRbr Y59F Y127F. For the mutant Y127F none of the purified fractions had the expected amount of iron. The results of the TPTZ method are corroborated by the ICP results and also by the ERP experiments (see section 3.5).

Table 3.1: Quantifications performed for all final fractions from the protein purifications.

Protein	Cellular yield (g of cells/Litre of growth)	Protein yield (mg/Litre of growth)	Iron (Atoms/Monomer of protein)
DRbr WT	6.4	23	4.19
DRbr Y59F	6.5	25	4.22
DRbr Y127F	6	47	1.17
DRbr Y59F Y127F	6.9	22	2.89

3.3.3 UV-Visible spectra

Immediately after the purification UV-Visible spectra of all the final fractions were acquired. The spectra are in Figure 3.9 and Figure 3.10 shows the overlap of all spectra for an easier comparison between the different proteins.

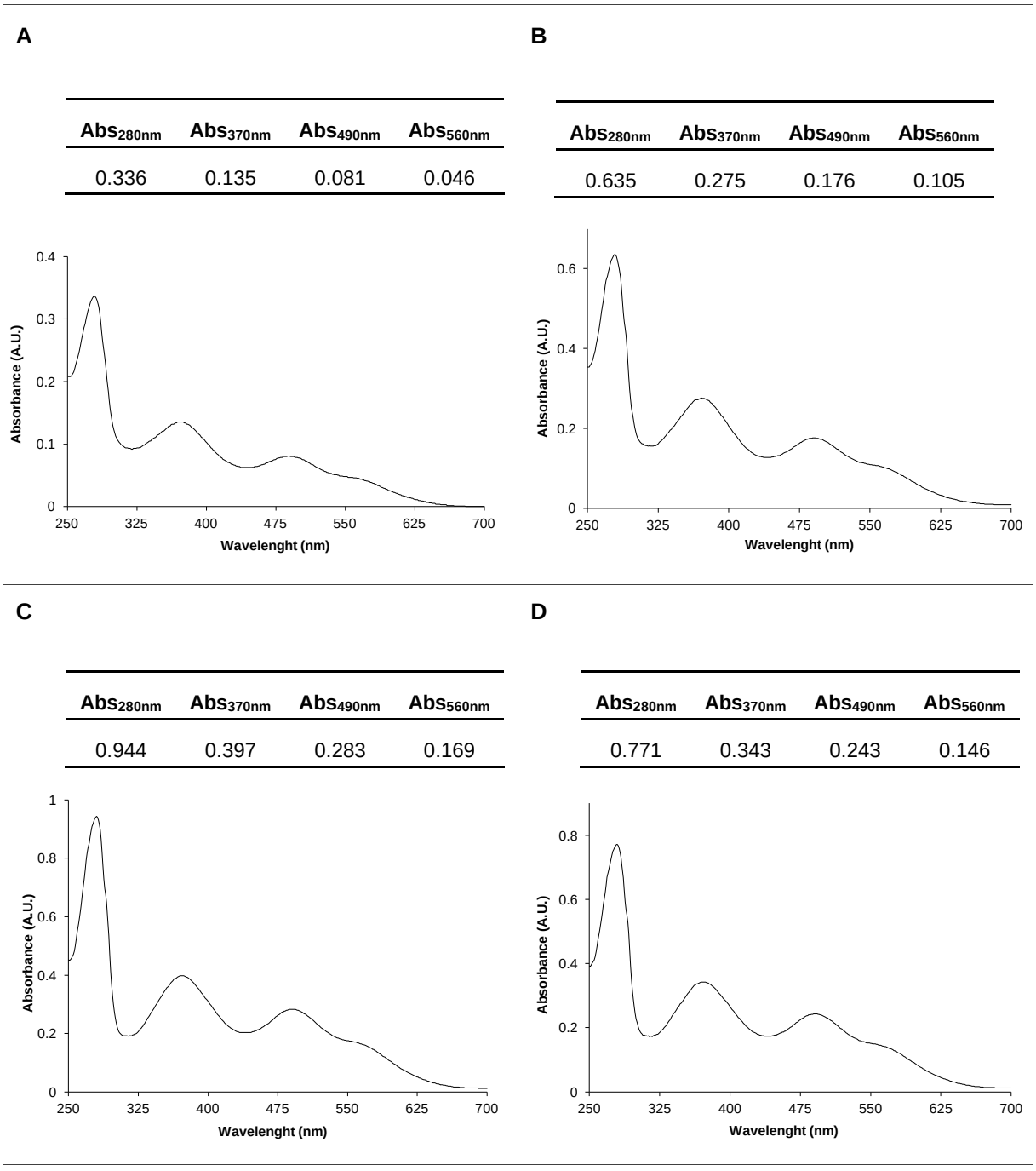

Figure 3.9: UV-Visible spectra from final fractions of DRbr proteins. Protein was in 20 mM Tris-HCl pH 7.2 with 150 mM NaCl **(A)** DRbr Wt **(B)** DRbr Y59F **(C)** DRbr Y127F **(D)** DRbr Y59F Y127F.

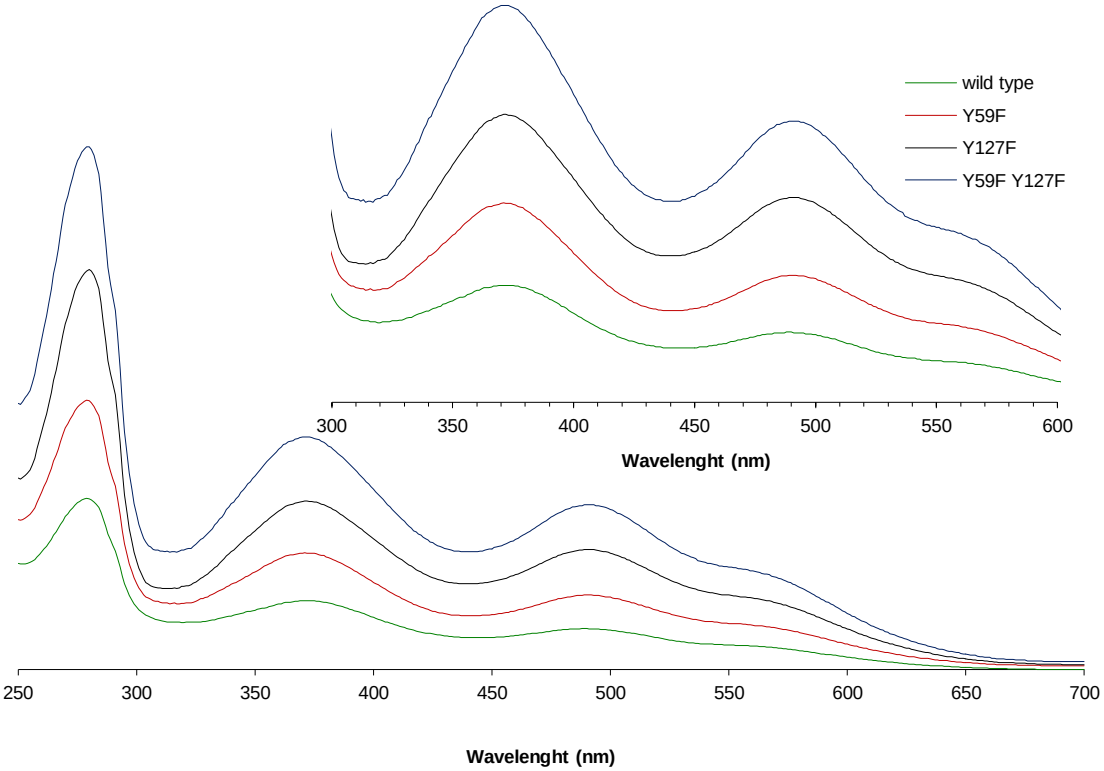

Figure 3.10: Overlap of the UV-Visible absorption spectra of wild type and desulforubrerythrin mutants.

To compare the fractions of the different purified proteins the ratios between the absorbance peaks were calculated and are summarized in Table 3.2.

Table 3.2: Absorbance ratios between the different absorbance bands.

Protein	Abs_{280}/Abs_{490}	Abs_{370}/Abs_{560}	Abs_{490}/Abs_{560}	Abs_{370}/Abs_{490}
DRbr WT	4.2	2.9	1.8	1.7
DRbr Y59F	3.6	2.6	1.7	1.6
DRbr Y127F	3.5	2.4	1.7	1.4
DRbr Y59F Y127F	3.2	2.4	1.7	1.4

3.3.4 Oligomerization state in solution

In order to determine the oligomerization state of the proteins in solution the samples were applied in an analytical S-200 column. A calibration was previously performed with adequate molecular mass standards. The elution volumes are listed in Table 3.3.

Table 3.3: Elution volumes of the molecular mass standards of the S-200 calibration. V_0 corresponds to the elution volume of blue dextran and is the dead volume of the column. V_t is the column volume. V_e is the elution volume for each protein. K_{av} is the partition coefficient and is obtained by the equation $K_{av} = (v_e-v_0) / (v_t-v_0)$. For proteins with a similar shape the formula can bbe linearized and $K_{av} = - A \log Mm + B$, where A is the slope of the curve and be is the interception of the y-axis.

Standard	Mm	log (Mm)	V_e (mL)	K_{av}
Aprotinin	6600	3.820	18.530	0.630
Myoglobin	17600	4.246	16.950	0.539
Chimiotripsogen	25000	4.398	16.800	0.529
Albumin	66000	4.820	15.318	0.441
Canalbumin	76600	4.884	14.330	0.383
Aldolase	158000	5.199	13.386	0.327
Catalase	240000	5.380	12.973	0.305
Ferritin	440000	5.643	11.156	0.194

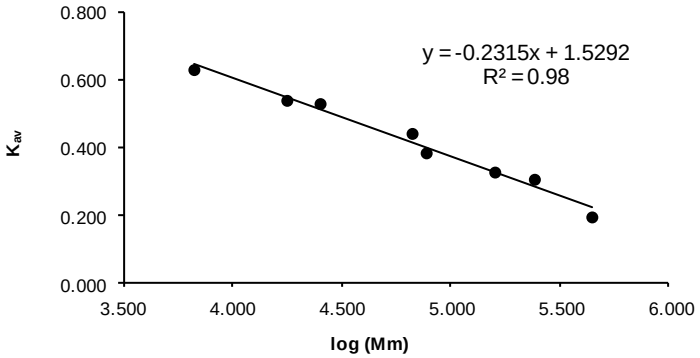

Figure 3.11: Calibration curve of the size exclusion column. The theoretical curve was adjusted to the experimental points via the mean root square method.

After the standards, the samples were applied in the column and the chromatograms and the retention volumes were recorded. The chromatogram of each protein is Figure 3.12.

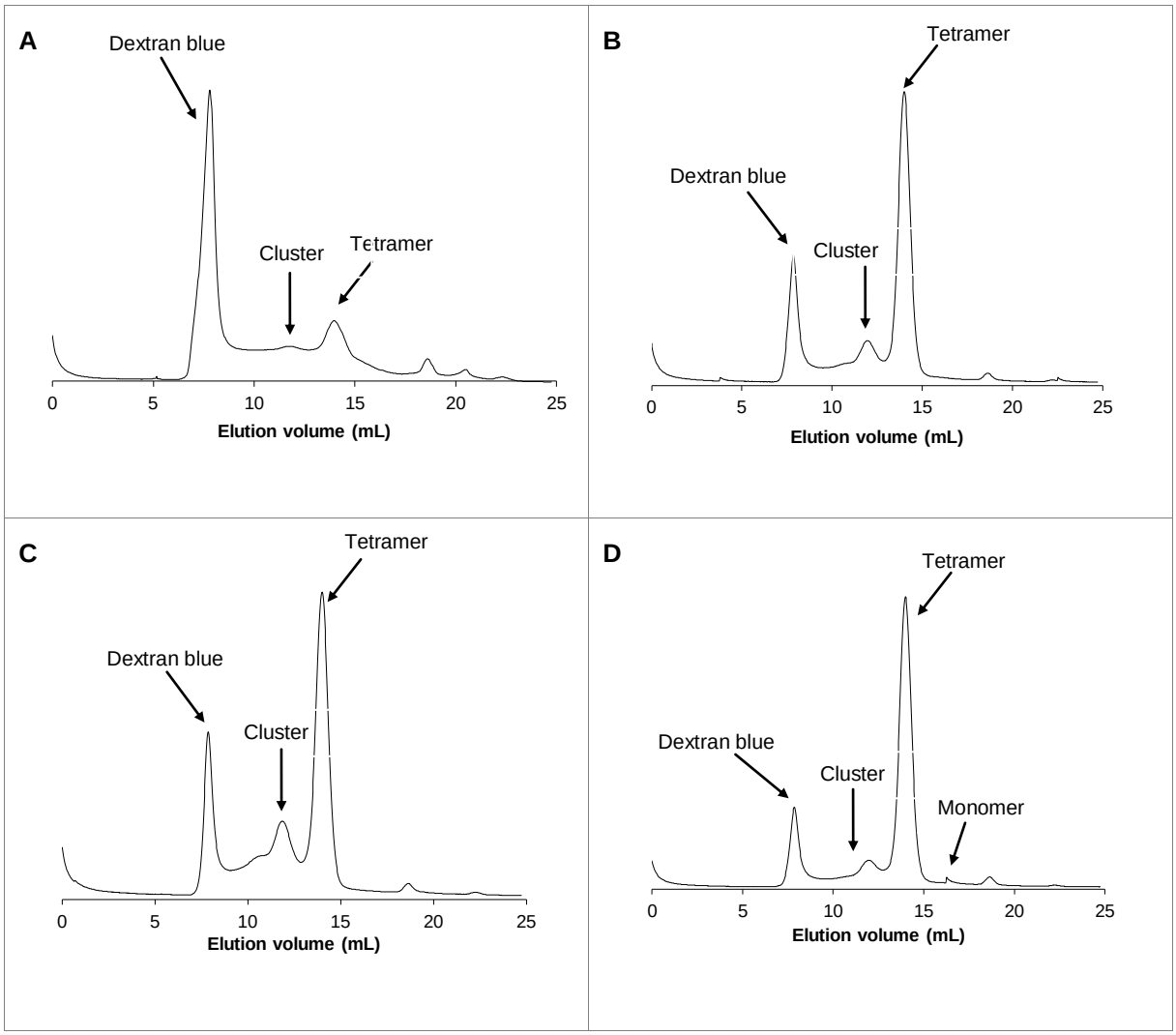

Figure 3.12: Elution profiles of DRbr proteins from the analytical size exclusion column. The y-axis corresponds to absorbance at 280 nm. **(A)** DRbr WT. **(B)** DRbr Y59F. **(C)** DRbr Y127F. **(D)** DRbr Y59F Y127F.

The mean dead volume of the column is 7.836 mL (± 0.025) and was calculated from the dextran blue elution volume obtained in each experiment and the column had a volume of 24.742 mL

In all samples the protein is mainly in a tetrameric state, but for the wild type protein the tetrameric form exists in a smaller proportion when compared with the mutants. In all samples also is possible to identify the presence of a cluster of elevate molecular mass (≈ 370 kDa) composed approximately of 14 to 16 subunits. The monomeric form of the protein was only detected for the double mutant and in a very small amount. In all chromatograms was possible to detect the presence of peaks with molecular masses inferior to the monomer, probably originate by protein degradation or contaminants. The results obtained are summarized in Tables 3.4 and 3.5.

Table 3.4: Elution volumes and molecular masses of WT and DRbr mutants and its degradation products. The molecular masses were calculated using the elution volumes from the size exclusion column and the calibration curve obtained for the standard proteins.

DRbr	V_e (mL)	Mm (kDa)	Subunits	V_e (mL)	Mm (kDa)	Subunits
WT	12	37	15	14	108	4
Y59F						
Y127F						
Y59F Y127F						

Table 3.5: Elution volumes and molecular masses of WT and DRbr mutants and its degradation products (continued from Table 3.4)

DRbr	V_e (mL)	Mm (kDa)	Subunits	V_e (mL)	Mm (kDa)	V_e (mL)	Mm (kDa)	V_e (mL)	Mm
WT	-	-	-	19	7	20	2.3	22	790
Y59F									
Y127F						-	-		
Y59F Y127F	16	28	1	-	-			-	-

3.3.5 N-terminal sequencing

To determine the origin of the bands detected in the SDS-PAGE gel of the mutant proteins one sample of the mutant Y59F was sent to N-terminal sequencing. In order to do that the sample was applied in a 15% SDS-PAGE gel and was transferred to a PVDF membrane. The bands ranging from 10 to 40 kDa were isolated and its N-terminal sequencing was performed (Figure 3.13). The results obtained for each band are in Table 3.6.

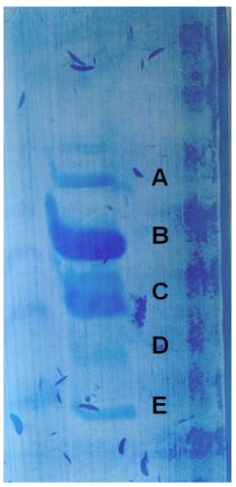

Figure 3.13: PVDF membrane after the protein transference and before the bands were cut.

Table 3.6: Results of the N-terminal sequencing

Band	Molecular mass (kDa) (approximate)	N-terminal sequence
A	40	DIQVG
B	24	MRQYETY
C	20	-
D	14	MRQYE
E	10	MRQYE

3.4 Crystallization experiments

The mutant DRbr Y127F previously dialyzed into 100 mM MES pH 6.2 with 500 mM NaCl and concentrated to approximately 20 mg/mL was submitted to crystallization trials. An initial screen was performed, using a 96 well plate in the nanorobot. The crystallization assays started by performing a screen using the Structure Screen 1 and 2 (Molecular Dimension). The set up method was the vapour diffusion sitting drop technique and the plate remained at 20ºC. For each condition were tested three proportions of protein (P) and reservoir solution (R): 1:2, 1:1, 2:1 (P:R). Small needle-shaped crystals appeared in the following conditions: 100 mM Hepes pH 7.5, 10% Isopropanol, 20% PEG 4K (1:1); 100 mM Tris-HCl pH 8.5, 10 mM $NiCl_2$, 20% PEG 2K (1:1, 1:2, 2:1); 100 mM Bicine pH 9.0, 100 mM NaCl, 30% PEG 550 (1:1); 100 mM Hepes pH 7.5, 10% PEG 6K, 5% MPD (1:1) (Figure 3.14).

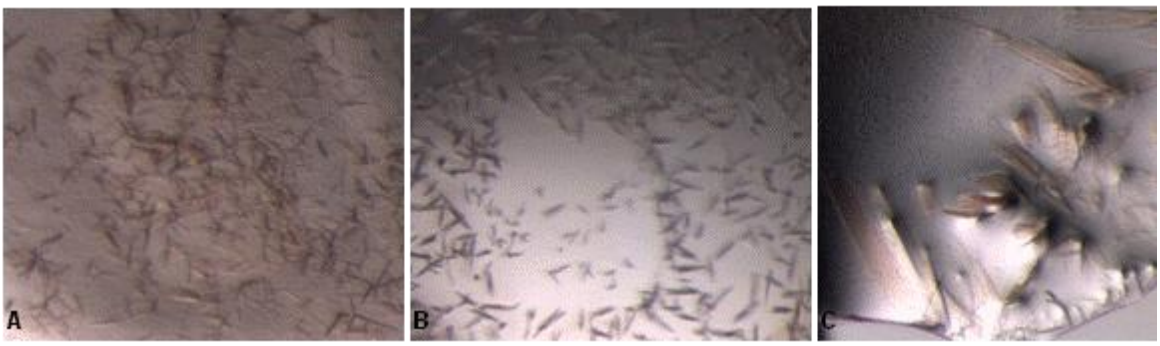

Figure 3.14: Examples of some DRbr Y127F crystals obtained using the Structure Screen 1 & 2. **(A)** 100 mM Bicine pH 9, 30 % PEG 550. **(B)** 100 mM Tris-HCl pH 8.5, 10 mM $NiCl_2$, 10% PEG 6K. **(C)** 100 mM Hepes pH 7.5, 10% isopropanol, 20% PEG 4K.

These conditions were reproduced in a 24 well plate using the hanging drop technique. Some variations were done, namely in the concentration of the precipitant agents. In none of the conditions appeared crystals suitable for X-ray diffraction. The work proceeded by doing drastic alterations in the crystallization solutions, namely in the pH value, the buffer and the precipitant reagents. Still no improvement on the crystals was achieved. The conditions tested are resumed in the schemes of Figures 3.15, 3.16, 3.17, 3.18 and 3.19.

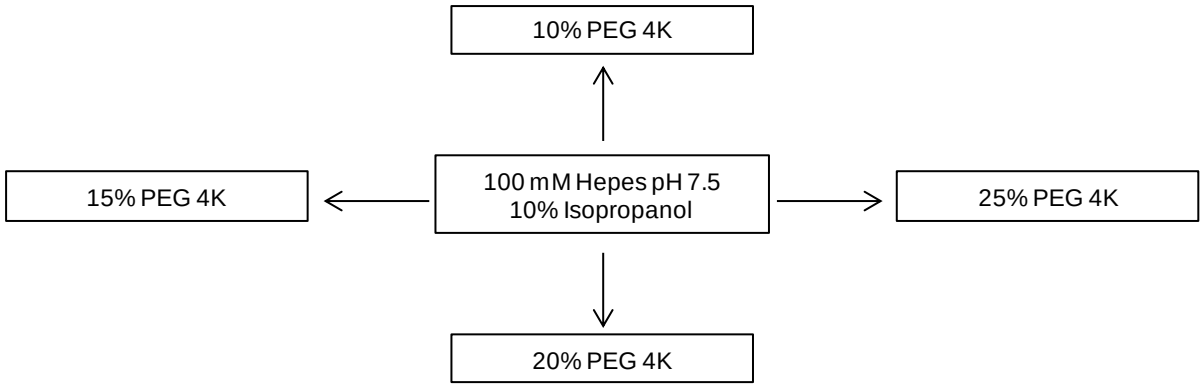

Figure 3.15: Crystallizations conditions tested for the protein DRbr Y127F with 100 mM Hepes pH 7.5 and 10% isopropanol with different concentrations of PEG 4K.

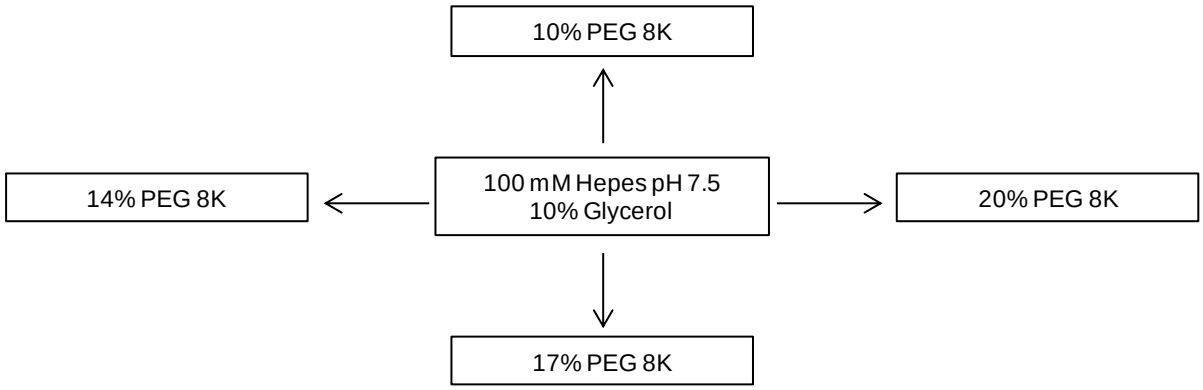

Figure 3.16: Crystallizations conditions tested for the protein DRbr Y127F with 100 mM Hepes pH 7.5 and 10% glycerol with different concentrations of PEG 8K.

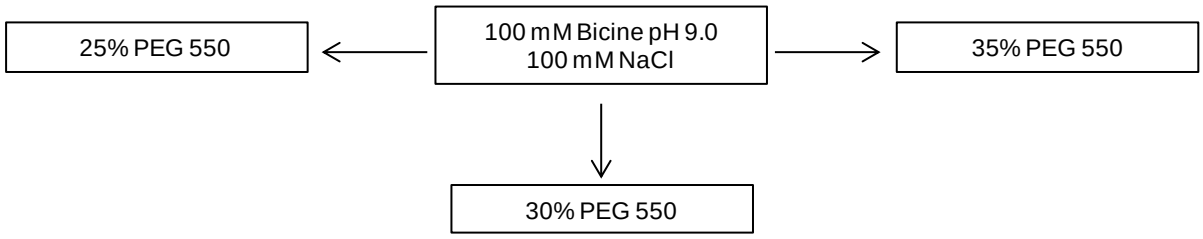

Figure 3.17: Crystallizations conditions tested for the protein DRbr Y127F with 100 Bicine pH 9.0 and 100 mM NaCl with different concentrations of PEG 550.

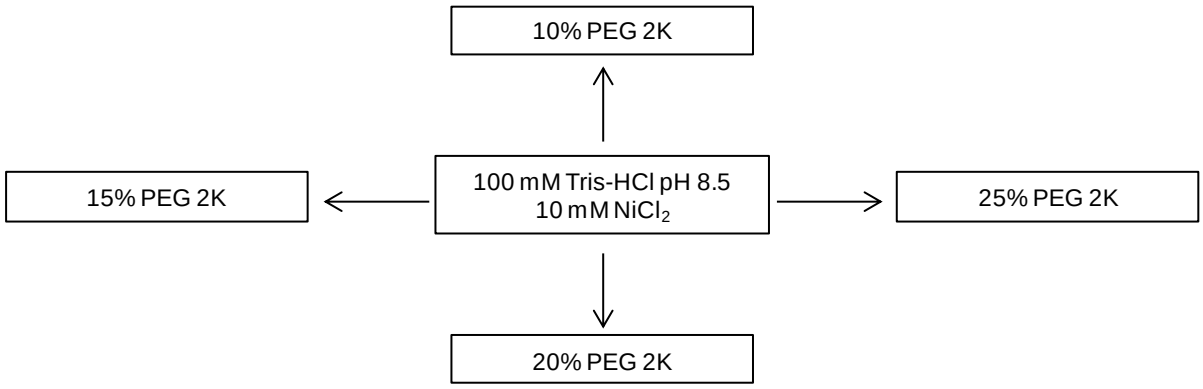

Figure 3.18: Crystallizations conditions tested for the protein DRbr Y127F with 100 mM Tris-HCl pH 8.5 and 10 mM $NiCl_2$ with different concentrations of PEG 2K.

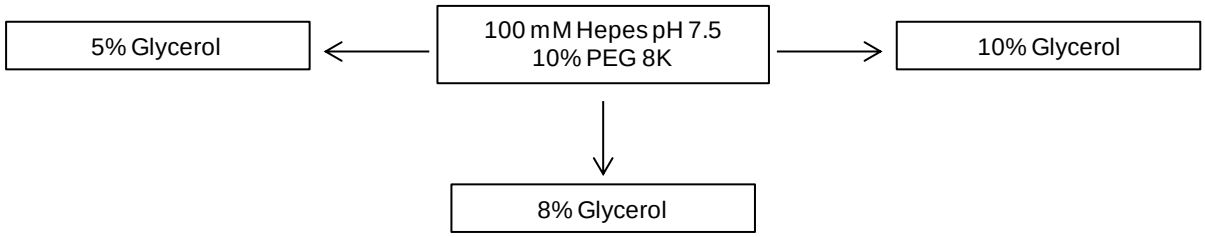

Figure 3.19: Crystallizations conditions tested for the protein DRbr Y127F with 100 mM Hepes pH 7.5 and 10 % PEG 8K with different concentrations of glycerol.

The work continued with the other proteins. The conditions tested were based on the results obtained for the Y127F mutant and on previous results obtained for the wild type protein. This time no screen was performed and the experiments begun using a 24 well plate. The conditions that produced better crystals were: 100 mM Hepes pH 7.5, 14% PEG 8K, 10% glycerol; 100 mM Hepes pH 7.5, 5% isopropanol, 10 % PEG 4K; 100 mM Hepes pH 7.5, 5% isopropanol, 10 % PEG 4K; 100 mM Hepes pH 7.5, 10% isopropanol, 10 % PEG 4K; 100 mM Hepes pH 7.5, 14% PEG 8K, 10% glycerol; 100 mM Hepes pH 7.5, 5% isopropanol, 10 % PEG 4K. In some assays was used 100 mM TCEP as additive but it did not produce any improvement in the crystals. All the conditions tested are described in the schemes of Figures 3.20 and 3.22.

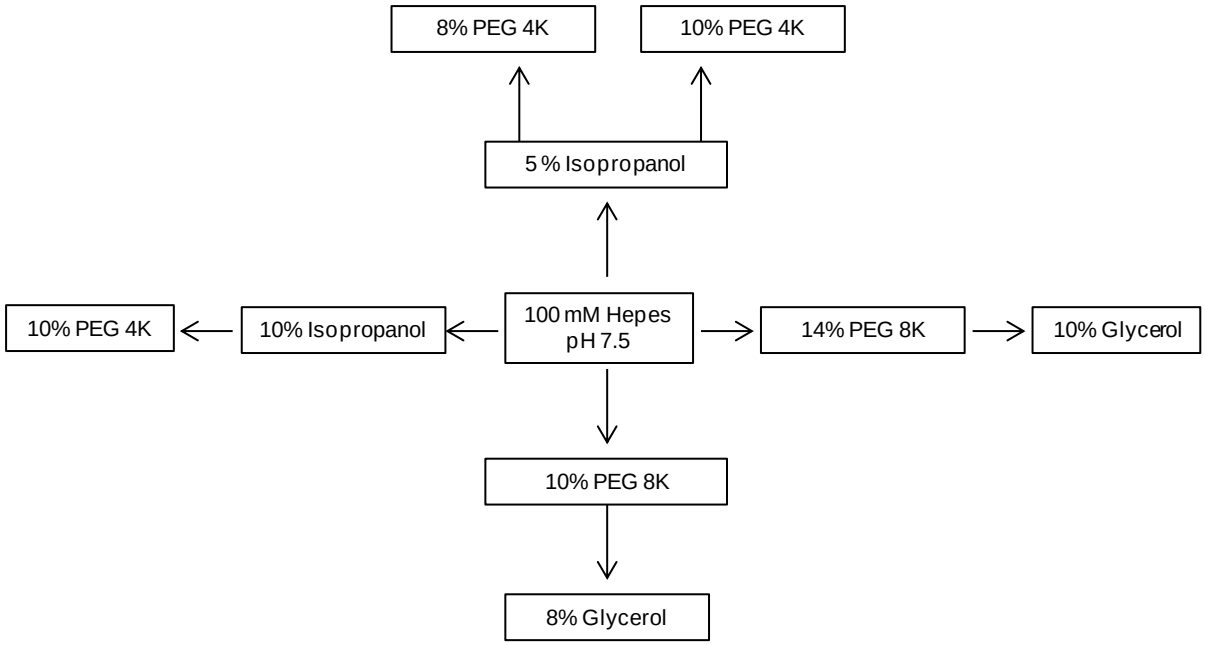

Figure 3.20: Resume of all crystallization conditions tested for the wild type protein.

For the wild type protein the following conditions produced crystals suitable for X-ray diffraction: 100 mM Hepes pH 7.5, 5% isopropanol. 10% PEG 4K; 100 mM Hepes pH 7.5, 14% PEG 8K, 10% glycerol (Figure 3.21). The crystals were cryoprotected in the respective reservoir solution plus 20 % glycerol before flash-cooling in liquid nitrogen.

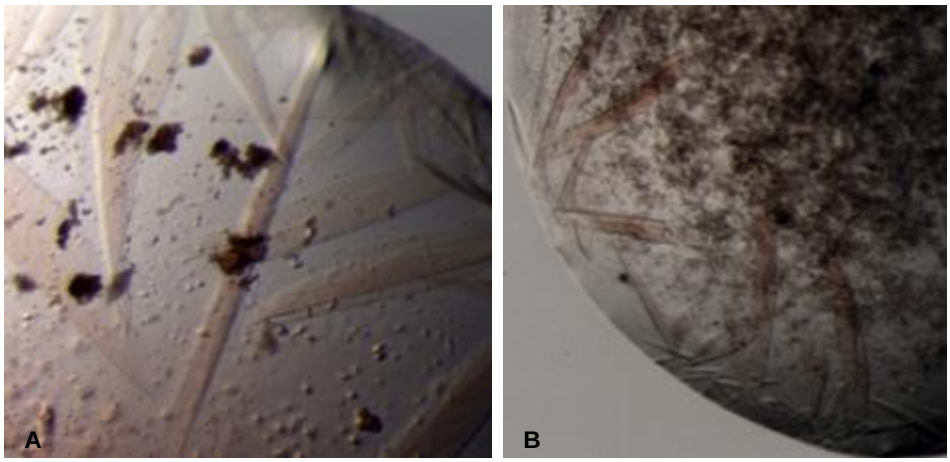

Figure 3.21: Example of crystals obtained for the wild type protein. **(A)** 100 mM Hepes pH 7.5, 14% PEG 8K, 10% glycerol (1:1). **(B)** 100 mM Hepes pH 7.5, 5% isopropanol, 10 % PEG 4K (1:2).

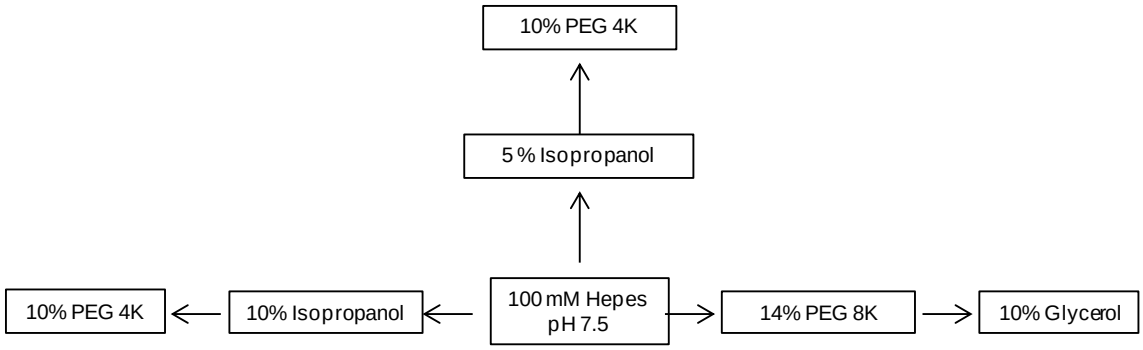

Figure 3.22: Resume of all crystallization conditions tested for DRbr Y59F and DRbr Y59F Y127F.

For the mutant Y59F crystals were obtained using the following conditions: 100 mM Hepes pH 7.5, 5% isopropanol, 10 % PEG 4K; 100 mM Hepes pH 7.5, 10 % isopropanol, 10 % PEG 4K (Figure 3.23). The crystals were cryoprotected in the liquid reservoir plus 20% glycerol prior to flash-cooling in liquid nitrogen and X-ray diffraction data were collected.

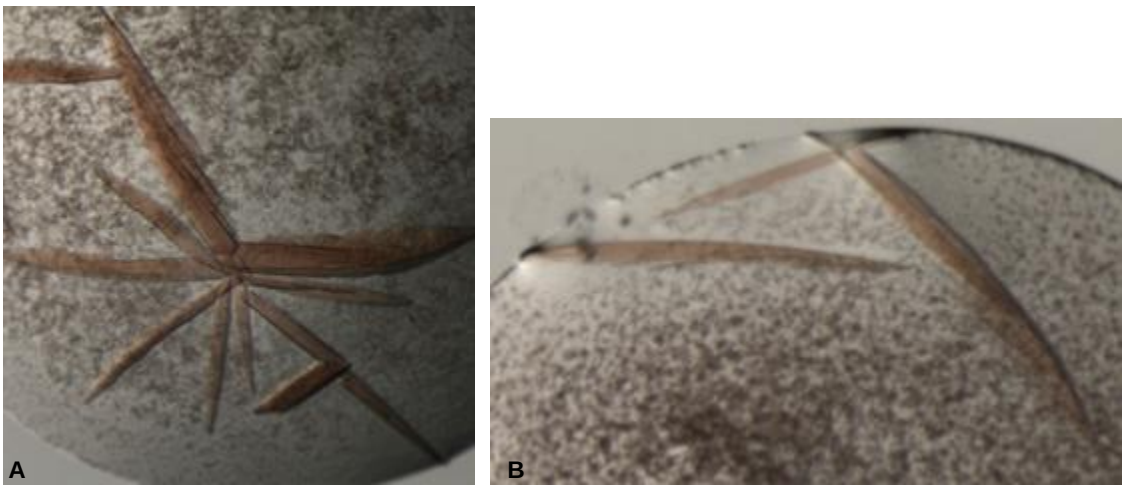

Figure 3.23: Crystals obtained for DRbr Y59F **(A)** 100 mM Hepes pH 7.5, 5% isopropanol, 10 % PEG 4K (1:2) **(B)** 100 mM Hepes pH 7.5, 10% isopropanol, 10 % PEG 4K.

The double mutant crystals appeared in the following conditions: 100 mM Hepes pH 7.5, 5% isopropanol, 10 % PEG 4K; 100 mM Hepes pH 7.5, 14 % PEG 8K, 10 % glycerol (Figure 3.24). The crystals were flash-cooled in liquid nitrogen after being immersed in a cryoprotectant solution with liquid reservoir and 20 % glycerol. X-ray diffraction data were collected.

Figure 3.24: Crystals obtained for DRbr Y59F Y127F. **(A)** 100 mM Hepes pH 7.5, 14% PEG 8K, 10% glycerol **(B)** 100 mM Hepes pH 7.5, 5% isopropanol, 10 % PEG 4K (1:1).

3.5 EPR studies

3.5.1 EPR spectra

The EPR spectra were collected at a temperature of 7 K, with a microwave power of 2 mW and at a frequency of 9.4 GHz. Unless otherwise stated the protein concentration was 100 μM in 50 mM Tris-HCl pH 7.2. When necessary a solution of sodium ascorbate was used to substoichiometricly reduce the proteins.

The first spectrum to be acquired concerns the as isolated wild type protein (Figure 3.25, green line). The spectrum presents the g-signals expected for the protein metallic centres: rubredoxin domain (9.3, 4.85, and 3.65), diiron centre (1.98, 1.76, and 1.66) and desulforedoxin domain (8.0 and 5.6).

The spectra of the mutant proteins were also collected in the same conditions. The DRbr Y59F spectra are also shown in Figure 3.25 (red and pink lines). The spectrum of the as isolated protein shows the g-signals of all metallic centres. After reduction with sodium ascorbate the resonances attributed to the diiron centre and the Dx domain disappear. Only the resonances from the Rd domain still remain visible in the spectrum.

The procedure described for DRbr Y59F was done for DRbr Y127F: spectra of the as isolated and reduced protein were acquired and are represented by the black and grey lines, respectively, in Figure 3.25. The as isolated protein shows only resonances with g-values from the Rd and Dx domains. The absence of signal of the diiron centre could be due to its absence in the protein or it could be fully oxidized or fully reduced (less probable, since the protein is oxidized by oxygen). To verify if the diiron centre was fully oxidized, sodium ascorbate was added to the protein, but no changes were observed in the spectrum around g-values typical for diiron centres.

Finally, the spectra of the double mutant were acquired just like previously was done for the other proteins (blue lines inFigure 3.26). The results obtained are very similar to those obtained for the Y127F mutant. Once again the resonances which would originate from the diiron centre are absent from both spectra.

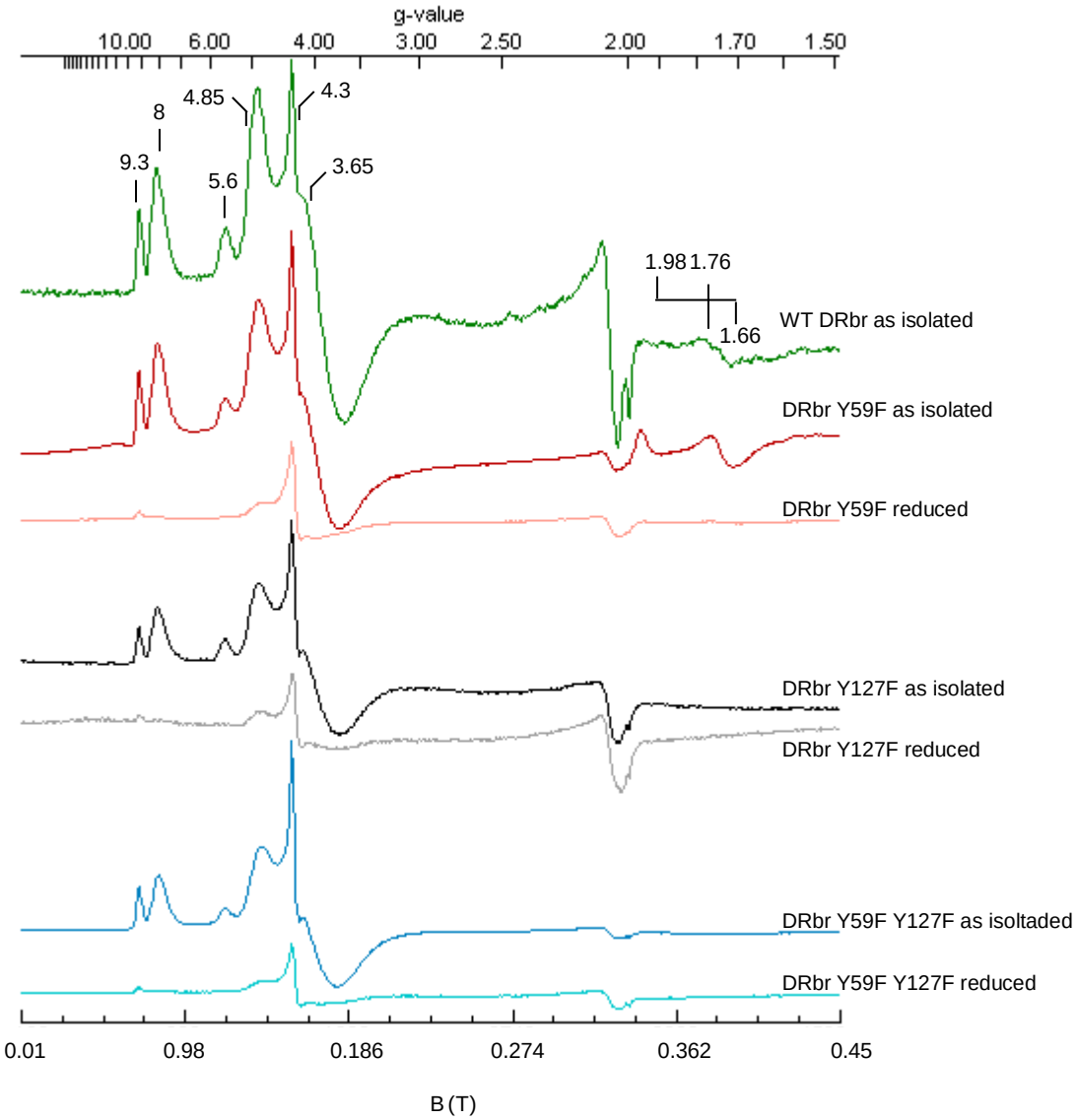

Figure 3.25: EPR spectra of DRbr proteins. When indicated proteins were reduced with sodium ascorbate. Proteins concentration was 100 μM in 50 mM Tris-HCl pH 7.2. The experimental conditions were: T: 7K; microwave power: 2 mW; microwave frequency: 9.4 GHZ.

3.5.2 Diiron centre reconstitution

Apparently the mutant Y127F and the double mutant were lacking the diiron site. This was taken as an advantage to try a process for the reconstitution of the diiron centre. The reconstitution was done by incubating 100 μM of DRbr Y127F with 2 M of DTT and 300 μM of Fe^{2+} for half an hour, in anaerobic conditions. After removing the excess of iron the success of the process was confirmed by the EPR spectrum (Figure 3.26). The spectrum acquired immediately after the reconstitution lacks the resonances usually attributed to the diiron centre, but after addition of sodium ascorbate a signal appears around g values 1.7, thus an indication that the process was successful.

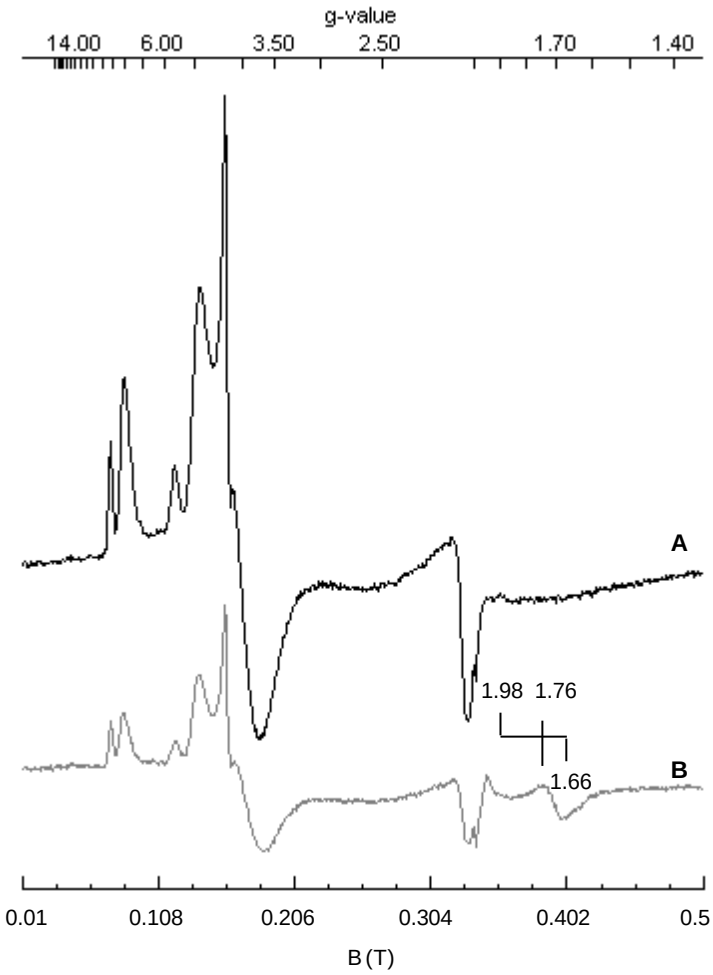

Figure 3.26: EPR spectra of the DRbr Y127F before **(A)** and after **(B)** the diiron centre reconstitution. Protein concentration was 100 μM in 20 mM Tris-HCl pH 7.2 with 150 mM NaCl.

3.5.3 Redox titration of the wild type protein

Due to limitations in the amount of protein purified with the correct amount of iron this experiment was only done for the wild type protein.

The redox titration was performed under argon in 50 mM Tris-HCl pH 7.2. To the protein at a concentration of 80 μM were added redox mediators from -225 mV to + 430 mV each at a concentration of 80 μM. The spectra are shown in Figure 3.27.

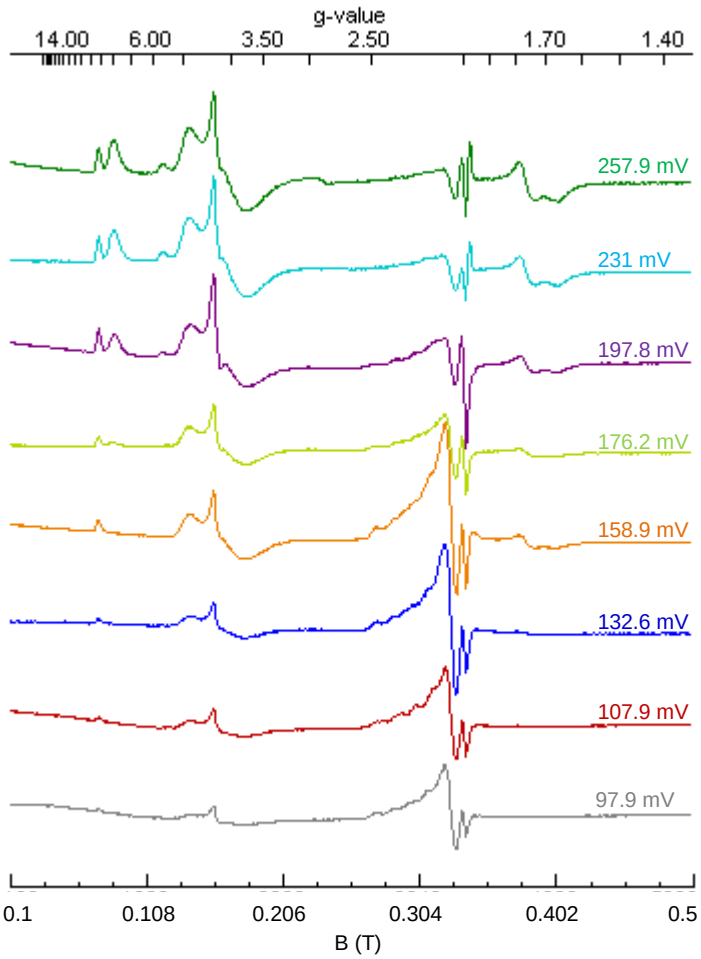

Figure 3.27: Redox titration of desulforubrerythrin wild type. The protein concentration was 80 μM.

The data were analysed using the Nernst equation [$E = E_0 - RT/nF \ln Q$; R: Universal gas constant, F: Faraday constant, n: number of electrons involved in the transition, Q: quotient between the concentrations of the species involved in the reaction]. In this case the coefficient of the reaction is expressed by the amplitude of the signal correspondent for each transition. Given that the amplitude of the signal is not necessarily dependent on the concentration of the species all amplitudes were normalized considering the maximum signal for each g-value.

For the diiron centre were considered two consecutive single electron transitions. The first transition corresponds to the reduction of the first atom of iron, given rise to the mixed-valence state ($Fe^{3+}/Fe^{3+} \rightarrow Fe^{3+}/F^{2+}$) – which gives the EPR signal. The second transition corresponds to the fully reduction of the diiron centre ($Fe^{3+}/Fe^{2+} \rightarrow Fe^{2+}/Fe^{2+}$). This process was followed by the resonances at g-values of 1.76 and 1.66. The concentration of the mixed-valence state can be calculated by the following Nernst equation: $[Fe^{3+}/Fe^{2+}] = 10^{[(E1 - E)/(RT/nF)]} / (1+10^{[(E1-E)/(RT/nF)]} + 10^{[(E1+E2-2E)/(RT/nF)]})$. The potential of each transition is noted by E_1 and E_2, respectively for the first and second transitions and E is the redox potential of the solution at a certain moment. The equation fits the experimental data for potentials of 270 and 235 mV, for the first and second transitions (Figure 3.28).

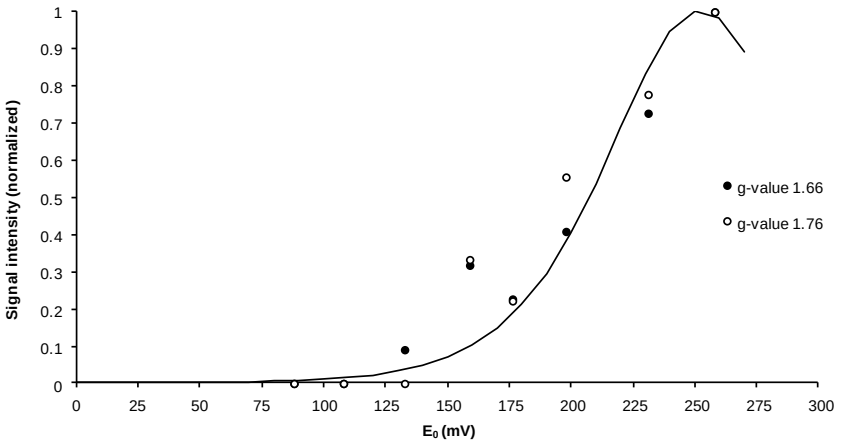

Figure 3.28: Redox titration of DRBr WT followed by EPR spectroscopy. The redox changes of the diiron centre were monitored by the changes in the amplitudes at g-values 1.66 and 1.76.

For the rubredoxin and desulforedoxin domains the same approach was used but considering only one electronic transition. In these cases the Nernst equation assumes a simpler form: $[Fe^{3+}]=10^{[(E-E1)/(RT/nF)]} / (1+10^{[(E-E1)/(RT/nF)]})$. The theoretical data fit the experimental values for potentials of 170 and 200 mV for the rubredoxin and desulforedoxin domain, respectively (Figure 3.29 and Figure 3.30).

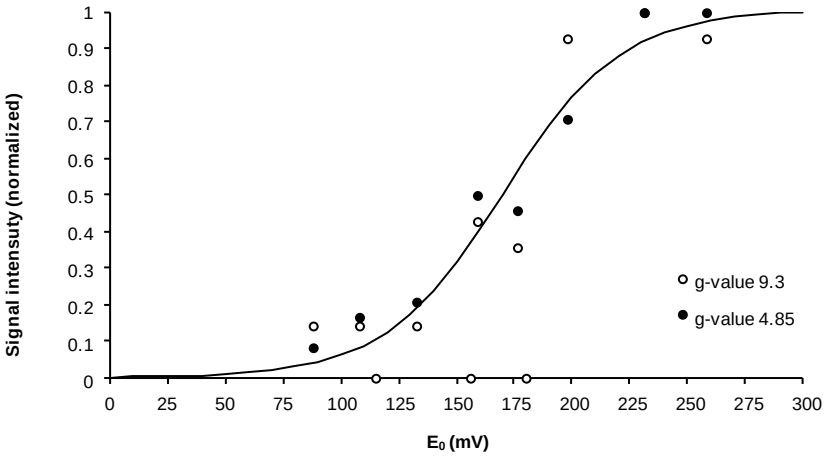

Figure 3.29: Redox titration of DRBr WT followed by EPR spectroscopy. The redox changes of the rubredoxin domain were monitored by the changes in the amplitudes at g-values 9.3 and 4.85.

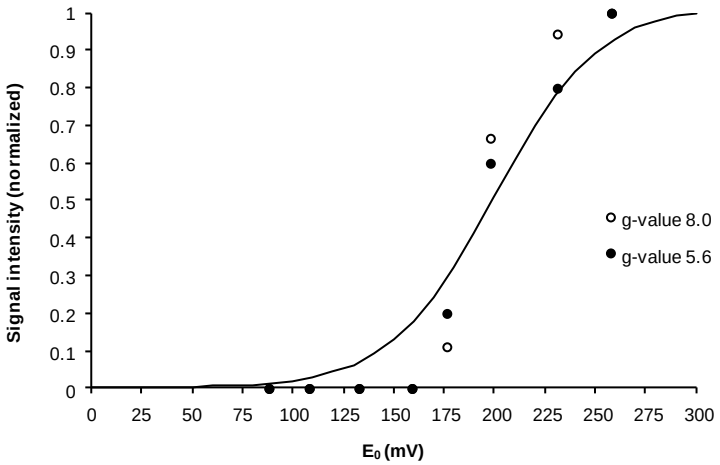

Figure 3.30: Redox titration of DRbr WT followed by EPR spectroscopy. The redox changes of the rdesulforedoxin domain were monitored by the changes in the amplitudes at g-values 8 and 5.6.

4 DISCUSSION

4.1 Diiron proteins

Diiron proteins are widespread among the three life domains. Rubrerythrins and ribonucleotide reductases (RNR) are examples of two families of proteins with this feature. RNR are proteins responsible to reduce ribonucleotides making deoxyribonucleotides available to DNA synthesis. They are usually divided in three classes. Class I RNR are composed of two subunits: the small subunit contains a diiron centre and its mechanism relies in the formation of a tyrosil radical that is transported to the large subunit of the protein where the reduction reaction takes place (Zhang *et al.*, 2011).

To try to find other common features between the two families of proteins a sequence alignment was performed between several rubrerythrins and the small subunit of four RNR. The RNR proteins chosen are representative from organisms with different levels of complexity: a virus (Epstain-Barr), a bacterium (*E. coli*), a fungus (*Saccharomyces cerevisiae*) and a mammal (*Homo sapiens*).

As can be seen in Figure 4.1, in all rubrerythrins analysed the iron ligands are aligned in positions 174 (E), 209 (E), 212 (H), 266 (E), 269 (E), 300 (E) and 303 (H). In erythrin only one ligand (the first glutamate) is aligned with the other rubrerythrins, due to the small size of the protein. The tyrosines hydrogen bonded to glutamate involved in iron coordination (positions 182 and 274) are conserved in all rubrerythrins, supporting the idea that these residues should be important for protein function.

Three iron ligands (positions 266, 300 and 303) are highly conserved in all proteins analysed, including the RNR. In the eukaryotic RNR the glutamate in the position 174 is also conserved. The tyrosine responsible for radical formation in *E.coli* RNR is aligned with the first tyrosine hydrogen bonded to glutamate in rubrerythrins (position 182) that corresponds to amino acid 122 in the protein sequence. In the other RNR the tyrosine is the position 199 (Zhou *et al.*, 2005). Curiously, the other tyrosine locate immediately after the highly conserved glutamate is replaced by a phenylalanine in all RNR (position 274), thus eliminating the possibility of another radical at this site.

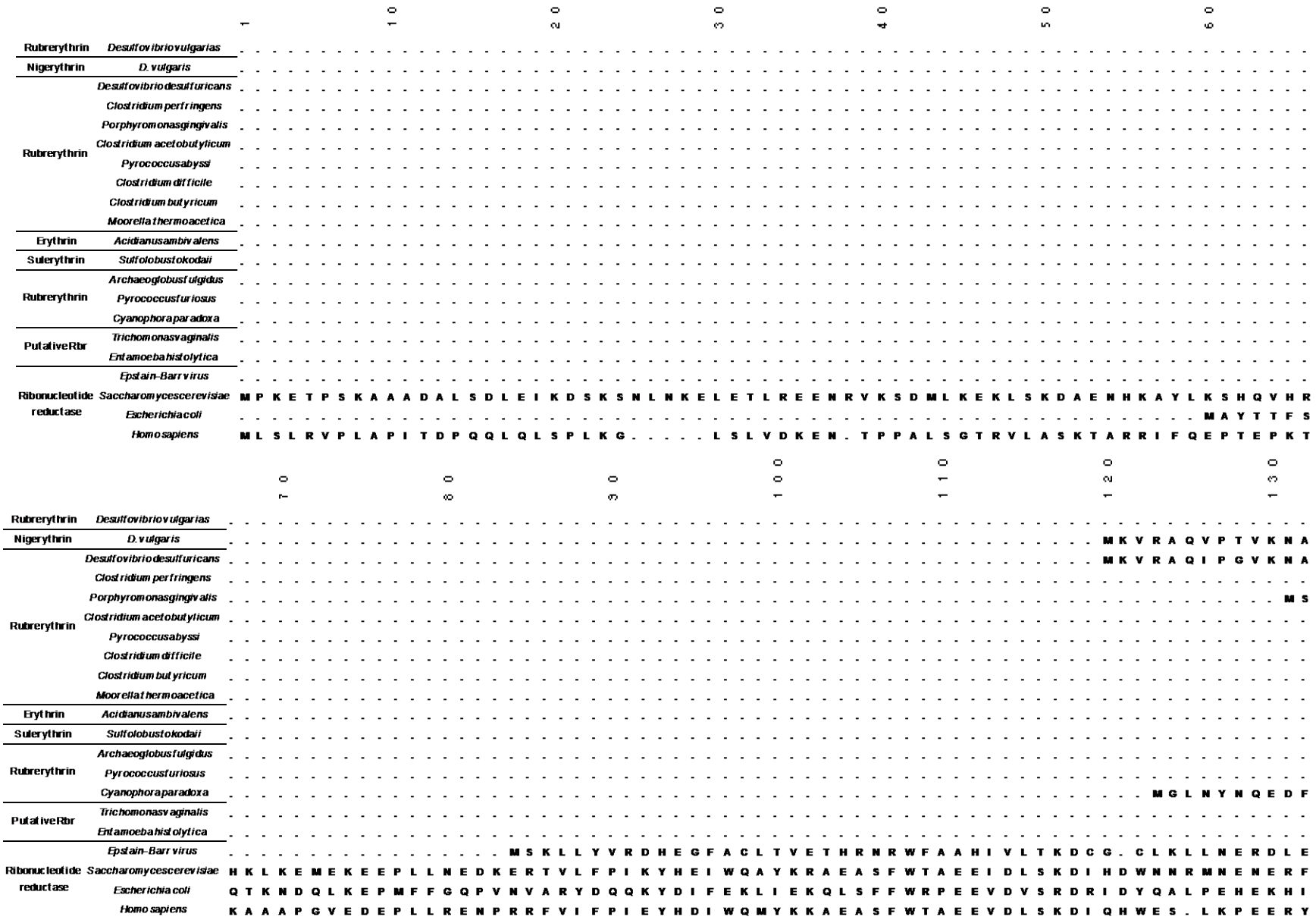
1 10 20 30 40 50 60
Rubrerythrin Desulfovibriovulgarias
Nigerythrin D.vulgaris
Desulfovibriodesulfuricans
Clostridiumperfringens
Porphyromonasgingivalis
Rubrerythrin Clostridiumacetobutylicum
Pyrococcusabyssi
Clostridiumdifficile
Clostridiumbutyricum
Moorellathermoacetica
Erythrin Acidianusambivalens
Sulerythrin Sulfolobustokodaii
Archaeoglobusfulgidus
Rubrerythrin Pyrococcusfuriosus
Cyanophoraparadoxa
PutativeRbr Trichomonasvaginalis
Entamoebahistolytica
Epstain-Barrvirus
Ribonucleotide reductase Saccharomycescerevisiae MPKETPSKAAADALSDLEIKDSKSNLNKELETLREENRVKSDMLKEKLSKDAENHKAYLKSHQVHR
Escherichiacoli MAYTTFS
Homosapiens MLSLRVPLAPITDPQQLQLSPLKG....LSLVDKEN.TPPALSGTRVLASKTARRIFQEPTEPKT
70 80 90 100 110 120 130
Rubrerythrin Desulfovibriovulgarias
Nigerythrin D.vulgaris MKVRAQVPTVKNA
Desulfovibriodesulfuricans MKVRAQIPGVKNA
Clostridiumperfringens
Porphyromonasgingivalis MS
Rubrerythrin Clostridiumacetobutylicum
Pyrococcusabyssi
Clostridiumdifficile
Clostridiumbutyricum
Moorellathermoacetica
Erythrin Acidianusambivalens
Sulerythrin Sulfolobustokodaii
Archaeoglobusfulgidus
Rubrerythrin Pyrococcusfuriosus
Cyanophoraparadoxa MGLNYNQEDF
PutativeRbr Trichomonasvaginalis
Entamoebahistolytica
Epstain-Barrvirus MSKLLYVRDHEGFACLTVETHRNRWFAAHIVLTKDCG.CLKLLNERDLE
Ribonucleotide reductase Saccharomycescerevisiae HKLKEMEKEEPLLNEDKERTVLFPIKYHEIWQAYKRAEASFWTAEEIDLSKDIHDWNNRMNENERF
Escherichiacoli QTKNDQLKEPMFFGQPVNVARYDQQKYDIFEKLIEKQLSFFWRPEEVDVSRDRIDYQALPEHEKHI
Homosapiens KAAAPGVEDEPLLRENPRRFVIFPIEYHDIWQMYKKAEASFWTAEEVDLSKDIQHWESS.LKPEERY


Rubrerythrin Desulfovibrio vulgaris
Nigerythrin D. vulgaris
Desulfovibrio desulfuricans
Clostridium perfringens
Porphyromonas gingivalis
Rubrerythrin Clostridium acetobutylicum
Pyrococcus abyssi
Clostridium difficile
Clostridium butyricum
Moorella thermoacetica
Erythrin Acidianus ambivalens
Sulerythrin Sulfolobus tokodaii
Archaeoglobus fulgidus
Rubrerythrin Pyrococcus furiosus
Cyanophora paradoxa
Trichomonas vaginalis
Putative Rbr
Entamoeba histolytica
Epstain-Barr virus
Ribonucleotide reductase Saccharomyces cerevisiae
Escherichia coli
Homo sapiens

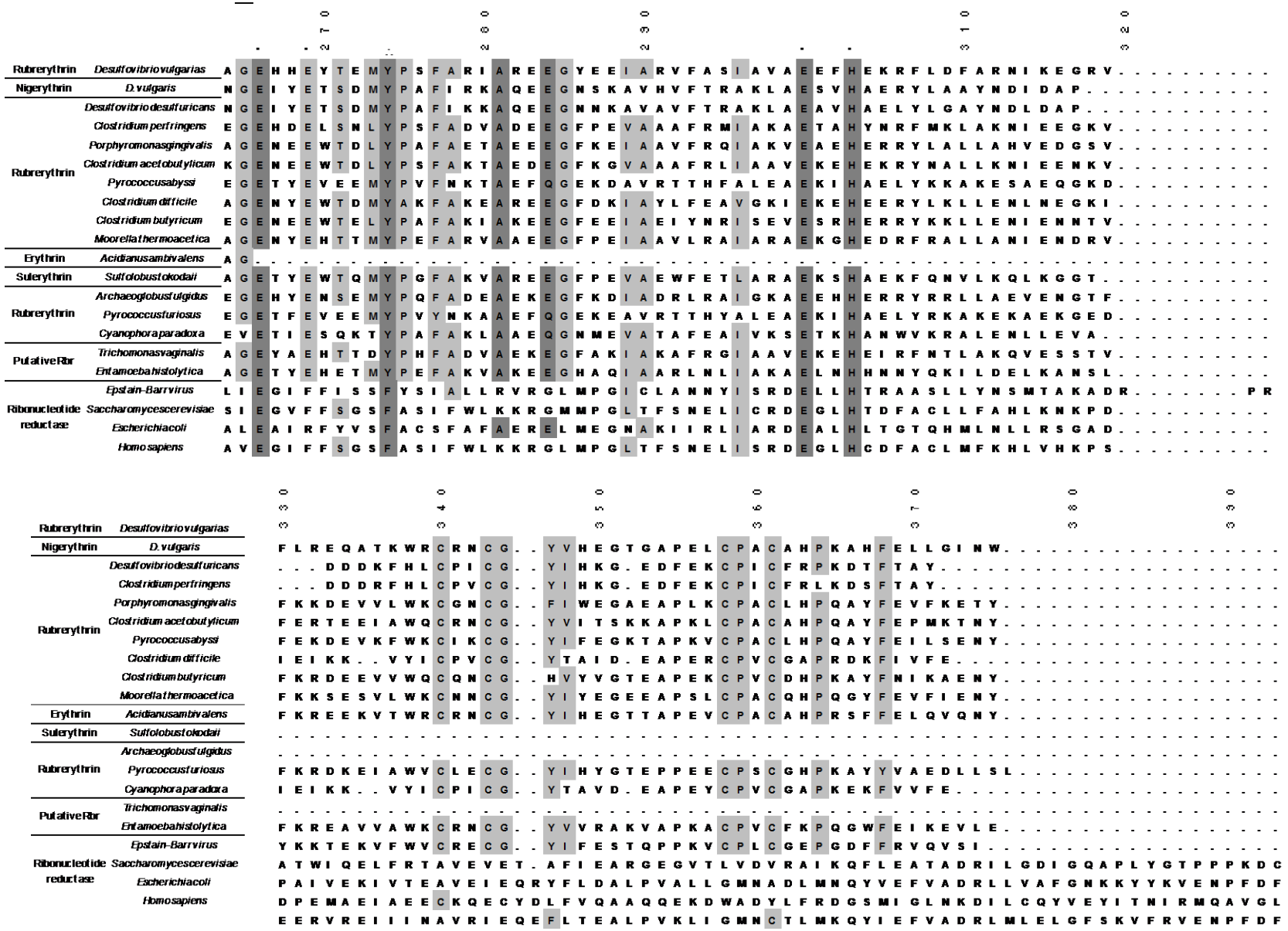
Rubrerythrin Desulfovibrio vulgarias
Nigerythrin D. vulgaris
Desulfovibrio desulfuricans
Clostridium perfringens
Porphyromonas gingivalis
Rubrerythrin Clostridium acetobutylicum
Pyrococcus abyssi
Clostridium difficile
Clostridium butyricum
Moorella thermoacetica
Erythrin Acidianus ambivalens
Sulerythrin Sulfolobus tokodaii
Archaeoglobus fulgidus
Rubrerythrin Pyrococcus furiosus
Cyanophora paradoxa
Putative Rbr Trichomonas vaginalis
Entamoeba histolytica
Epstein-Barr virus
Ribonucleotide reductase Saccharomyces cerevisiae
Escherichia coli
Homo sapiens

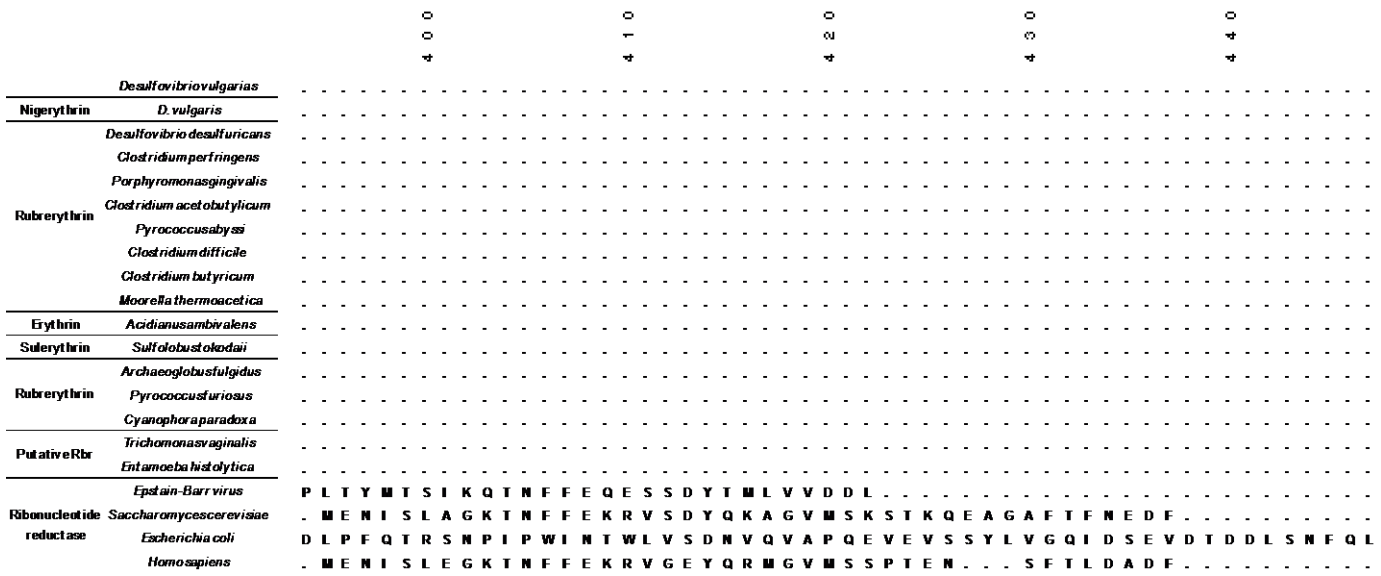

Figure 4.1: Amino acid sequence alignment of rubrerythrins and ribonucleotide reductases. Dark grey boxes represent highly conserved residues and light grey boxes represents conserve residues in the presented sequences. The boxes limited by black rectangles are the tyrosil radicals in RNR. The residues identified with "*" are iron ligands and residues identified with "∴" are the tyrosines possibly involved in radical formation in Rbrs. Alignment performed with Clustal X. The protein sequences are from the UniProt website:
D. vulgaris rubrerythrin: P24931, *D. vulgaris* nigerythrin: P30820, *D. desulfuricans*: Q30W15, *C. perfringens*: P51591, *P. gingivalis*: Q9AGG3, *C. acetobutylicum*: Q97FZ9, *P. abyssi*: Q9V0A0, *C. difficile*: C9XM55, *C. butyricum*: B1R052, *M. thermoacetica*: Q2RIY9, *A. ambivalens*: Q8X273, *S.tokodaii*: F9VPE5, *A. fulgidus*: O29427, *P. furiosus*: Q9UWP7, *C.paradoxa*: P48329, *T. vaginalis*: A2EHC4, *E. histolytca*: C4M030, *Epstain-Barr* virus: P0CAP6, *S.cerevisiae*: P09938, *E. coli*: P69924, *H. sapiens*: P31350.

4.2 Protein expression tests for desulforubrerythrin mutants

The protein expression tests were performed in three *E. coli* strains: BL21DE3 GOLD, STAR and BL21DE3. Analyzing the gel images in Figure 3.1 it is possible to observe that all strains successfully expressed the mutant proteins. The *E.coli* BL21DE3 GOLD cells apparently expressed more DRbr proteins but also more contaminants, although this perception may be due to an excess of sample applied on the gel. It also seems that a great amount of protein is not in the soluble fraction, but this may be caused by incomplete cellular lysis or the protein may be localized in inclusion bodies.

A closer look into the gels, particularly the results obtained for *E. coli* STAR and *E. coli* BL21DE3, reveals that the mutants have a slightly different migration pattern when compared with the wild type protein (Figure 3.1 B and C).

Considering the obtained results and having in mind that the wild type protein had already been successfully over expressed in *E. coli* BL21DE3 GOLD this cellular strain was chosen to over express the mutant proteins.

4.3 Proteins expression

The cells over expressing the proteins were grown in M9 medium supplemented with iron. This is fundamental given that iron is an essential prosthetic group. The M9 medium was chosen instead of LB medium because the last contains zinc in its composition that would be incorporated in the protein instead of iron. Transformed cells were selected due to ampicilin resistance conferred by the pMAL plasmid.

After harvesting the cells by centrifugation their weight was registered and the cellular yield was determined. Although only two growths of each protein were performed the expression of the different proteins does not seem to influence the cellular yield.

Similarly to what had been done to the expression tests samples of the non-induced and induced cells were analyzed in a 15% SDS-PAGE (Figure 3.2). In spite of the contaminants it is possible to observe the systematic over expression of other proteins along with the DRbr mutants, particularly in non-soluble fraction (Figure 3.2). Once again a considerable amount of the protein appears in the non-soluble fraction. Considering the high levels of protein obtained it is probably due to the formation of inclusion bodies. Anyway, given the high amount of protein in the soluble fraction there was no need to solubilise the protein from the inclusion bodies.

4.4 Biochemical characterization

The first step to study each protein was its purification. All protein containing samples obtained from the last purification step were analysed by UV-Vis spectroscopy and by SDS-PAGE.

4.4.1 Proteins purification

All proteins were successfully purified in three steps: anionic exchange, adsorption and size exclusion. During the purification is crucial that all steps are anaerobically performed to avoid protein

degradation. For the wild type protein this strategy seems efficient, given that the gels performed immediately after the purification showed no degradation of the protein (Figure 3.3). For the mutant proteins some degradation is observed in the gels, but this degradation is visible in the gels performed right after the growths (Figure 3.2), so that was not due to the purification process.

4.4.2 UV-Vis spectra

The UV-Vis spectra of all as isolated proteins are very similar (Figure 3.10). That means the mutations did not induce alterations in the UV-Vis spectra. UV-Vis spectra of diiron protein usually have a band between 300 and 400 nm (Makris *et al.*, 2010) (Figure 4.2), but in this case this is not visible due to the large molar absorptivity of the rubredoxin-like domains in that area of the spectrum. Given that the mutations under study are located near the diiron centre changes in the UV-Vis spectra were not expected.

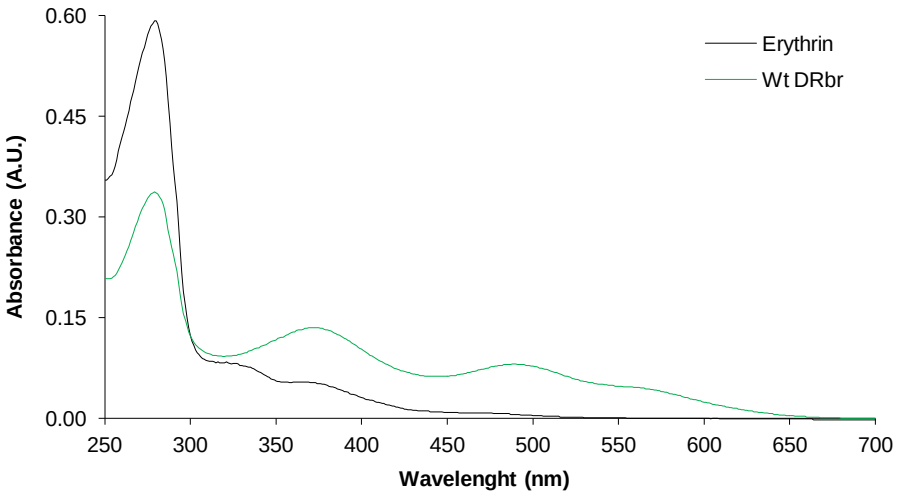

Figure 4.2: UV-Visible spectra of erythrin and desulforubrerythrin. The black line represents the UV-Vis spectrum of as isolated erythrin from *A. ambivalens* in 200 mM KPi pH 7.2. [4] The green line is the spectrum of as isolated wild type desulforubrerythrin in 20 mM Tris-HCl pH 7.2 plus 150 mM NaCl.

The absorption at 490 and 560 nm are typical features from rubredoxin-like domains (*e.g.*: Auchere *et al.*, 2004; Bruschi *et al.*, 1977; Shimizu *et al.*, 1989; Yoon, *et al.*, 1999) and are due to the ferric iron coordinated by four cysteines. The absorption at 370 is due to the $Fe(Cys)_4$ but also to the diiron centres in the ferric state (Coulter *et al.*, 1999; Coulter *et al.*, 2000).

Previously was determined a characteristic absorbance ratio of 3.7 between Abs_{280}/Abs_{490} for the wild type desulforubrerythrin (Pinto, 2012). For the mutant Y59F and Y127F proteins was possible to have, at least, one fraction with a ratio very close to 3.7 but for the wild type protein and for the double mutant this ratio was more distant from the reference value (Table 3.2). This could indicate the presence of contaminants or, given that the absorbance at 490 nm is dependent of the iron occupancy of Rd and Dx domains, another explanation could be the absence of iron in some protein monomers.

[4] Work performed by Joana Carrilho from the Metalloenzymes and Molecular Bioenergetics Group, ITQB-UNL.

In the case of the wild type protein neither option seems viable given that the sample in the SDS-PAGE gel is apparently free of contaminants and the TPTZ quantification yielded a result of 4 atoms of iron per monomer of protein. For the double mutant an explanation could be the absence of iron, but this hypothesis does not seem viable for two reasons: first, all the other absorbance ratios are very similar in all proteins; second, the EPR spectra of this protein show resonances characteristic from Rd and Dx domains.

The remainder ratios have some differences between the wild type protein and the Y59F mutant (both with 4 atoms of iron per monomer) and the Y127F mutant and the double mutant (with less than 4 atoms of iron per monomer). These small differences could be due to the absence of iron in some Dx or Rd domains.

4.4.3 Quantifications

The protein in the fractions resulting from the S-200 column was quantified through the BCA method. This allowed to evaluate the yield of each protein. The values obtained are around 23 mg of protein per litre of growth, except for the Y127F mutant which yield was 47 mg of protein per litre of growth (Table 3.1). In both set of growths the mutant Y127F always rendered more protein.

4.4.4 Oligomerization state in solution

The oligomerization state of the protein was determined by size exclusion chromatography. All proteins are present in a large cluster with a molecular mass between 353 kDa and 368 kDa. For the mutants the protein is in a tetrameric conformation with a molecular mass ranging between 106 and 109 kDa; accordingly with the monomeric molecular mass of the protein the tetramer should have approximately 97 kDa. The wild type protein is also present in this tetrameric form but the intensity of this peak much more reduced (Figure 3.12). Previous work performed with other rubrerythrins showed that rubrerythrins are isolate in solution as dimers, although they crystallize as tetramers (*e.g.*: Coulter *et al.*, 1999; Fushinobu *et al.*, 2003: Jin *et al.*, 2002; Li *et al.*, 2003), suggesting that the tetramer results from the dimerization of a dimer.

4.4.5 N-terminal sequencing

As seen in panel D from Figure 3.4, 3.5 and 3.6 the SDS-PAGE gels of the mutant proteins present several bands besides the 24 kDa one. To determine if these bands are the result of protein degradation or are contaminants a sample of the Y59F mutant was separated by electrophoresis and transferred to a PVDF membrane. The N-terminal sequences of each band were determined (Figure 3.13 and Table 3.6). The results for the N-terminal sequencing confirmed the 24 kDa band as being desulforubrerythrin. For all the other bands the results obtained are not so simple to interpret. The band with nearly 40 kDa is probably a contaminant, given that the determined sequence does not match the protein sequence. The band with 20 kDa presented an inconclusive result given the possibility of several different amino acids for each position. Given that none of the possibilities match

the sequence of the protein this should be a contaminant instead of a degradation product. All the bands with inferior molecular match the beginning of the protein. Their origin should be due to protein degradation, but the bands corresponding to the other product(s) of degradation are not visible in the SDS-PAGE gel, possibly due to their small size.

4.5 Into desulforubrerythrin metallic sites: EPR studies

EPR studies were performed to study the metallic centres of DRbr. This technique allows one to study the metallic centres, its composition and the redox state of each centre.

The spectrum of the as isolated wild type protein shows resonances characteristic of all iron centres proposed for the protein. The attribution of the resonances to each domain is made by comparison with spectra from other proteins known by sharing metallic sites with DRbr. The resonances at g-values lower than 2 are characteristic of diiron centres in the mixed-reduced state with S=1/2 (Kao *et al.*, Legall *et al.*, 1988; 2008; *Pierik et al.*, 1993; Yamasaki *et al.*, 2004). The resonances at higher g-values are typical for systems with S= 5/2. The assignment of the rubredoxin and desulforedoxin resonances is possible by comparing the spectrum with rubredoxins, desulfoferrodoxins, desulforedoxin from *D. gigas* and rubrerythrin from *D. vulgaris*. The resonances at g-values 3.65, 4.85 and 9.3 are due to the rubredoxin domain (Auchere *et al.*, 2004; Legall *et al.*, 1988; Zeng *et al.*, 1996). The desulforedoxin domain has resonances at g-values 8, 5.6 and 3.6 (Moura *et al.*, 1980). The resonance with g-value 4.3 is attributed to heterogeneous ferric sites (Pinto *et al.*, 2011).

The reduction potential of each metallic centre was determined by redox titration followed by EPR analysis. The rubredoxin centre has the lowest potential: 170 mV making this centre the entrance point for electrons. The diiron centre has potentials of 270 and 235 mV, respectively for the first and second transitions. This means that the rubredoxin domains receives the first electron and then transfers it to the diiron centre. After that another electron reduces the rubredoxin domain that, again, transfers the electron to the diiron domain. Just after the complete reduction of the diiron centre the rubredoxin will be reduced. The desulforedoxin domain was a potential of 200 mV and its function is still unknown. Accordingly with the redox potentials this domain should be reduced after the complete reduction of the diiron centre.

The only reduction potentials within the range of previously calculated values to rubrerythrins belong to the diiron centre (Gupta *et al.*, 1995). The reduction potential calculated for the rubredoxin is higher than its usual value in rubredoxins but lower than its value for rubredoxin domains in rubrerythrins. Rubredoxins usually have potentials between – 100 mV to 50 mV (Luo *et al.*, 2010; Moura *et al.*, 1979; Lee *et al.*, 1995) and between 230 and 281 mV in rubrerythrins (Legall *et al.*, 1988; Pierik *et al.*, 1993). The desulforedoxin domain has a potential much higher than desulforedoxin domains in desulfoferrodoxin that usually have values around 0 mV (Moura *et al.*, 1994; Verhagen *et al.*, 1993). Desulforedoxin from *D. gigas* has a potential of -35 mV (Archer *et al.*, 1999).

To try to find an explanation for the great diversity of values for rubredoxins and rubredoxin domains a multiple sequence alignment was performed. The proteins chosen have potentials ranging from -87 mV to +230 mV and belong to organisms from all life domains. Accordingly to some authors the reduction potential of rubredoxins may be influenced by the residues charge around the active site and also by hydrogen bonds (Bönisch *et al.*, 2007; Lin *et al.*, 2005).

To test the effect of hydrogen bonds strength in the reduction potential Lin and collaborators made studies on *Clostridium pasteurianum* rubredoxin. As they observed that rubredoxins with lower potential have a valine in the second position after the last cysteine ligand while rubredoxins with higher reduction potentials usually have an alanine. *C. pasteurianum* rubredoxin has a reduction potential of -77 mV and has a valine in position 44. In this study the authors constructed several mutants where the valine has replaced by a glycine, an alanine, an isoleucine and valine. For each protein they determined the reduction potential and the hydrogen bond length between residue 44 and the sulphur from cysteine 42 (Table 4.1). They also did the same considering valine in position 8 and cysteine in position 6. Their work showed a relation in the length of the hydrogen bond and in the reduction potential: amino acids in position 44 that establish a short hydrogen bond will increase the reduction potential. For the substitutions in position 8 the changes in the reduction potential are not so pronounced (Lin *et al.*, 2005).

Table 4.1: Reduction potentials of WT *C.pasteurianum* and its mutants (Adapted from Lin *et al.*, 2005).

Protein	Reduction potential (mV)
V44G	0
V44A	-24
V44I	-53
WT	-77
V44L	-87

Analysing the protein alignment in Figure 4.3 is possible to observe that all proteins with a valine two residues after the last cysteine that is involved in iron coordination have a negative reduction potential. In proteins with positive potential that position is mainly occupied by an alanine, but in some cases a tyrosine, a lysine or a serine replace the alanine. The rubredoxin domain of *C. jejuni* DRbr has an alanine and a potential of +170 mV, which is in agreement with the observed results for *C. pasteurianum* rubredoxin. Although this analysis helps to understand the different reduction potentials in rubredoxins this is not sufficient to explain the large range of values observed in these proteins, especially the high reduction potentials observed in rubrerythrins.

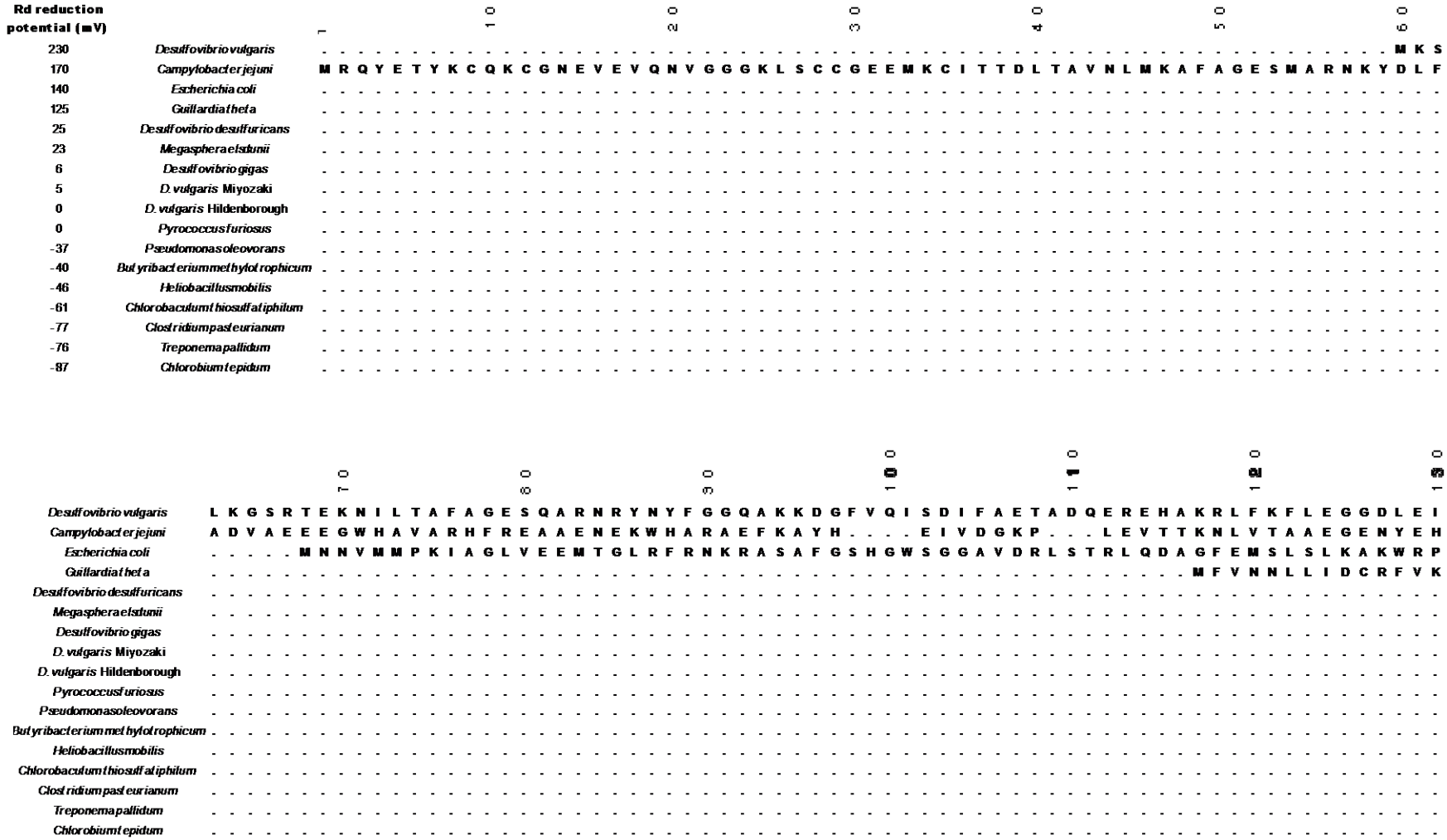
Rd reduction potential (mV)
1
10
20
30
40
50
60
70
80
90
100
110
120
130
230 Desulfovibrio vulgaris M K S
170 Campylobacter jejuni M R Q Y E T Y K C Q K C G N E V E V Q N V G G G K L S C C G E E M K C I T T D L T A V N L M K A F A G E S M A R N K Y D L F
140 Escherichia coli
125 Guillardia theta
25 Desulfovibrio desulfuricans
23 Megasphera elsdunii
6 Desulfovibrio gigas
5 D. vulgaris Miyozaki
0 D. vulgaris Hildenborough
0 Pyrococcus furiosus
-37 Pseudomonas oleovorans
-40 Butyribacterium methylotrophicum
-46 Heliobacillus mobilis
-61 Chlorobaculum thiosulfatiphilum
-77 Clostridium pasteurianum
-76 Treponema pallidum
-87 Chlorobium tepidum
Desulfovibrio vulgaris L K G S R T E K N I L T A F A G E S Q A R N R Y N Y F G G Q A K K D G F V Q I S D I F A E T A D Q E R E H A K R L F K F L E G G D L E I
Campylobacter jejuni A D V A E E E G W H A V A R H F R E A A E N E K W H A R A E F K A Y H . . . . E I V D G K P . . . L E V T T K N L V T A A E G E N Y E H
Escherichia coli . . . . . M N N V M M P K I A G L V E E M T G L R F R N K R A S A F G S H G W S G G A V D R L S T R L Q D A G F E M S L S L K A K W R P
Guillardia theta . . . . . M F V N N L L I D C R F V K
Desulfovibrio desulfuricans
Megasphera elsdunii
Desulfovibrio gigas
D. vulgaris Miyozaki
D. vulgaris Hildenborough
Pyrococcus furiosus
Pseudomonas oleovorans
Butyribacterium methylotrophicum
Heliobacillus mobilis
Chlorobaculum thiosulfatiphilum
Clostridium pasteurianum
Treponema pallidum
Chlorobium tepidum

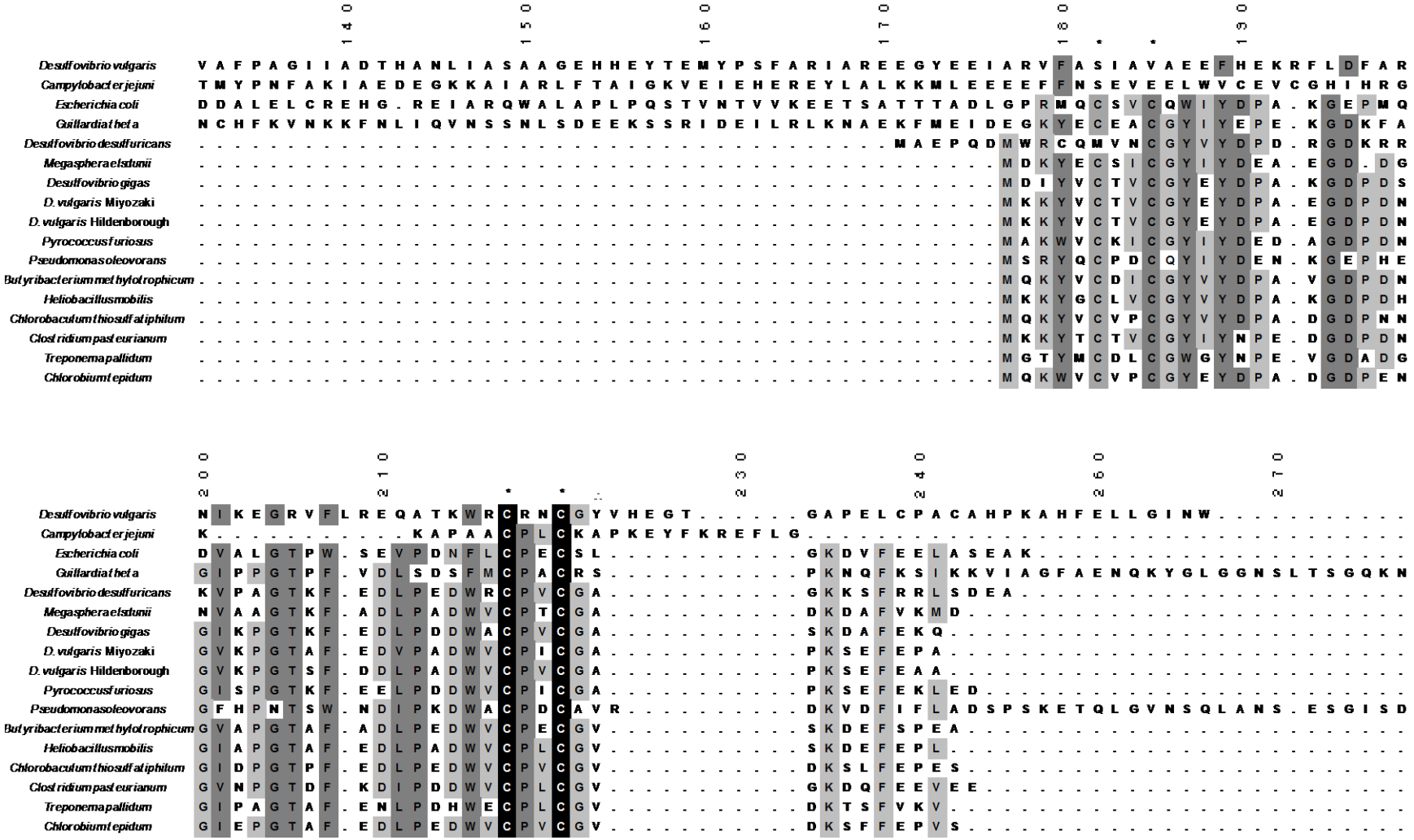
140
150
160
170
180
190
Desulfovibrio vulgaris V A F P A G I I A D T H A N L I A S A A G E H H E Y T E M Y P S F A R I A R E E G Y E E I A R V F A S I A V A E E F H E K R F L D F A R
Campylobacter jejuni T M Y P N F A K I A E D E G K K A I A R L F T A I G K V E I E H E R E Y L A L K K M L E E E E E F F N S E V E E L W V C E V C G H I H R G
Escherichia coli D D A L E L C R E H G . R E I A R Q W A L A P L P Q S T V N T V V K E E T S A T T T A D L G P R M Q C S V C Q W I Y D P A . K G E P M Q
Guillardia theta N C H F K V N K K F N L I Q V N S S N L S D E E K S S R I D E I L R L K N A E K F M E I D E G K Y E C E A C G Y I Y E P E . K G D K F A
Desulfovibrio desulfuricans . . . . . M A E P Q D M W R C Q M V N C G Y V Y D P D . R G D K R R
Megasphaera elsdunii . . . . . M D K Y E C S I C G Y I Y D E A . E G D . D G
Desulfovibrio gigas . . . . . M D I Y V C T V C G Y E Y D P A . K G D P D S
D. vulgaris Miyazaki . . . . . M K K Y V C T V C G Y E Y D P A . E G D P D N
D. vulgaris Hildenborough . . . . . M K K Y V C T V C G Y E Y D P A . E G D P D N
Pyrococcus furiosus . . . . . M A K W V C K I C G Y I Y D E D . A G D P D N
Pseudomonas oleovorans . . . . . M S R Y Q C P D C Q Y I Y D E N . K G E P H E
Butyribacterium methylotrophicum . . . . . M Q K Y V C D I C G Y V Y D P A . V G D P D N
Heliobacillus mobilis . . . . . M K K Y G C L V C G Y V Y D P A . K G D P D H
Chlorobaculum thiosulfatiphilum . . . . . M Q K Y V C V P C G Y V Y D P A . D G D P N N
Clostridium pasteurianum . . . . . M K K Y T C T V C G Y I Y N P E . D G D P D N
Treponema pallidum . . . . . M G T Y M C D L C G W G Y N P E . V G D A D G
Chlorobium tepidum . . . . . M Q K W V C V P C G Y E Y D P A . D G D P E N
200
210
230
240
260
270
Desulfovibrio vulgaris N I K E G R V F L R E Q A T K W R C R N C G Y V H E G T . . . . . G A P E L C P A C A H P K A H F E L L G I N W . . . . . .
Campylobacter jejuni K . . . . . K A P A A C P L C K A P K E Y F K R E F L G . . . . . .
Escherichia coli D V A L G T P W . S E V P D N F L C P E C S L . . . . . G K D V F E E L A S E A K . . . . . .
Guillardia theta G I P P G T P F . V D L S D S F M C P A C R S . . . . . P K N Q F K S I K K V I A G F A E N Q K Y G L G G N S L T S G Q K N
Desulfovibrio desulfuricans K V P A G T K F . E D L P E D W R C P V C G A . . . . . G K K S F R R L S D E A . . . . . .
Megasphaera elsdunii N V A A G T K F . A D L P A D W V C P T C G A . . . . . D K D A F V K M D . . . . . .
Desulfovibrio gigas G I K P G T K F . E D L P D D W A C P V C G A . . . . . S K D A F E K Q . . . . . .
D. vulgaris Miyazaki G V K P G T A F . E D V P A D W V C P I C G A . . . . . P K S E F E P A . . . . . .
D. vulgaris Hildenborough G V K P G T S F . D D L P A D W V C P V C G A . . . . . P K S E F E A A . . . . . .
Pyrococcus furiosus G I S P G T K F . E E L P D D W V C P I C G A . . . . . P K S E F E K L E D . . . . . .
Pseudomonas oleovorans G F H P N T S W . N D I P K D W A C P D C A V R . . . . . D K V D F I F L A D S P S K E T Q L G V N S Q L A N S . E S G I S D
Butyribacterium methylotrophicum G V A P G T A F . A D L P E D W V C P E C G V . . . . . S K D E F S P E A . . . . . .
Heliobacillus mobilis G I A P G T A F . E D L P A D W V C P L C G V . . . . . S K D E F E P L . . . . . .
Chlorobaculum thiosulfatiphilum G I D P G T P F . E D L P E D W V C P V C G V . . . . . D K S L F E P E S . . . . . .
Clostridium pasteurianum G V N P G T D F . K D I P D D W V C P L C G V . . . . . G K D Q F E E V E E . . . . . .
Treponema pallidum G I P A G T A F . E N L P D H W E C P L C G V . . . . . D K T S F V K V . . . . . .
Chlorobium tepidum G I E P G T A F . E D L P E D W V C P V C G V . . . . . D K S F F E P V S . . . . . .

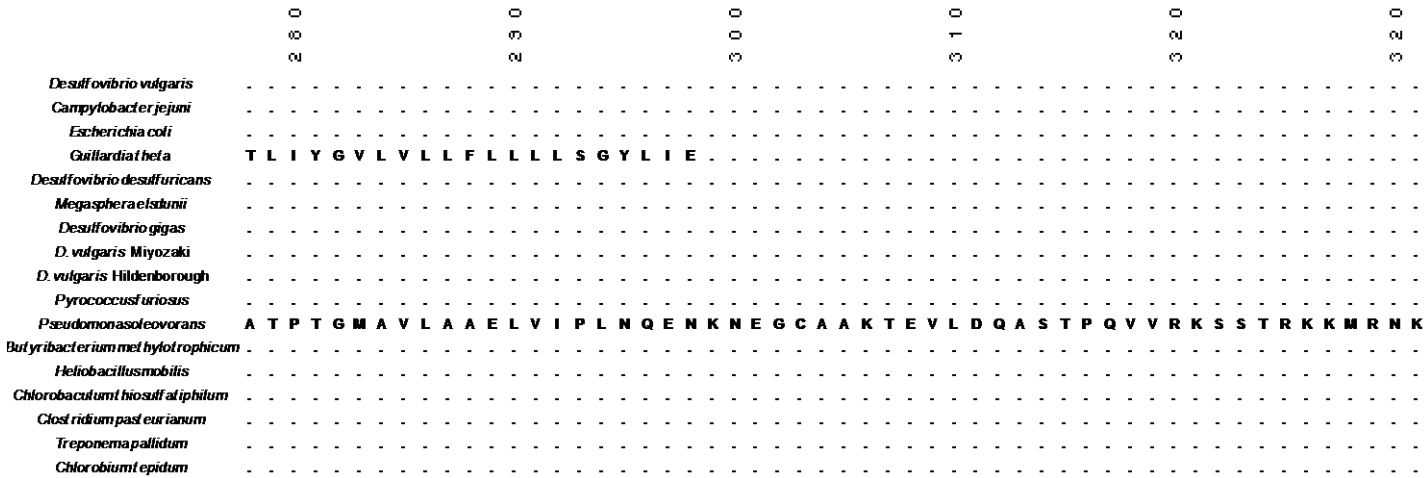

Figure 4.3: Multiple sequence alignment of rubrerythrins using Clustal X. Strictly conserved residues are in black boxes, dark grey boxes point highly conserved residues and light grey boxes mark conserved residues. Iron ligand are indicated by "*" and residue corresponding to alanine 47 in *C. pasteurianum* rubredoxin is indicated by "∴".
All sequences are from the Uniprot website. *D. vulgaris* rubrerythrin: P24931; *C. jejuni* DRbr: Q0PCB3; *E. coli* rubredoxin: F9CLA6; *Guillardia theta* rubredoxin: Q9XG40; *D. desulfuricans* Rubredoxin: Q93PP8; *Megasphaera elsdenii* rubredoxin: P00271; *D. gigas* rubredoxin: P00270; *D. vulgaris* Miyazaki rubredoxin: P15412; *D. vulgaris* Hildenborough rubredoxin; *Pyrococcus furiosus* rubredoxin: P24297; *Pseudomonas oleovarans* rubredoxin: P12692; *Butyribacterium methylotrophicum* rubredoxin: P14071; *Heliobacillus mobilis* rubredoxin: P5663; *Chlorobaculum thiosulfatiphilum* rubredoxin. B3QL56; *Treponema pallidum* rubredoxin O83956; *Clostridium pasteurianum* rubredoxin: P00268; *Chlorobium tepidum* rubredoxin: P58025.

4.6 Final remarks

The work here described pretends to be a step in the comprehension of resistance to reactive oxygen species in microorganisms. In this particular case the protein under study belongs to a pathogenic bacterium responsible for a high number of gastroenteritis all over the world. As with other bacteria the resistance to antibiotics is a serious problem, which makes unviable the use of these substances to control the presence of *C. jejuni* in chicken and poultry, in which it inhabits as a commensal. The resistance to antibiotics can also become a problem in the treatment of infected humans. This makes urgent to identify new targets with anti-microbial function. To accomplish that objective is important to understand the metabolism of the microorganism, mainly the pathways involved with survival inside the host. One of the defences of the innate immune system against pathogens is the production of reactive oxygen species, so pathogen bacteria must be well equipped to fight these species. A profound knowledge of how bacteria overcome that barrier may help to provide new drugs to combat bacterial infections.

To verify the existence of the DRbr in other *C. jejuni* strains, and eventually in other bacteria of the same genus a search was performedat the Uniprot website. The results showed that 19 strains of *C. jejuni* have a protein with 100% of identity with the protein under study. Moreover, 42 strains of *C. jejuni* also have a protein 99 % identical with *C. jejuni* NCTC 11168 DRbr. Finally, proteins with 97 % of identity are present in several strains of *Campylobacter coli*. So, this protein is present in all strains of *Campylobacter.*

As seen before, detoxification of hydrogen peroxide is performed by a great diversity of proteins, so at first sight studying another protein with the same function may seem redundant. It is important to refute that idea. Although all proteins have the same function they are active under different circumstances that depend on substrate concentration, co-factors availability (iron, manganese), availability of reduction potential in the cell (NAD(P)H) and of other electron donor proteins (Winterbourn, 2008). Hydrogen peroxide is able to penetrate membranes and gives rise to the hydroxyl radical, so cells cannot rely on one single type of molecule to reduce hydrogen peroxide to water.

With this work was possible to biochemically characterize three proteins expressed for the first time. It was shown that the mutations did not affect the biochemical properties of the protein. Also, the metallic domains were found in all proteins.

It was possible to obtain crystals suitable for Xray diffraction for the wild type, Y59F and double mutants and solve their structures.

The next step in this work would be the determination of the NADH:peroxidase activities for the mutant proteins and compare with the values previously determined to the wild type protein. One intriguing aspect that remains is the function of the desulforedoxin domain. Given the reduction potentials of the domains and the spatial localization, it is not likely to transfer electrons to the catalytic one. One possibility is that this domain function as a sensor of hydrogen peroxide, leading to protein degradation upon exposure to high concentrations of hydrogen peroxide. In a more advanced phase of the work would be important to perform complementation assays using a broad range of

concentrations of H_2O_2 in *E. coli* strains lacking some hydrogen peroxide detoxifying proteins to confirm the *in vivo* function of the protein and also to determine the range of substrate concentrations in which it is active. Finally would be desirable to perform that complementation tests in *C. jejuni* and try to identify the physiological electron donors of the protein.

5 REFERENCES

Agnez-Lima, L.F., Melo, J.T., Silva, A.E., Oliveira, A.H., Timoteo, A.R., Lima-Bessa, K.M., Martinez, G.R., Medeiros, M.H., Di Mascio, P., Galhardo, R.S. and Menck, C.F. 2012. DNA damage by singlet oxygen and cellular protective mechanisms. Mutation research 751: 15-28.

Aguirre, J.D. and Culotta, V.C., 2012. Battles with iron: manganese in oxidative stress protection. The Journal of biological chemistry 287: 13541-13548.

Alfadda, A.A and Sallam, R.M. 2012. Reactive Oxygen Species in Health and Disease. Journal of Biomedicine and Biotechnology 2012

Alterkruse, S.F., Stern, N.J., Fields, P.I. and Swerdlow, D.L. 1999. *Campylobacter jejuni* – An Emerging Foodborne Pathogen. Emerging Infection Diseases 5: 28-35

Andrews, S.C., 1998. Iron storage in bacteria. Advances in microbial physiology 40: 281-351.

Andrews, S.C., 2010. The Ferritin-like superfamily: Evolution of the biological iron storeman from a rubrerythrin-like ancestor Biochimica et biophysica acta 1800: 691-705

Atack, J.M., Harvey, P., Jones, M.A. and Kelly, D.J. 2008. The *Campylobacter jejuni* Thiol Peroxidases Tpx and Bcp Both Contribute to Aerotolerance and Peroxide-Mediated Stress Resistance but Have Distinct Substrate Specificities. Journal of Bacteriology 190: 5279-5290

Atack, J.M. and Kelly, D.J. 2009. Oxidative stress in *Campylobacter jejuni*: responses, resistance and regulation. Future Microbiology 4: 677-690.

Archer, M., Huber, R., Tavares, P., Moura, I., Moura, J.G., Carrondo, M.A., Sieker, L., C., LaGall, J., and Romão, M.J. 1995. Crystal Structure of Desulforedoxin from *Desulfovibrio vulgarisi* Determined at 1.8 Å Resolution: A Novel Non-heme Iron Protein Structure. Journal of Molecular Biology 251: 690-702.

Archer, M., Carvalho, A.L., Teixeira, S., Moura, I., Moura, J.J., Rusnak, F. and Romao, M.J. 1999. Structural studies by X-ray diffraction on metal substituted desulforedoxin, a rubredoxin-type protein. Protein science: a publication of the Protein Society 8: 1536-1545.

Auchere, F., Sikkink, R., Cordas, C., Raleiras, P., Tavares, P., Moura, I. and Moura, J.J.G. 2004. Overexpression and purification of *Treponema pallidum* rubredoxin; kinetic evidence for a superoxide-mediated electron transfer with the superoxide reductase neelaredoxin. Journal of Biological Inorganic Chemistry 9: 839-849.

Baillon, M.L.A., van Vliet, A.H.M., Ketley, J.M., Constantinidou, C. and Penn, C.W. 1999. An iron-regulated alkyl hydroperoxide reductase (AhpC) confers aerotolerance and oxidative stress resistance to the microaerophilic pathogen *Campylobacter jejuni*. Journal of bacteriology 181: 4798-4804.

Bartz, R.R. and Piantadosi, C.A., 2010. Clinical review: oxygen as a signaling molecule. Critical Care 14: 234-243.

Bentrop, D., Capozzi, F. and Luchinat, C. 2001. Iron-Sulfur Proteins With Known Structures. In Handbook on Metalloproteins (I. Bertini, A. Sigel and H. Sigel eds), pp 357 - 447, Marcel Dekker, New York

Bingham-Ramos, L.K. and Hendrixson, D.R. 2008. Characterization of Two Putative Cytochrome *c* Peroxidases of *Campylobacter jejuni* Involved in Promoting Commensal Colonization of Poultry. Infection and Immunity 76: 1105:1114

Birben, E., Sahiner, U.M., Sackesen, C., Erzurum and S., Kalayci, O. 2012. Oxidative stress and antioxidant defense. The World Allergy Organization journal 5: 9-19.

Bönisch, H., Schmidt, C.L., Bianco, P. and Ladenstein, R. 2007. Ultrahigh-resolution study on *Pyrococcus abyssi* rubredoxin: II. Introduction of an O-H···Sγ-Fe hydrogen bond increased the reduction potential by 65 mV. Journal of Biological Inorganic Chemistry 12: 1163-1171.

Brenner, D.J., Krieg, N.R. and Staley, J.T. 2005. Bergey's Manual of Systematic Bacteriology, Volume Two, Part C. Springer, USA

Brieger, K., Schiavone, S., Miller, F.J., Jr. and Krause, K.H. 2012. Reactive oxygen species: from health to disease. Swiss medical weekly 142.

Bucher, J., Flint, A., Stahl, M. and Stintz A. 2010. *Campylobacter* Fur and PerR Regulons in Iron Uptake and Homeostasis in Microorganisms (P. Cornelis and S.C. Andrews eds.) pp167-195, Caister Academic Press, Northfolk UK.

Burton, G.J. and Jauniaux, E., 2011. Oxidative stress. Best practice & research. Clinical obstetrics & gynaecology 25: 287-299.

Butcher, J., Sarvan, S., Brunzelle, J., Couture, J-F. and Stintzi, A. 2012. Structure and regulon of *Campylobacter jejuni* ferric uptake regulator Fur define apo-Fur regulation. Proceedings of the National Academy of Sciences of the Unites States of America 19: 10047-10052.

Bruschi, M., Hatchikian, C.E., Golovleva, L.A. and Gall, J.L. 1977. Purification and characterization of cytochrome c3, ferredoxin, and rubredoxin isolated from *Desulfovibrio desulfuricans* Norway. Journal of bacteriology 129: 30-38.

Cooley, R.B., Arp, D.J. and Karplus, P.A. 2011. Symerythrin structures at atomic resolution and the origins of rubrerythrins and the ferritin-like superfamily. Journal of molecular biology 413: 177-194.

Cornelis, P. and Andrews, S.C. 2010. Iron Uptake and Homeostasis in Microorganisms. Caister Academic Press, Northfolk, UK

Coulter, E.D., Shenvi, N.V., and Kurtz, D.M. 1999. NADH peroxidase activity of rubrerythrin. Biochemical and biophysical research communications 255: 317-323.

Coulter, E.D., Shenvi, N.V., Beharry, Z.M., Smith, J.J., Prickril, B.C., and Kurtz, D.M. 2000. Rubrerythrin-catalyzed substrate oxidation by dioxygen and hydrogen peroxide. Inorganica Chimica Acta 297: 231-241

Damo, S., Chazin, W.J., Skaar, E.P. and Kehl-Fie, T.E., 2012. Inhibition of bacterial superoxide defense: a new front in the struggle between host and pathogen. Virulence 3: 325-328.

Dasti, J.I., Tareen, A.M., Lugert, R., Zautner, A.E. and Groβ, U. 2010. *Campylobacter jejuni*: A brief overview on pathogenecity-associated factors and disease-mediating mechanisms. International Journal of Medical Microbiology 300: 205-211

Day, W. A.Jr., Sajecki, J.L., Pitts, T.M. and Joens, L.A. 2000. Role of Catalase in *Campylobacter jejuni* Intracellular Survival. Infection and Immunity 68: 6337-6345

Droge, W., 2002. Free radicals in the physiological control of cell function. Physiological reviews 82: 47-95.

Engberg, J., Aarestrup, F.M., Taylor, D.E., Gerner-Smidt, P. and Nachamkin, I. 2001. Quinolone and macrolide resistance in *Campylobacter jejuni* and *C. coli*: Resistance mechanisms and trends in human isolates. Emerging infectious diseases 7: 24-34.

Finnegan, M., Linley, E., Denyer, S.P., McDonnell, G., Simons, C. and Maillard, J.Y., 2010. Mode of action of hydrogen peroxide and other oxidizing agents: differences between liquid and gas forms. The Journal of antimicrobial chemotherapy 65: 2108-2115.

Fischer, D.S. and Price, D. C. 1964. A Simple Serum Iron Method Using the New Sensitive Chromogen Tripyridyl-s-triazine. Clinical Chemistry 10: 21-31

Fridovich, I., 2013. Oxygen: how do we stand it? Medical principles and practice. International journal of the Kuwait University, Health Science Centre 22: 131-137.

Fushinobu, S., Shoun, H. and Wakagi, T. 2003. Crystal structure of sulerythrin, a rubrerythrin-like protein from a strictly aerobic archaeon, *Sulfolobus tokodaii* strain 7, shows unexpected domain swapping. Biochemistry 42: 11707-11715.

Gupta, N., Bonomi, F., Kurtz, D.M., Ravi, N., Wang, D.L. and Huynh, B.H. 1995. Recombinant *Desulfovibrio vulgaris* Rubrerythrin - Isolation and Characterization of the Diiron Domain. Biochemistry 34: 3310-3318.

Gupta, R.S. 2006. Molecular signatures (unique proteins and conserved indels) that are specific for the epsilon proteobacteria (*Campylobacterales*). BMC Genomics 7: 167

Hagen, W.R. 2006. EPR spectroscopy as a probe of metal centres in biological systems. Dalton Transactions 37: 4415-4434

Hoffman, P.S. and Goodman, T.G. 1982. Respiratory Physiology and Energy Conservation Efficiency of *Campylobacter jejuni*. Journal of Bacteriology 150: 319-326

Holmes, K., Mulholland, F., Pearson, B.M., Pin, C., McNicholl-Kennedy, J., Ketley, J.M. and Wells, J.M. 2005. *Campylobacter jejuni* gene expression in response to iron limitation and the role of Fur. Microbiology 151: 243-257.

Hu, L., Bray, M.D., Osorio, M. and Kopecko, D.J. 2006. *Campylobacter jejuni* Induces Maturation and Cytokine Production in Human Dendritic Cells. Infection and Immunity 74:2697-2705

Huergo, L.F., Rahman, H., Ibrahimovic, A., Day, C.J. and Korolik, V. 2013. *Campylobacter jejuni* Dps Protein Binds DNA in the Presence of Iron or Hydrogen Peroxide. Journal of Bacteriology 195: 1970-1978.

Ishikawa, T., Mizunoe, Y., Kawabata, S., Takade, A., Harada, M., Wai, S.N. and Yoshida, S. 2003. The Iron-Binding Protein Dps Confers Hydrogen Peroxide Stress Resistance to *Campylobacter jejuni*. Journal of Bacteriology 185: 1010-1017.

Janssen, R., Krogfelt,K.A., Cawthraw, S.A., van Pelt, W., Wagenaar, J.A. and Owen, R.J. 2008. Host-Pathogen Interactions in *Campylobacter* Infections: the Host Perspective. Clinical Microbiology Reviews 21:505-518.

Jin, S., Kurtz, D.M., Liu, Z.J., Rose, J. and Wang, B.C. 2002. X-ray crystal structures of reduced rubrerythrin and its azide adduct: A structure-based mechanism for a non-heme diiron peroxidase. Journal of the American Chemical Society 124: 9845-9855.

Jena, N.R. 2012. DNA damage by reactive species: Mechanisms, mutation and repair. Journal of biosciences 37: 503-517.

Kaakoush N.O., Miller, W.G., Reuse, H.D. and Mendz, G.L. 2007. Oxygen requirement and tolerance of *Campylobacter jejuni*. Research in Microbiology 158: 644-650.

Kassem, I.I, Khatri, M., Esseili, M., Sanad, Y.M., Saif, Y.M., Olson, J.W. and Rajashekara, G. 2012. Respiratory proteins contribute differentially to *Campylobacter jejuni*'s survival and in vitro interactions with hosts' intestinal cells. BMC Microbiology 12.

Kao, W.C., Wang, V.C.C., Huang, Y.C., Yu, S.S.F., Chang, T.C. and Chan, S.I. 2008. Isolation, purification and characterization of hemerythrin from *Methylococcus capsulatus* (Bath). Journal of Inorganic Biochemistry 102: 1607-1614.

Kim, M., Hwang, S., Ryu, S. and Jeon, B. Regulation of *perR* Expression by Iron and *PerR* in *Campylobacter jejuni*. Journal of Bcateriology 193:6171-6178

Konkel, M.E., Klena, J.D., Rivera-Amill, V., Monteville, M.R., Biswas, D., Raphael, B. and Mickelson J. 2004. Secretion of Virulence Proteins from *Campylobacter jejuni* Is Dependent on a Functional Flagellar Export Apparatus. Journal of Bacteriology 186:3296-3303.

Lee, W.Y., Brune, D.C., Lobrutto, R. and Blankenship, R.E. 1995. Isolation, Characterization, and Primary Structure of Rubredoxin from the Photosynthetic Bacterium, *Heliobacillus mobilis*. Archives of biochemistry and biophysics 318: 80-88.

Legall, J., Prickril, B.C., Moura, I., Xavier, A.V., Moura, J.J.G. and Huynh, B.H. 1988. Isolation and Characterization of Rubrerythrin, a Non-Heme Iron Protein from *Desulfovibrio vulgaris* That Contains Rubredoxin Centers and a Hemerythrin-Like Binuclear Iron Cluster. Biochemistry 27: 1636-1642.

Li, M., Liu, M.Y., Le Gall, J., Gui, L.L., Liao, J., Jiang, T., Zhang, J.P., Liang, D.C. and Chang, W.R. 2003. Crystal structure studies on rubrerythrin: enzymatic activity in relation to the zinc movement. Journal of Biological Inorganic Chemistry 8: 149-155.

Lin, I.J., Gebel, E.B., Machonkin, T.E., Westler, W.M. and Markley, J.L. 2005. Changes in hydrogen-bond strengths explain reduction potentials in 10 rubredoxin variants. Proceedings of the National Academy of Sciences of the United States of America 102: 14581-14586.

Lindmark, B., Rompikuntal, P.K., Vaitkevicius, K., Song, T., Mizunoe, Y., Uhlin, B.E., Guerry, P. and Wai, S.N. 2009. Outer membrane vesicle-mediated release of cytolethal distendingtoxin (CDT) from *Campylobacter jejuni*. BMC Microbiology 9:220.

Linley, E., Denyer, S.P., McDonnell, G., Simons, C. and Maillard, J.Y., 2012. Use of hydrogen peroxide as a biocide: new consideration of its mechanisms of biocidal action. The Journal of antimicrobial chemotherapy 67: 1589-1596.

Lumpio, H.L., Shenvi, N.V, Summers, A.O., Voordouw, G. and Kurtz, D.M. Jr. 2001. Rubrerythrin and Rubredoxin Oxidoreductase in *Desulfovibrio vulgaris*: a Novel Oxidative Stress Protection System. Journal of Bacteriology 183: 101-108.

Luo, Y., Ergenekan, C.E., Fischer, J.T., Tan, M.L. and Ichiye, T. 2010. The Molecular Determinants of the Increased Reduction Potential of the Rubredoxin Domain of Rubrerythrin Relative to Rubredoxin. Biophysical journal 98: 560-568.

Makris, T.M., Chakrabarti, M., Munck, E. and Lipscomb, J.D. 2010. A family of diiron monooxygenases catalyzing amino acid beta-hydroxylation in antibiotic biosynthesis. Proceedings of the National Academy of Sciences of the United States of America 107: 15391-15396.

Miyamoto, T., Asahina, Y., Miyazaki, S., Shimizu, H., Ohto, U., Noguchi, S. and Satow, Y. 2011. Structures of the SEp22 dodecamer, a Dps-like protein from *Salmonella enterica* subsp. *enteric* serovar Enteritidis. Acta Crystallographica 67: 17-22

Moura, I., Moura, J.J.G., Santos, M.H., Xavier, A.V. and Legall, J. 1979. Redox Studies on Rubredoxins from Sulfate and Sulfur Reducing Bacteria. FEBS letters 107: 419-421.

Moura, I., Huynh, B.H., Hausinger, R.P., Le Gall, J., Xavier, A.V. and Munck, E. 1980. Mossbauer and EPR studies of desulforedoxin from *Desulfovibrio gigas*. The Journal of biological chemistry 255: 2493-2498.

Moura, I., Tavares, P. and Ravi, N. 1994. Characterization of three proteins containing multiple iron sites: rubrerythrin, desulfoferrodoxin, and a protein containing a six-iron cluster. Methods in enzymology 243: 216-240.

Mydel, P., Takahashi, Y., Yumoto, H., Sztukowska, M., Kubica, M., Gilbson, F.C., Kurtz, D.M., Travis, J., Collins, L.V, Nguyens, K., Genco, C.A. and Potempai J. 2006. Roles of the Host Oxidative Immune Response and Bacterial Antioxidant Rubrerythrin during *Porphyromonas gingivalis* Infection. PLOS Pathogens 2: 712-725.

Ohara, M., Oswald, E. and Sugai M. 2004. Cytolethal Distending Toxin: A Bacterial Bullet Targeted to Nucleus. Journal of Biochemistry 136:409-413

Palyada, K., Threadgill, D. and Stintzi, A.2004. Iron Acquisition and Regulation in *Campylobacter jejuni*. Journal of Bacteriology 186:4714-4729

Palyada, K. Sun, Y.Q., Flint, A., Butcher, J., Naikare, H. and Stintzi, A. 2009. Characterization of the oxidative stress stimulon and PerR regulon of *Campylobacter jejuni*. BMC Genomics 10:481

Parkhill, J., Wren, B.W., Mungall, K. Ketley, J.M., Churcher, C., Basham, D., Chillingworth, T., Davies, R.M., Feltwell, T., Holroyd, S., Jagels, K., Karlyshev, A.V., Moule, S., Pallen, M.J., Pennk, C.W., Quail, M.A., Rajandream, M-A., Rutherford, K.M., van Vliet, H.M., Whitehead, S. and Barrel, B.G. 2000. The genome sequence of the food-borne pathogen *Campylobacter jejuni* reveals hypervariable sequences. Nature 403: 665-668

Pesci, E.C., Cottle, D.L. and Picket, C.L. 1994. Genetic, Enzymatic, and Pathogenic Studies of the Iron Superoxide Dismutase of *Campylobacter jejuni*. Infection and Immunity 62: 2687-2694.

Pi, H.L., Jones, S.A., Mercer, L.E., Meador, J.P., Caughron, J.E., Jordan, L., Newton, S.M., Conway, T. and Klebba, P.E. 2012. Role of Catecholate Siderophores in Gram-Negative Bacterial Colonization of the Mouse Gut. PloS one 7.

Pierik, A.J., Wolbert, R.B., Portier, G.L., Verhagen, M.F. and Hagen, W.R. 1993. Nigerythrin and rubrerythrin from *Desulfovibrio vulgaris* each contain two mononuclear iron centers and two dinuclear iron clusters. European journal of biochemistry / FEBS 212: 237-245.

Pinto, A.F., Todorovic, S., Hildebrandt, P., Yamazaki, M., Amano,F., Igimi, S., Romão, C.V. and Teixeira, M. 2011. Desulforubrerythrin from *Campylobacter jejuni*, a novel multidomain protein. Journal of Biological Inorganic Chemistry 13: 501-510

Pinto, A.F. 2012. Reductive scavenging of reactive oxygen species in prokaryotes, Rubrerythrin and Superoxide Reductase. Ph.D Thesis. Instituto de Tecnologia Química e Biológica, Universidade Nova de Lisboa

Putz, S., Gelius-Dietrich, G., Piotrowski, M. and Henze, K. 2005. Rubrerythrin and peroxiredoxin: Two novel putative peroxidases in the hydrogenosomes of the microaerophilic protozoon *Trichomonas vaginalis*. Molecular and biochemical parasitology 142: 212-223.

Rhee, S.G., Woo, H.A., Kil, I.S. and Bae, S.H., 2012. Peroxiredoxin functions as a peroxidase and a regulator and sensor of local peroxides. The Journal of biological chemistry 287: 4403-4410.

Sahu I.D., McCarrick, R.M. ND Lorigan, G.A. 2013. Use of Electron Paramagnetic Resonance To Solve Biochemical Problems. Biochemistry 52: 5967-5984

Sansonetti, P.J. and Di Santo, J.P. 2007. Debugging how bacteria manipulate the immune response. Immunity 26: 149-161.

Shimizu, F., Ogata, M., Yagi, T., Wakabayashi, S. and Matsubara, H. 1989. Amino-Acid-Sequence and Function of Rubredoxin from *Desulfovibrio-Vulgaris* Miyazaki. Biochimie 71: 1171-1177.

Smith, M.A., Finel, M., Korolik, V. and Mendtz G.L. 2000. Characteristics of the aerobic respiratory chains of the microaerophilics *Campylobacter jejuni* and *Helicobacter pylori*. Archives of Microbiology 174: 1-10

Sztukowsaka M., Bugno M., Potempa, J., Travis, J. and Kurtz, D.M. 2002. Role of rubrerythrin in the oxidative stress responseof *Porphyromonas gingivalis*. Molecular Microbiology 44: 479-488

Todar, K. 2008. Important groups of Procaryotes. Version 1st September 2013. http://textbookofbacteriology.net/procaryotes.html in Todar's Online Textbook of Bacteriology, http://textbookofbacteriology.net

Verhagen, M.F., Voorhorst, W.G., Kolkman, J.A., Wolbert, R.B. and Hagen, W.R. 1993. On the two iron centers of desulfoferrodoxin. FEBS letters 336: 13-18.

Vliet, A.H. van, Ketley, J.M., Park, S.F. and Penn, C.W. 2002. The role of iron in *Campylobacter* gene regulation, metabolism and oxidative stress defense. FEMS microbiology reviews 26: 173-186.

Wainwright, L.M., Elvers,K.T., Park., S.F. and Poole, R.K. 2005. A truncated haemoglobin implicated in oxygen metabolism by the microaerophilic food-borne pathogen *Campylobacter jejuni*. Microbiology 151: 4079-4091

Wakagi, T. 2003. Sulerythrin, the smallest member of the rubrerythrin family, from a strictly aerobic and thermoacidophilic archaeon, *Sulfolobus tokodaii* strain 7. FEMS Microbiology Letters 222: 33-37

Weinberg, M.V., Jenney, F.E., Jr., Cui, X. and Adams, M.W., 2004. Rubrerythrin from the hyperthermophilic archaeon *Pyrococcus furiosus* is a rubredoxin-dependent, iron-containing peroxidase. Journal of bacteriology 186: 7888-7895.

Wiinterbourn, C.C. 2008. Reconciling the chemistry and biology of reactive oxygen species. Nature Chemical Biology. 4:278-286.

Wood, P.M., 1988. The potential diagram for oxygen at pH 7. The Biochemical journal 253: 287-289.

Yamasali, M., Igimi, S., Katayama, Y., Yamamoto, S. and Amano, F. 2004. Identification of an oxidative stress-sensitive protein from *Campylobacter jejuni*, homologous to rubredoxin oxidoreductase/rubrerythrin. FEMS Microbiology Letters 235: 57-63

Yoon, K.S., Hille, R., Hemann, C. and Tabita, F.R. 1999. Rubredoxin from the green sulfur bacterium *Chlorobium tepidum* functions as an electron acceptor for pyruvate ferredoxin oxidoreductase. Journal of Biological Chemistry 274: 29772-29778.

Young, K., Davis, L.M., DiRita, V.J. 2007. *Campylobacter jejuni*: molecular biology and pathogenesis. Nature Reviews Microbiology 5: 665-679.

Zhang, Y., Liu, L., Wu, X., An, X., Stubbe, J. and Huang, M. 2011. Investigation of in vivo diferric tyrosyl radical formation in *Saccharomyces cerevisiae* Rnr2 protein: requirement of Rnr4 and contribution of Grx3/4 AND Dre2 proteins. The Journal of biological chemistry 286: 41499-41509.

Zeng, Q.D., Smith, E.T., Kurtz, D.M. and Scott, R.A. 1996. Protein determinants of metal site reduction potentials: Site-directed mutagenesis studies of *Clostridium pasteurianum* rubredoxin. Inorganica Chimica Acta 242: 245-251.

Zheng, J., Meng, J., Zhao, S., Singh, R. and Song, W. 2008. *Campylobacter*-Induced Interleukin-8 Secretion in Polarized Human Intestinal Epithelial Cells Requires *Campylobacter*-Secreted Cytolethal Distending Toxin- and Toll-Like Receptor-Mediated Activation of NF-κB. Infection and Immunity 76: 4498-4508.

Zhou, B., Shao, J., Su, L., Yuan, Y.C., Qi, C., Shih, J., Xi, B., Chu, B. and Yen, Y. 2005. A dityrosyl-diiron radical cofactor center is essential for human ribonucleotide reductases. Molecular cancer therapeutics 4: 1830-1836.

6 APPENDIX

6.1 Electronic Paramagnetic Resonance

Electronic Paramagnetic Resonance (EPR) is a technique used to study species with unpaired electrons, which limits the use of this technique but also increases its specificity. Each electron has an associated spin number (S) with a value of 1/2 and can exist with a quantum state ±1/2. In the absence of a magnetic field those states are degenerate (have the same energy), but when a magnetic field is applied the energy of the negative state decreases and the energy of the positive state increases. The energy between the two levels is $g\beta_e B_0$, where g is a characteristic of the electron, β_e is the electron Bohr magneton and B_0 is the magnetic affecting the electron (that results both from the external magnetic field applied and the field generate by the molecule nucleus). In an EPR experiment the frequency of the radiation is constant and the field varies within a determined range. When the microwave radiation energy equals the energy difference between the two levels there is absorption of energy that is converted into a spectrum. Usually the result is shown as the derivative of the signal and not the signal itself. At this point is possible to determine the g-value of the system, which allows characterize the system.

In biology EPR is particularly useful in the study of molecules with transition metals (*e.g.*: Fe, Co, Mn) or molecules harbouring radicals (Hagen 2006; Sahu *et al.*,2013)

6.2 List of reagents and proteins used to perform the experimental work

Product	Brand/Seller
Acetic acid glacial	Panreac
Acrylamide 30%	Roth
Agar	Fragon
Aldolase	Sigma Aldrich
Albumin, from chicken egg	Sigma Aldrich
Ammonium acetate	Fisher Chemicals
Ammonium hydroxide	Fluka
Ammonium chloride	Panreac
Ammonium Persulfate (APS)	Roth
Ampicilin sodium salt	Sigma Aldrich
Anthraquinone-2-sulfonic	Sigma Aldrich
Aprotinin	Sigma Aldrich
BCA Reagents A and B	Pierce
BSA, protein standard for BCA	Sigma Aldrich
Bicine	Sigma Aldrich
Blue Dextran	Sigma Aldrich
Brilliant Blue G	ACROS
Bromophenol Blue	Sigma Aldrich
Calcium chloride dihydrate	Merck
Cyclohexylamino propanesulphonic acid (CAPS)	Roth
Catalase	Sigma Aldrich
Conalbumin	Sigma Aldrich
di-Sodium Hydrogen Phospate (Na_2HPO_4)	Panreac
di-Potassium Hydrogen Phosphate anhydrous (K_2HPO_4)	Panreac
D-Glucose	Roth
DNAse I	Applichem
Ethanol (Absolute)	Scharlau
Ferritin, type I from horse spleen	Sigma Aldrich

Glutathione reduced form GSH	Sigma Aldrich
Glycerol 86-88%	Scharlau
Glycerol 99.5%	Sigma Aldrich
Glycine	Roth
Hepes	Roth
Hydrochloric acid (HCl) 37%	Panreac
Hydrogen peroxide	Sigma Aldrich
Iron Standard for ICP	Fluka
Iron (II) sulfate heptahydrate	Merck
Isopropyl β-D-1-thiogalactopyranoside (IPTG)	Apollo Scientific
Lysozyme	Sigma Aldrich
LMW calibration kit for SDS electrophoresis (14.4-97kDa)	GE Healthcare
Magnesium sulphate anhydrous (MgSO4)	Fluka
MES hydrate	Sigma
Menadione	Sigma Aldrich
Methanol 99.8%	Sigma Aldrich
Myoglobin	Sigma Aldrich
Nickel (II) chloride hexahydrate ($NiCl_2$)	Merck
n,n-dimethyl-p-phenylendiamine sulfate	Sigma Aldrich
N, N,N',N'-Tetrametyldiamine 99% (TEMED)	ACROS Organics
N,N,N,N-tetramethyl-1,4- phenylenodiamine	ACROS
Phenazine	Sigma Aldrich
Potassium dihydrogen phosphate (KH_2PO_4)	Panreac
Potassium Indigotrisulfonate	Sigma Aldrich
plumbagin	Sigma Aldrich
Polyethylene glycol methyl ether 550 (PEG 550)	Fluka
Polyethylene glycol monomethylether 2000 (PEG 2 K)	Fluka
Polyethylene glycol 4000 (PEG 4 K)	Merck
Polyethylene glycol 6000 (PEG 6K)	Merck
Polyethylene glycol 8000 (PEG 8K)	Sigma

Potassium ferricyanide	Merck
Prestained SDS PAGE marker (6-203 kDa)	BioRad
quinhydrone 98%	Merck
Sodium chloride (NaCl)	José Manuel Gomes dos Santos
Sodium dithionite	Sigma Aldrich
Sodium dodecyl sulphate (SDS)	Panreac
Sucrose	Sigma Aldrich
Trichloroacetic Acid (TCA)	Roth
Trimethylhydroquinone 97%	Sigma Aldrich
Triptone	Cultimed
Tris-(hydroxymethyl)aminomethane (Tris)	Panreac
Tris-(2-Carboxyethyl)phosphine hydrochloride (TCEP)	Sigma Aldrich
Urea	Harnstoff
Yeast extract	Cultimed
1,2 Naphthoquinone	Fluka
1,4- Napthoquinone hydrate 97%	Sigma Aldrich
1,2-naphtoquinone-4-sulfonic acid, sodium salt 99%	Sigma Aldrich
2-Hydroxy-1,4-naphthoquinone	Sigma Aldrich
2-Mercaptoethanol	Sigma Aldrich
2-Methyl-2,4 pentanediol (MPD)	Merck
2- Propanol	Riede-deHaën
2, 4, 6 Tris (2-pyridyl) – S-triazine (TPTZ)	Sigma Aldrich
(+)-sodium L - ascorbate	Sigma Aldrich